Inaugural dissertation

for

obtaining the doctoral degree

of the

Combined Faculty of Mathematics, Engineering and Natural Sciences

of the

Ruprecht - Karls - University

Heidelberg, Germany

Presented by

M.Sc. Marco Torben Siekmann

born in: Ludwigsburg, Germany

Oral examination: 27th February 2023

Organoid assembloids
modelling the role of serotonin
during human cortical development

Referees: Prof. Dr. Valerie Grinevich

Prof. Dr. Philipp Koch

I. Table of Content

II. List of Figures

III. List of Tables

IV. List of Abbreviations

Abbreviation	Full name
%	percent
°C	degree Celsius
2D	two-dimensional
3D	three-dimensional
5-HT	5-hydroxytryptamine / Serotonin
5-HT_1	serotonin receptor 1
5-HT_2	serotonin receptor 2
AA	ascorbic acid
ADHD	Attention deficit / hyperactivity disorder
aPC	apical progenitor cell
aRG	apical radial glia cell
ASD	autism spectrum disorder
ATP	adenosine triphosphate
BBB	blood brain barrier
BDNF	Brain-derived neurotrophic factor
bPC	basal progenitor cell
bRG	Basal radial glia cell
BW	BW723C86
cAMP	cyclic-adenosine monophosphate
cDNA	complementary DNA
CNS	central nervous system
CO	cortical organoid
CP	CP 809101 hydrochloride
Ct	threshold cycle
DAPI	4,6-diamidino-2-phenylindole

Abbreviation	Full name
DAPT	N-[N-(3,5.Difluorophenacetyl)-L-anlanyl]-S-phenylglycine t-butyl ester
DCN	deep cerebellar neurons
ddH2O	double-distilled water
DEPC	diethyl pyrocarbonate
DMEM	dulbecco's modified eagle medium
DMSO	dimethyl sulfoxide
DNA	desoxyribonucleic acid
dNTP	desoxynucleotide triphosphate
E	embryonic day (rodents)
e.g.	*exempli gratia* (for example)
E8	essential 8
EB	embryoid body
EDTA	Ethylenediaminetetraacetic acid
EMX1	Empty spiracles homebox 1
et al.	Et alia (and others)
FBS	fetal bovine serum
FGF	fibroblast growth factor
FOX	forkhead box
g	gram
GABA	γ-aminobutyric acid
GAD65	glutamate decarboxylase 65
gDNA	genomic DNA
GDNF	glial cell-derived neurotrophic factor
GPCR	G protein-coupled receptor

Abbreviation	Full name
GW	gestation week (human)
HEK	human embryonic kidney
HOX	homebox
IP	Intermediate progenitor cell
IPS	ipsapirone
iPSC	induced pluripotent stem cell
iSVZ	inner SVZ
Ket	Ketanserin
l	liter
LAAP	L-ascorbic acid 2-phospate
m	milli
M	molar
MAO	monoamine oxidase
MAP2	microtubule-associated protein 2
MEM	minimum essential media
min	minute
mRNA	messenger RNA
n	nano
n.s	not significant
N/A	not applicable
NES	neuroepithelial stem cell
NKX	NK homebox
OLIG2	oligodendrocyte transcription factr 2
oSVZ	outer SVZ
OTX2	orthodenticle homebox2
p	significance level
PAX	paired box
PBS	phosphate buffered saline
PCR	polymerase chain reaction

Abbreviation	Full name
PFA	paraformaldehyde
pH3	phosphorylated histone 3
PHOX2B	paired-like homebox 2B
PTC	patched
PTPRZ1	protein tyrosine phosphatase receptor type Z1
qPCR	quantitative PCR
R	rhombomer
RIN	rin integration number
RNA	ribonucleic acid
RO	raphe nuclei organoid
ROCK inhibitor	rho-associated protein kinase inhibitor
rpm	revolutions per minute
RT	room temperature
RT-PCR	reverse transcription PCR
SB	SB 242084 hydrochloride
SCN	suprachiasmatic nucleus
sDarken	serotonin darkening 5-HT_{1A} receptor-based sensor
SEM	standard error of the mean
seq	sequencing
SERT	serotonin transporter
SHH	Sonic hedgehog
SMAD	small mothers against decapentaplegic
Smo	smoothened
SOX	sex-determining region Y-box
SP	subplate
SSRI	selective serotonin reuptake inhibitors

Abbreviation	Full name
SVZ	subventricular zone
TBR	T-box, brain
TGF-β	transforming growth factor β
TH	tryptophan hydroxylase
TPH	Tryptophan-5-hydroxylase
TUBB3	beta-III-tubulin
v/v	volume percent
VMAT2	vesicular monoamine transporter 2
VZ	ventricular zone
w/v	weight percent
Wnt	wingless/integrated
µ	micro

1 Abstract

The development of the human cortex involves the coordinated interplay between cell proliferation, migration and differentiation. Serotonergic projections from the raphe nuclei were shown to reach the developing cortex at early stages, prior to the main expansion period. Subsequently, serotonin has been linked to several aspects of corticogenesis, including proliferation. However, the lack of appropriate models impedes deepening our understanding of the role of serotonin in human corticogenesis. In this context, human induced stem cell (hiPSC)-derived culture systems became of interest as regionalized brain organoids have been shown to faithfully recapitulate certain aspects of human brain development.

In this thesis, hiPSC-derived 2D and 3D model systems were applied to decipher the effect of serotonin on distinct cortical progenitor pools. Thus, apical progenitor cells (aPCs) were identified as recipients of serotonin. Specifically, activation of the serotonergic receptor 5-HT_{2C} was required and sufficient to induce proliferation. Secondly, a mitogenic effect of serotonin was also observed in basal progenitor cells (bPCs), a precursor type fundamental for human brain development, e.g. human-specific cortical expansion. The increased proliferation was here mediated by the receptor 5-HT_{2A}. Interestingly, no change in proliferation behavior was observed in intermediate progenitors (IPs).

To closer resemble the interplay between serotonergic neurons and the developing cortex, cortical-raphe assembloids were established. Whereby, a new organoid model was developed mimicking the raphe nuclei. At early time points, raphe organoids (RO) were composed of progenitors exhibiting expression of characteristic markers of serotonergic precursors including NKX2.2 and FOXA2. RO ultimately generated serotonergic neurons marked by TPH2, VMAT2 and serotonin itself. Moreover, by applying the serotonin sensor sDarken the endogenous release of serotonin could be detected.

By fusing raphe with cortical organoids (CO) to assembloids, a model system was created representing the influence of serotonergic innervation on human corticogenesis. Specifically, RO-derived serotonergic projections were observed in cortical structures and the utilization of sDarken in CO demonstrated serotonergic innervation. Finally, ventricular zones showed elevated proliferation in the presence of serotonergic projections.

Taken together, hiPSC-derived organoids displayed distinct mitogenic effects of exogenous serotonin on different progenitor populations, namely aPCs and bPCs but not IPs. Moreover, the generated assembloid proved valuable by displaying endogenous serotonergic innervation and recapitulating the mitogenic effect of serotonin. Thus, RO-CO assembloids enable further decipherment of the serotonergic role during human corticogenesis and open the possibility to study associated diseases, including autism spectrum disorder.

2 Zusammenfassung

Die Entwicklung des menschlichen Kortex beruht auf die koordinierte Abfolge von Zellproliferation, -wanderung und -differenzierung. Serotonerge Projektionen ausgehend von den Raphe Kerne wurden bereits an frühen Entwicklungsstadien im Kortex nachgewiesen, sogar vor der Hauptexpansionsphase des Kortexes. Folglich wurde Serotonin mit verschiedenen Aspekten der Gehirnentwicklung in Verbindung gebracht, unteranderem mit der Proliferation. Jedoch hat der Mangel an geeigneten humanen Modellen eine tiefere Erforschung der Rolle von Serotonin bis jetzt verhindert. Neue Möglichkeiten schaffen humanen induzierte pluripotente Stammzellen (hiPSCs) und regionalspezifischen Gehirnorganoidmodellen, welche bereits bestimmte Aspekte der menschlichen Gehirnentwicklung replizieren konnten.

In dieser Thesis wurde mithilfe von auf hiPSCs-basierenden 2D und 3D Zellkulturmodellsystemen der Effekt von Serotonin auf verschiedene kortikale Progenitorpopulationen untersucht. Apikale Progenitoren (aPCs) wurden als Rezipienten von Serotonin erkannt, wobei diese bei Aktivierung des 5-HT_{2C} eine erhöhte Proliferation zeigten. Ein mitogenischer Effekt von Serotonin konnte ebenso für basale Progenitoren (bPCs) identifiziert werden, welche eine fundamentale Funktion in der humanen kortikalen Expansion haben. Die erhöhte Proliferation beruhte auf der Aktivierung des Rezeptors 5-HT_{2A}. Interessanterweise konnte keine Veränderung des Zellteilungsverhaltens bei intermediären Progenitoren festgestellt werden.

Um eine höhere Vergleichbarkeit mit der natürlichen serotonergen Innervierung auf den sich entwickelnden Kortex zu schaffen, wurden Raphe-Kortex Assembloids entwickelt. Dabei wurde ein neues Organoidsystem geschaffen, welches die Raphe Kerne imitiert. An frühen Zeitpunkten exprimierten die Progenitoren des Raphe Organoids (RO) charakteristische Marker von serotonergen Vorläuferzellen wie zum Beispiel NKX2.2 und FOXA2. Schlussendlich generierten RO serotonerge Neurone, welche anhand von TPH2, VMAT2 sowie Serotonin identifiziert wurden. Mithilfe des serotonergen Sensors sDarken konnte sogar die endogene Ausschüttung von Serotonin detektiert werden.

Durch die Fusion von Raphe- mit Kortikalen Organoiden zu Assembloids wurde ein Modelsystem geschaffen, welches den Einfluss von Serotonin auf die menschliche Kortikogenese repräsentieren kann. Serotonerge Projektionen des RO konnten in kortikalen Strukturen nachgewiesen werden und der Einsatz von sDarken demonstrierte serotonerge Innervierung. Es konnte außerdem festgestellt werden, dass Ventrikularstrukturen eine erhöhte Proliferation zeigten, wenn serotonerge Ausläufer vorhanden sind.

In dieser Arbeit konnte mithilfe von auf hiPSC-basierenden Organoiden definierte mitogenische Effekte auf bestimmte Zellpopulationen, nämlich aPCs and bPCs, aber nicht IPs, identifiziert werden. Der Wert der RO-CO Assembloids konnte durch die serotonerge endogene Innervierung sowie durch die Replizierung des serotonergen mitogenen Effekt bewiesen werden. Dadurch erlauben die Assembloids die weitere Untersuchung der Rolle von Serotonin in der Kortikogenese und öffnet die Möglichkeit assoziierte Erkrankung, wie die Autismus-Spektrum-Störung zu modellieren.

3 Introduction

1.1 Serotonin

Serotonin is a monoamine and commonly known as major neuromodulator of the nervous system. It is synthesized from the amino acid tryptophan. The enzyme L-tryptophan-5-hydroxylase (TPH) hydroxylates tryptophan to 5-hydroxytryptophan (5-HTP) using the co-enzyme tetrahydrobiopterin (BH4). In a second step, 5-HTP is decarboxylated by the enzyme aromatic amino acid decarboxylase (AADC) to 5-hydroxytryptamine (5-HT), also known as serotonin. The rate limiting enzyme TPH exists in two different variants which are expressed by different cell populations (Walther et al., 2003; Walther & Bader, 2003). TPH-1 is the principal enzyme in the periphery and mainly present in enterochromaffin cells, (Kim et al., 2010; Paulmann et al., 2009; Stunes et al., 2011; Yasmine et al., 2012) while TPH-2 is expressed in enteric or central serotonergic neurons (Walther *et al.*, 2003). Enterochromaffin cells synthesize about 95% of the body's serotonin and provide it to the gut and blood (Berger, Gray and Roth, 2009; Gershon, 2013). About 98% of the serotonin is then bound and stored in platelets (Tamir *et al.*, 1985; El-Merahbi *et al.*, 2015). The term serotonin is derived from its function as vascular tone regulator (Elhusseiny and Hamel, 2001; Jähnichen, Glusa and Pertz, 2005; Kaumann and Levy, 2006): "sero" from serum and "tonin" from to induce constrictions (Rapport et al., 1948). The diverse peripheral functions of serotonin vary from modifying proliferation (Lesurtel *et al.*, 2006; Yadav *et al.*, 2008) and the regulation of blood sugar levels (Sumara *et al.*, 2012) to a mediating role with the immune system (Spohn *et al.*, 2016; Spohn and Mawe, 2017; Liu *et al.*, 2021).

Serotonin is an ancient neurotransmitter which is even present in single cell eukaryotes paramecium and tetrahymena (Csaba, 1993). Evolutionary, the receptor system was developed about 700-750 million years ago and is thus, older than other receptor classes like dopaminergic or adrenergic (Peroutka and Howell, 1994). Over the time, the serotonergic receptor system diverged and gave rise to 15 different types from which 14 are found in mammals (Nichols and Nichols, 2008; Qi *et al.*, 2014). This makes the serotonergic receptor system the largest G-protein coupled neurotransmitter receptor class (Nichols and Nichols, 2008). The serotonergic receptors are divided into seven families: 5-HT_1 – 5-HT_7. All are G-protein coupled neurotransmitter receptors (GPCR), except for the 5-HT_3 type which is a ligand-gated cation channel. The receptor types 5-HT_1 and 5-HT_5 are $G\alpha_i$-coupled. When activated, they inhibit the adenylyl cyclase and cause a decrease of intracellular cAMP (Lin *et al.*, 2002) and are therefore considered inhibitory. An excitatory effect is mediated by the 5-HT_2 receptor family which is coupled to $G\alpha_{q/11}$. Upon binding of serotonin, membranous phosphoinositol is recruited and cleaved into diacyl glycerol (DAG) and inositol triphosphate (IP3). This in turns, activates protein kinase C (PKC) and triggers a calcium release from the endoplasmic reticulum, leading to an increased intracellular

calcium concentration (Roth *et al.*, 1984). Among the receptor subtypes, the 5-HT_{2A} is one of the most studied ones, as it his vastly expressed in the human CNS (Willins et al., 1997). It received great attention for its binding potential of psychedelics as LSD or psilocybin (Nichols and Nichols, 2008). Furthermore, the receptor has been identified as an effective target for different mental illnesses like schizophrenia and psychoses (Abdolmaleky *et al.*, 2011; Meltzer and Roth, 2013). A second widely expressed subtype is the 5-HT_{2c} type. Among other areas, it is present in the choroid plexus or ventral tegmental area and has been reported to regulate adult neurogenesis (Millan *et al.*, 2005; Klempin *et al.*, 2010). The receptor types 5-HT_4, 5-HT_6 and 5-HT_7 are coupled to Ga_s and activate adenyl cyclase which facilitate the conversion of ATP to cAMP (Bockaert, Sebben and Dumuis, 1990).

Table 1: List of human serotonergic receptors and their functions

5-HT types	Subtype	Receptor type	function
5-HT_1	5-HT_{1A}	GPCR, Inhibitory auto and hetero receptor	$G\alpha_i$-coupled, inhibit adenyl cyclase, reduce intracellular cAMP
	5-HT_{1B}		
	5-HT_{1D}		
	5-HT_{1E}		
	5-HT_{1F}		
5-HT_2	5-HT_{2A}	GPCR, Excitatory hetero receptor	$G\alpha_{q/11}$-couped, increase in DAG and IP3, activates PKC
	5-HT_{2B}		
	5-HT_{2C}		
5-HT_3		Ligand-gated ion channel Excitatory heteroreceptor	Influx of cations (calcium, potassium, sodium)
5-HT_4		GPCR, Excitatory heteroreceptor	Ga_s-coupled, activate adenyl cyclase, increase intracellular cAMP
5-HT_5	5-HT_{5A}	GPCR, Excitatory heteroreceptor	Ga_s-coupled, activate adenyl cyclase, increase intracellular cAMP
	5-HT_{5B}		
5-HT_6		GPCR, Excitatory heteroreceptor	Ga_s-coupled, activate adenyl cyclase, increase intracellular cAMP
5-HT_7		GPCR, Excitatory heteroreceptor	Ga_s-coupled, activate adenyl cyclase, increase intracellular cAMP

Serotonergic receptors offer a large heterogeneity and can cause various, even opposing downstream effects. Moreover, serotonergic receptors are expressed by many different cell types and occur also pre-synaptically. Besides, it is estimated that one serotonergic neuron targets at least 500,000 cells (Jacobs and Azmitia, 1992). This enables serotonin to modulate numerous functions on different levels in a very precise manner (Avery and Krichmar, 2017). However, this also gives rise to a complex effect machinery and makes it very difficult to decipher the specific serotonergic mechanisms.

Serotonin is rapidly removed from the synaptic cleft by the presynaptic serotonin transporter (SERT). Subsequently, serotonin can again be stored in vesicles under the support of vesicular monoamine transporter 2 (VMAT2) and ultimately, released in the synaptic cleft again. It can also be degraded to 5-hydroxy-3-indolacetaldehyde (5-HIAL) by monoamine oxidase (MAO) and finally processed to 5-hydroy-3-indolacetic acid (5-HIAA) by aldehyde dehydrogenase.

Although the vast amount of serotonin is produced in the periphery, it can not enter the brain. Serotonin is not able to pass the blood brain barrier (BBB) which separates the blood from the central nervous system (Bonnin *et al.*, 2011a). As early as gestation week (GW) 12, the tight junction proteins occluding and claudin-5 are vastly expressed, which allows the assumption of a certain level of functionality (Virgintino *et al.*, 2000). From GW 18 onwards, the BBB provides a structure of tight junction proteins as it is found in adults (Virgintino *et al.*, 2000). At this developmental stage, the enteritic serotonin system is just partially developed and the enterochromaffin cells do not express the rate limiting enzyme TPH-1 yet (Kliman *et al.*, 2018). Interestingly, endothelial cells of the fetus are already able to take up serotonin by SERT and to degrade it using MAO (Kliman *et al.*, 2018). Additionally, several receptors have been identified being expressed at this early development stages in the brain (Hillion *et al.*, 1993; Buznikov, Lambert and Lauder, 2001; Bonnin *et al.*, 2006). PET-1 is a crucial transcription factor involved in the development of murine serotonergic neurons. Interestingly, PET-1 knock-out mice present normal levels of serotonin in the developing forebrain indicating a minor role of the endogenous system at early stages (Bonnin and Levitt, 2011; Bonnin *et al.*, 2011a). The initial source of serotonin has been identified as maternal (Côté *et al.*, 2007; Bonnin *et al.*, 2011a). Serotonin can be directly taken up by the placenta of the maternal blood stream or even directly be synthesized in the placenta (Bonnin *et al.*, 2011a; Kliman *et al.*, 2018). The placenta releases serotonin in the fetal blood stream where it is taken up by platelets via SERT and transported to the developing brain (Bonnin *et al.*, 2011a; Baković *et al.*, 2021).

1.2 Serotonin in the CNS

The CNS is supplied with serotonin by around 250,000 serotonergic neurons which are mainly located in the raphe nuclei (Baker *et al.*, 1991). The raphe nuclei are a diverse group of nuclei with a mixed population of neuron types with distinct projections (Wylie *et al.*, 2010; Sos *et al.*, 2017). The nuclei have weakly defined edges and are located around the midline, stretching from the rostral to the caudal extension of the pons in the mid- and hindbrain (Alonso *et al.*, 2013). The raphe nuclei consist of two nuclei clusters based on their location and projections (Jacobs and Azmitia, 1992). The rostral group make up for around 85 % of all serotonergic neurons in the brain and innervate virtually the entire brain (Hornung, 2003). The two main nuclei are the median and dorsal raphe. The dorsal raphe nucleus is located in the mesencephalon and the median extends caudally from the superior cerebellar

perduncle in the rostral pons (Alonso *et al.*, 2013). The major projections are to the cerebral cortex, hypothalamus, amygdala, thalamus, basal ganglia and hippocampus(Bang *et al.*, 2012). The caudal group of the raphe nuclei is separated by the rostral group by a gap in the pons. Raphe magnus, obscurus and pallidus are the main contributor to the caudal cluster and are stretching from the caudal pons to the caudal medulla oblongata (Hornung, 2003). Their major projections expand to the brainstem and to the spinal cord (Deneris and Gaspar, 2018a).

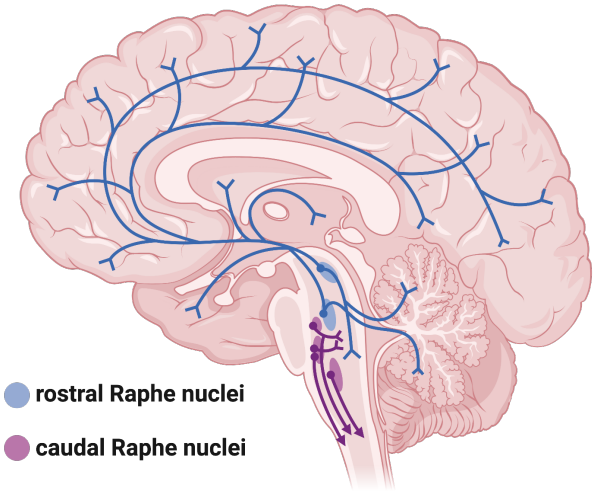

Figure 1: Schematic overview of projections from the rostral and caudal raphe nuclei cluster throughout the CNS

1.3 Serotonergic function

Serotonin has a reported effect on a large variety of brain function. Due to its wide range of target cells and diversity of receptors, it can modulate processes on several levels (Jacobs and Azmitia, 1992; Nichols and Nichols, 2008; Berger, Gray and Roth, 2009). A schematic overview of the range of functions is depicted in figure 2 of which just a very limit amount can be introduced here.

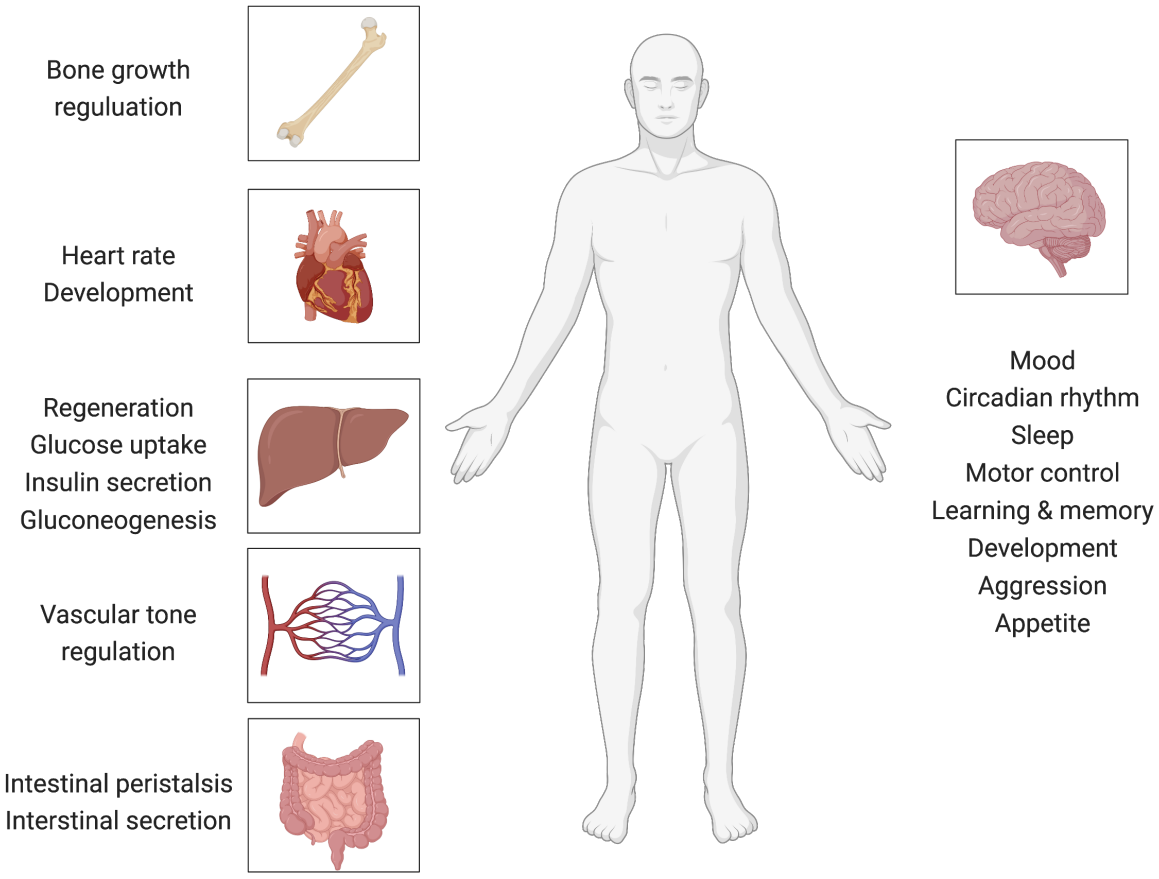

Figure 2: Schematic overview of diverse functions of serotonin in body and brain

1.3.1 Mood

Generally, serotonin has a strong association with mood as the major therapeutic depression agents are inhibiting SERT (selective serotonin reuptake inhibitors; SSRIs). The idea is that serotonin then remains longer in the synaptic cleft and subsequently, has a prolonged receptor binding which then elevates the mood (Invernizzi *et al.*, 1997). However, SSRIs are just effective in a subset of patients, demonstrating that the concentration of serotonin might just be part of the answer to depression (Melander *et al.*, 2008). Serotonin has been implicated in the cognitive processing of emotional information. Acute tryptophan deletion experiments revealed for instance, a negative bias in perception and a focus towards punishment and negative information (Murphy *et al.*, 2002; Chamberlain *et al.*, 2006; van der Veen *et al.*, 2007). Similar to outcomes, which have been also identified in depressed patients (Murphy *et al.*, 1999, 2002). The lack of serotonin might thus result in a negative perception bias. As mood is dependent on how we perceive outcomes, this might then cause lowered mood, anti-social behavior and even depression (Bjork *et al.*, 1999; Eldar *et al.*, 2016; Steenbergen *et al.*, 2016). Subsequently, elevation of serotonergic levels by tryptophan supplementation or SSRIs might then cause a positive re-balancing of perception which in the end increases mood (Murphy *et al.*, 2006; Steenbergen *et al.*, 2016). Additionally, Michely and colleagues

proposed a computational model based on serotonin's increase of subjective reward perception increases mood over time giving an explanation for the delayed onset of SSRIs (Michely *et al.*, 2020).

1.3.2 Circadian rhythm and sleep

The suprachiasmatic nucleus (SCN), the central pace maker of the circadian clock has few direct neuronal connections. Beside retinohypothalamic connections from the retina as main input, SCN has reciprocal connections to the rostral raphe (Moore, Halaris and Jones, 1978; Malek *et al.*, 2007). Serotonin has the capabilities to induce non-photic phase shifts in the SCN (Mistlberger *et al.*, 2000). Moreover, serotonin also regulates photic-shifts by reducing the light input on the SCN by activating 5-HT_{1B} receptors on retinal projection neurons (Pickard and Rea, 1997; Pickard *et al.*, 1999; Smith *et al.*, 2001). The activation of this receptor decreases the innervation from the retinal ganglion cells. A reduction of retinal input could also be achieved by activating 5-HT_7 in the SCN (Smith *et al.*, 2001).

The release of serotonin in the brain is dependent on the time of the day and the activity state: the highest release of serotonin is during active wakefulness, decreased during sleep and lowest during rapid eye movement (REM) sleep (Trulson and Jacobs, 1979; Portas *et al.*, 1996, 1998). Hence, serotonin is since described as a promoting wakefulness agent, although the exact mechanisms remain poorly understood. The general model describes serotonin from the DRN as part of the waking system which then lead to an activation of the cortex and thalamus. Interestingly, they also inhibit sleep-promoting GABAergic neurons in the median and ventrolateral preoptic nucleus (Luppi and Fort, 2019) while on the other hand, GABAergic neurons from different regions inhibit the serotonergic raphe neurons during sleep (Gervasoni *et al.*, 2000). However, recent results highlight the importance of serotonin for sleeping as well and point to a crucial function towards the initiation and maintenance of sleep (Oikonomou *et al.*, 2019).

1.3.3 Motor function

Early studies found strong projections to brain regions responsible for motor control like basal ganglia, cerebellum and spinal cord (Imai, Steindler and Kitai, 1986; Bowker and Abbott, 1990). Among the nuclei of the basal nuclei, the substantia nigra seems the one having the most projections of the dorsal raphe nuclei (Imai, Steindler and Kitai, 1986). However, the actual effect remains elusive. The cerebellum harbors several nuclei involved in motor control. All of them, the pontine nuclei, cerebellar cortex, deep cerebellar nuclei and the inferior olive receive serotonergic input (Schweighofer, Doya and Kuroda, 2004). In general, the release of serotonin in the cerebellum is associated with a higher degree of motor activity (Mendlin *et al.*, 1996). The actual effect of serotonin on the cerebellar circuitry is poorly understood as many cell types express different receptor types and thus have different effects (Schweighofer, Doya and Kuroda, 2004; Kawashima, 2018). For instance, serotonin has an excitatory

effect on deep cerebellar neurons (DCNs) conducted on several levels. First of all, serotonin can depolarize DCN directly via 5-HT_5 (Saitow et al., 2009). Additionally, released serotonin can block inhibitory signals. DCNs receive inhibitory transmission from GABAergic purkinje cells. Those can be inhibited via 5-HT_{1B} activation directly as well as by serotonin stimulated inhibitory lugargo cells (Dieudonné and Dumoulin, 2000; Dean, Robertson and Edwards, 2003).

1.4 Human brain development

The entire human body develops from three distinct germ layers: endoderm forming internal organs, mesoderm giving rise to skeletal and muscle system and the ectoderm representing the most outer layer. The latter then differentiates to the neuroectoderm which forms the neural plate, folds to the neural groove and subsequently closes after 30 days to the neural tube (Piccolo *et al.*, 1996; Müller and O'Rahilly, 2006). The differentiation towards the three germ layers and the further development is guided by signaling molecules, called morphogens including Noggin, fibroblast growth factors (FGFs), wingless/Integrated (Wnt) and sonic hedgehog (SHH) (Brennan et al., 2001). Morphogens are secreted by certain organizing centers and activate distinct cellular responses by upregulating specific genes in a concentration dependent manner. Morphogens build up gradients, thus define distinct axes in the organism and along them, defined cell identities. For instance, the rostral-caudal axis of the developing neural tube is defined by Wnt signaling whereby, high levels drive the caudalization (McGrew, Hoppler and Moon, 1997; Kiecker and Niehrs, 2001). Additional caudalizing factors include FGFs and retinoic acid (Cox and Hemmati-Brivanlou, 1995; Hitoshi *et al.*, 2002).

SHH is secreted by the ventral notochord and defines cells along the ventral-dorsal axis (Echelard *et al.*, 1993). SHH signaling is mediated by the transmembrane proteins Patched (Ptc) and Smoothened (Smo). Smo is inhibited by Ptc until Ptc is bound by SHH which then allows Smo to transduce the signal intracellularly (Taipale *et al.*, 2002). Of note, bone morphogenetic protein (BMP) signaling emerges from the roof plate and has shown to inhibit the response of cells to SHH (Liem, Jessell and Briscoe, 2000). Thus, it facilitates a dorsalization and defines the cells' identity in the dorsal areas (Briscoe *et al.*, 2000).

Other morphogens support the definition of cell populations by forming additional secondary gradients and sharp boundaries (Kimelman and Kirschner, 1987; Crossley, Martinez and Martin, 1996). For instance, fibroblast growth factor 8 (FGF-8) plays a vital role defining the boundary between midbrain and hindbrain (mid-hindbrain boundary). Subsequently, shifting the boundary caudally results in diminished and displaced serotonergic population, while dopaminergic midbrain populations extended more caudally (Brodski *et al.*, 2003).

1.4.1 Raphe nuclei development

The brain develops from the caudal areas towards the anterior, therefore, serotonergic neurons from the hindbrain develop prior to cortical neurons (Kolk and Rakic, 2022). The early hindbrain is subdivided into eight distinct compartments called rhombomeres (R) (Figure 3A). The localization along the anterior-posterior axis of the rhombomeres gives rise to the raphe nuclei divisions (Alonso *et al.*, 2013). The precursors situated in R1-3 will develop the median and dorsal raphe nuclei while the posterior rhombomeres (R5-8) form the caudal raphe cluster (Alonso *et al.*, 2013; Okaty *et al.*, 2015). Interestingly, the rostral cluster arises 24 hours before the caudal one (Wallace and Lauder, 1983). R4 forms a gap between those serotonergic pools and develops visceral motor neurons (Pattyn *et al.*, 2000).

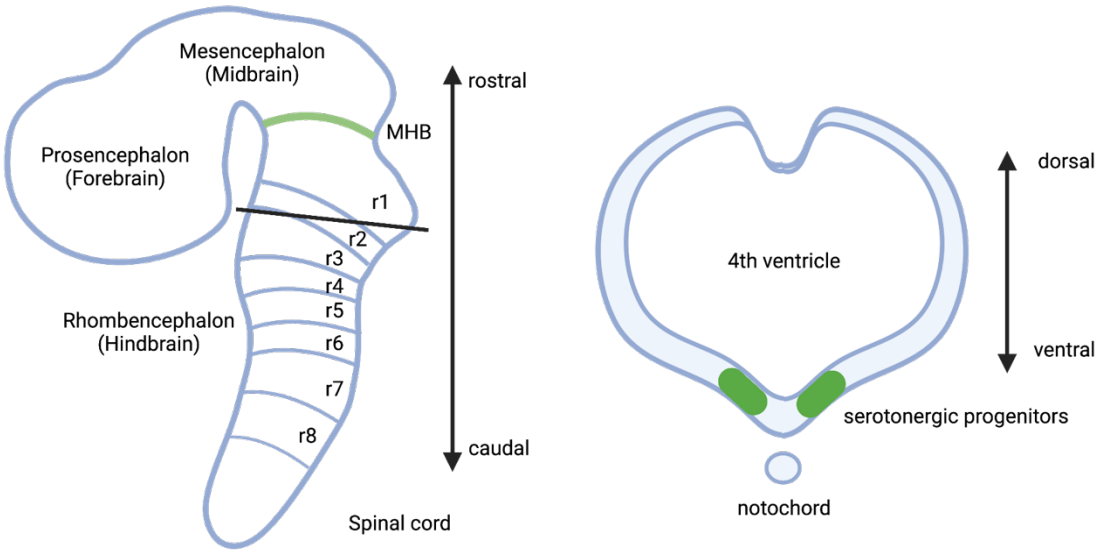

Figure 3: Schematic overview of the developing human brain.

(A) Lateral view of early regions prosencephalon, mesencephalon and rhombencephalon. The rhombencephalon can be subdivided into eight distinct compartments called rhombomers. (B) Transversal view on neural tube in rostral rhombencephalon. Serotonergic progenitors are located in the ventral p3 domain.

The progenitor cluster which will give rise to serotonergic neurons is located in the ventral p3 domain (Briscoe *et al.*, 2000). SHH is secreted by the ventral notochord and the floor plate and forms the gradient defining the cells' identity along the dorso-ventral axis (Figure 3 B). SHH is inducing the homeodomain transcription factors homeobox protein NK-6 Homolog 1 (NKX6.1), homeobox protein NK-2 Homolog 2 (NKX2.2) and forkhead transcription factor (FOXA2) in a concentration dependent manner (Briscoe and Ericson, 1999; Briscoe *et al.*, 2000). NKX2.2 and NKX6.1 have been identified as key players in the identification of serotonergic progenitor pools and are co-expressed in the p3 domain (Briscoe and Ericson, 1999; Cheng *et al.*, 2003; Craven *et al.*, 2004; Marklund *et al.*, 2014).

However, the p3 domain also gives rise to visceral motor neurons, therefore additional factors are needed (Pattyn *et al.*, 2003; Kiyasova and Gaspar, 2011). FOXA2 is initially expressed in the floor plate where the highest SHH concentration is present. Jacobs *et al* identified a time-dependent subsequent upregulation of FOXA2 in the p3 domain (Jacob *et al.*, 2007a). FOXA2 in turn downregulates the pro-motor neuronal transcription factor paired-like homebox 2b (PHOX2b) (Pattyn *et al.*, 2003; Jacob *et al.*, 2007a). In line, PHOX2b-knock out models showed a reduction of motor neurons and an early development of serotonergic neurons (Pattyn *et al.*, 2003). Thus, the subsequent upregulation of FOXA2 expression is a temporal switch from differentiating visceral-motor neurons towards serotonergic neurons (Jacob et al., 2007b; Deneris and Wyler, 2012; Smidt and van Hooft, 2013).

Together, NKX2.2, NKX6.1 and FOXA2 are initiating a cascade of transcription factors towards the serotonergic fate (Cheng *et al.*, 2003; Kittappa, Kehler and Barr, 2017). Among others, they upregulate downstream transcription factors like GATA2, GATA3, LMX1 and FEV which then initiate the expression of crucial serotonergic proteins like TPH2, VMAT2 and SERT (Craven *et al.*, 2004; Deneris and Wyler, 2012; Deneris and Gaspar, 2018b). Before any of those proteins are transcribed, the developing neuron start to migrate (Hawthorne *et al.*, 2010). The populations in the p3 domains fuse along the midline via somatic translocation and move towards their final position in the raphe nuclei system (Jacobs and Azmitia, 1992; Hawthorne *et al.*, 2010; Soiza-Reilly and Gaspar, 2020). Immunocytochemical studies found serotonergic neurons being present in the first trimester of embryonic development. Kinney and colleagues showed serotonergic neurons at GW7 and the work of Sundström e*t al* revealed serotonergic neurons in the caudal part already at GW 5 (Sundström *et al.*, 1993; Kinney *et al.*, 2007). In both studies, the observation was done at the earliest examined time point. Additionally, research in rodents showed that the rostral raphe cluster develops earlier than the caudal cluster, thus it might be possible that the first human serotonergic neurons are developing even before GW5 (Wallace and Lauder, 1983).

Shortly after being developed, serotonergic neurons start to extend their projections towards the target regions. The first serotonergic afferents in the developing cortex have been observed at GW 8 in the sub plate and intermediate zone at GW10 and entered the cortical plate at GW 13 (Verney, Lebrand and Gaspar, 2002). However, it is not clear from which timepoint on, human serotonergic neurons are indeed active and provide serotonin to the target regions. It is known however, that endogenous serotonin becomes the most important source 1.5 days after the first occurrence in the mouse cortex (Bonnin and Levitt, 2011; Bonnin *et al.*, 2011b).

1.4.2 Cortex development

At early stages, the neural tube consists of highly proliferative neuroepithelial stem cells (NES) which rapidly divide symmetrically and thus, increase the starting cell population for cortical neurons. NES are arranged in a monolayer but due to their apical-basal migration during the cell cycle, they have a pseudo-stratified organization (Götz and Huttner, 2005; Subramanian *et al.*, 2017). Around GW 7, NES convert to apical radial glia cells (aRGs) which are characterized by their radial processes spanning from the ventricular towards the basal surface. Their cell body can be located along their processes in the ventricular zone, it is however, confined at the ventricular lining during mitosis. Hence NES and aRGs can also be combined as apical progenitor cells (aPCs). The first neurons are generated by asymmetrical division of aRGs which then migrate radially along the radial processes to the forming pre-plate. ARGs can also indirectly generate neurons via asymmetrical division to intermediate progenitors (IPs). This progenitor type is developed at the ventricular lining and migrates out of the VZ and form the subventricular zone (Haubensak *et al.*, 2004). In contrast to radial glia progenitors, they retract their processes from the surfaces and downregulate astroglial marker (Cappello *et al.*, 2006). Instead, they express their characteristic marker TBR2, also known as EOMES (Cappello *et al.*, 2006). The morphology of IPs is divers and not well studied. The processes can be multipolar and extend and retract dynamically (Kalebic *et al.*, 2019). IPs can further be distinguished into a proliferative and a neurogenic type which differ also in their distribution (Florio and Huttner, 2014). The former can undergo symmetric division several rounds and increase the progenitor pool before giving rise to neurons (Hansen *et al.*, 2010). Neurogenic IPs just undergo one symmetric division and thus, generating two neurons (Haubensak *et al.*, 2004). As IPs are of limited proliferative capacity, they are also referred as transit-amplifying cells (Molnár *et al.*, 2019). Interestingly, lissencephalic animals have more often neurogenic IPs, while proliferative IPs are more common in gyrencephalic animals (Haubensak *et al.*, 2004; Betizeau *et al.*, 2013). The generated neurons quickly split the pre-plate into the subplate (SP) and the marginal zone and start forming the cortical plate (CP) (Nichols and Olson, 2010).

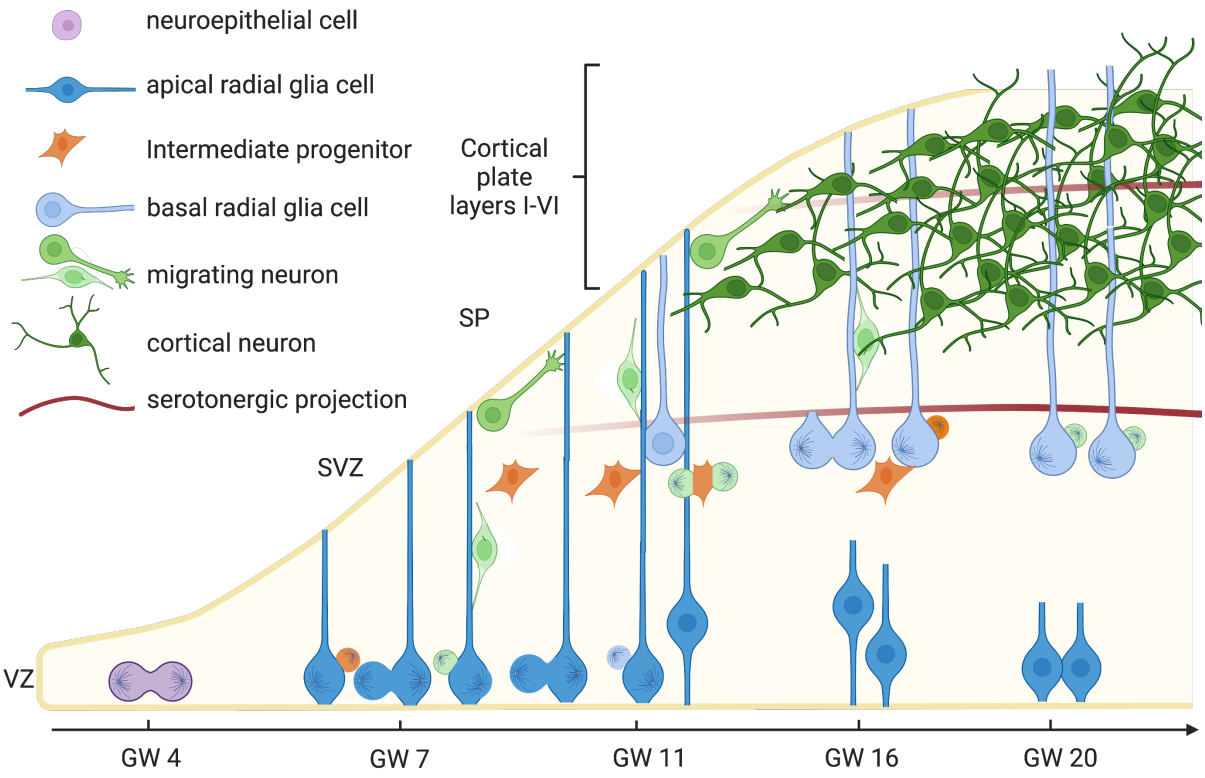

Figure 4: Schematic overview of corticogenesis

Neural epithelial cells (NES) proliferate and expand the neural tube surface (GW4). Subsequently, NESs give rise to a second class of apical progenitor cells (aPCs), apical radial glia cells (aRGs) which span their processes to pial surface (GW7). ARGs can self-renew or divide asymmetrically and thus generate the first neurons or intermediate progenitors. After migrating outside of the ventricular zone and start forming the subventricular zone, IPs can divide symmetrically to either self-renew or generate two neurons. Generated neurons are utilizing radial glia scaffold to migrate basally. Around GW11 basal radial glia cells are generated from aRGs and migrate to the SVZ which will subdivide into the inner and outer subventricular zone. BRGs mostly retract their apical connection and form a unipolar basal fiber. The dividing behavior of bRGs is divers as they can self-renew, generate neurons and IPs and will give rise at later stages to astrocytes and oligodendrocytes. Cortical neurons of the deeper layers (V and VI) are generated first, while upper layer neurons are born later and mainly generated from bRGs. Serotonergic neurons are generated around GW5 and reach cortical analogues at GW8 and are localized basally to the SVZ by GW 11.

The assumed most important progenitor type in the human brain is the basal radial glia cell (bRG) which can be identified by protein tyrosine phosphatase receptor type Z1 (PTPTRZ1) (Lewitus, Kelava and Huttner, 2013a; Pollen *et al.*, 2015). Around GW 11 aRGs divide symmetrically and give rise to bRGs (Hansen *et al.*, 2010; Xing *et al.*, 2020). BRGs delaminate from the apical lining and while some maintain their remnant apical process, most just form a unipolar fiber towards the basal surface (Hansen *et al.*, 2010; Pilz *et al.*, 2013). By GW 14, bRG have predominantly migrated to the SVZ and catalyze the division of the SVZ into the apical inner SVZ (iSVZ) and the basal outer SVZ (oSVZ) (Pollen *et al.*, 2015). Based on their location and proliferative capacity, bRGs are the largest contributors to the general class basal progenitor cells (bPC). The division occurs until GW 16 and represents the

localization of IPs (iSVZ) and bRGs (oSVZ), respectively (Fietz *et al.*, 2010; Hansen *et al.*, 2010). BRGs are capable to undergo multiple rounds of symmetric division and thus, massively enlarge the progenitor pool in humans (Betizeau *et al.*, 2013). In line, the largest expansion phase of the human neocortex occurs between GW 13 and 20 (Samuelsen *et al.*, 2003). While the proliferation and cell number in the oSVZ consistently increases, eventually the number of mitotic events in the VZ declines (Martínez-Cerdeño *et al.*, 2012; Nowakowski *et al.*, 2016). By asymmetrical division, bRGs can generate cortical neurons directly, or indirectly via the production of IPs. Thus, bRGs are thought to be the main contributor of the cortical neuron population (Florio and Huttner, 2014).

Pyramidal neurons arrange in distinct layers whereby the development occurs “inside out”. Deep layer neurons (V &VI) are mainly generated by the first neurogenesis phase by aRGs and IPs (Takahashi *et al.*, 1999; Stepien *et al.*, 2020). Around GW 16, the radial glia scaffold separates in the SVZ as aRGs lose their basal pial connection and retract their truncated processes (Nowakowski *et al.*, 2016). BRGs remain connected to the pial surface and generate primarily upper layer neurons in the following neurogenic phase (Nowakowski *et al.*, 2016). As bRGs are more prominent in primates compared to rodents, primate brains also display higher ratios of upper layer neurons (Pollen *et al.*, 2015). The resulting six-layer organization is noticeable by GW 18 (Budday, Steinmann and Kuhl, 2015). After this second neurogenesis phase, bRG produce large amount of different glia cell types, which ultimately, outnumber neurons (Rash *et al.*, 2019).

In the lissencephalic rodent brain, IPs mark the predominant progenitor type in the SVZ with a minor pool of more proliferative bRGs (Wang *et al.*, 2011). Interestingly, it was also shown that the proliferative capacity of rodent bRGs is lower than those in humans (Fietz *et al.*, 2010; Florio and Huttner, 2014). The amount of bRGs and the proportion of symmetric divisions is highly interspecies dependent and is significantly contributing to the expansion of the human cortex (Fietz *et al.*, 2010). Moreover, the higher abundance of bRGs and the expansion of the SVZ during evolution also drove the gyrification of the brain (Lewitus, Kelava and Huttner, 2013a). Gyrification describes increasing the cortical surface area by folding and this process starts by GW 24 (Takahashi et al., 2012). The precise mechanisms of the folding are still not well understood, however physical force is identified as important part (Karzbrun *et al.*, 2018). Same holds true for the involvement of bRGs, as gyrification could be induced by genetically increased bRG populations in mouse models (Stahl *et al.*, 2013; Florio *et al.*, 2015). Moreover, in humans, higher numbers of bRGs were observed underneath developing gyri than sulci (Nowakowski et al., 2016).

1.4.3 Corticogenesis is highly interconnected

The cortex does not develop isolated, but as an interplay with other brain regions. For instance, GABAergic interneurons have distinct functions already during brain development. GABA has a remarkable role during early stages as, in contrast to later stages, GABA causes a depolarization of target cells at this point. This is due to the expression and activity of the ion transporter NKCC1 during mid-gestation which builds up high levels of intracellular Cl^-. Activation of $GABA_A$ receptors opens Cl^- channels and causes an Cl^- efflux. Thus, GABA decreases proliferation and regulates migration of cortical neurons (LoTurco *et al.*, 1995; Heck *et al.*, 2007; Andäng *et al.*, 2008a). They further foster maturation of glutamatergic neurons and facilitate synaptogenesis (Wang and Kriegstein, 2008). Interestingly, those interneurons originate in the ganglionic eminences and migrate tangentially from the ventral- into the developing dorsal cortex. Whereby, the caudal ganglionic eminence (CGE) produces more than two-thirds of human cortical interneurons (Hansen *et al.*, 2013a; Kolk and Rakic, 2022). The first wave of interneurons is, however, originating in the lateral ganglionic eminence (LGE) which precedes the development of other regions. LGE-derived GABAergic neurons are entering the SVZ and IZ around GW10, closely followed by neurons generated in the medial ganglionic eminence (Letinic, Zoncu and Rakic, 2002; Hansen *et al.*, 2013b; Laclef and Métin, 2018). CGE-interneurons surpass the amount of interneurons in the cortex by GW14 and keep supplying the cortex with newly generated interneurons even after birth (Paredes *et al.*, 2016).

Other neurotransmitters were found to be involved in corticogenesis including noradrenalin and dopamine (Xing and Huttner, 2020). Noradrenalinergic neurons are derived from locus coeruleus in the brain stem and reach the developing cortex after GW10 and have shown to reduce synaptic density (Parnavelas and Blue, 1982). Dopamine mainly reduces progenitor proliferation and modifies interneuronal migration (Crandall *et al.*, 2004; Popolo, McCarthy and Bhide, 2004).

1.4.4 Serotonin and cortex development

Serotonin has been associated with a wide range of developmental processes. For instance, heart development is dependent on 5-HT signaling, mainly mediated by $5\text{-}HT_{2B}$ (Yavarone *et al.*, 1993; Nebigil *et al.*, 2000). Another example for serotonin's wide range would include the development of the mammary gland (Matsuda *et al.*, 2004), but here, shall be focused on serotonin's role during brain development.

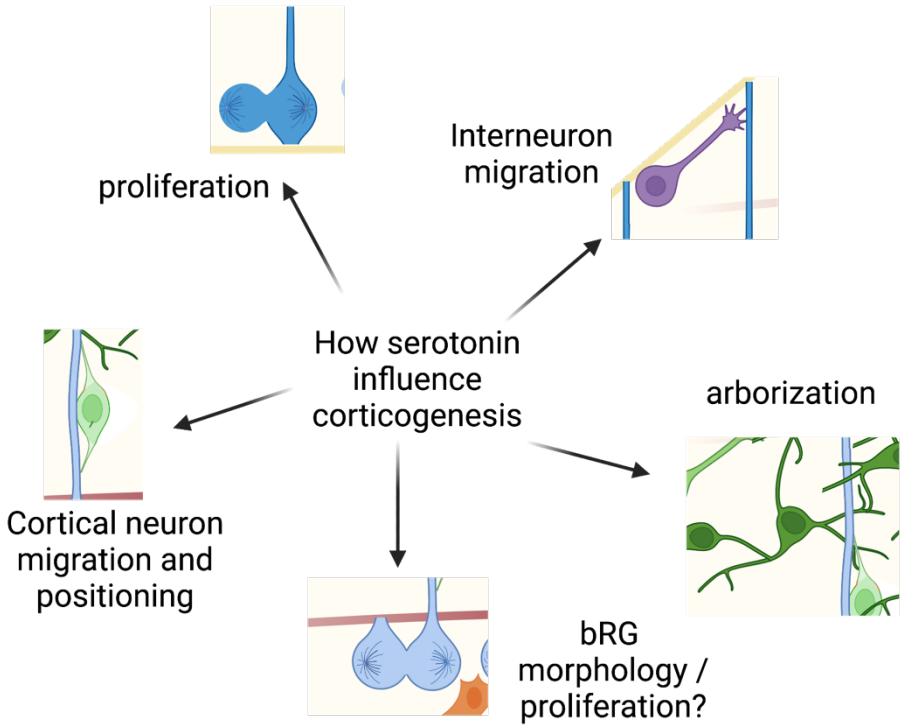

Figure 5: Schematic overview of serotonin influence on developmental processes

The development of the cortex relies on several precise steps which are described in figure 4. Numerous of those processes have been shown to be influenced by serotonin.

Bonnin and colleagues demonstrated that the maternal placenta provides serotonin before the fetal serotonergic system is developed, highlighting the importance of serotonin at early stages (Bonnin *et al.*, 2011a). From E10.5 onwards, serotonin is transported from the maternal bloodstream or synthesized directly in the placenta (Côté *et al.*, 2007; Kliman *et al.*, 2018). As the BBB is not developed yet, serotonin can enter the brain directly. The maternal source is predominant until E16.5 (Bonnin and Levitt, 2011; Bonnin *et al.*, 2011a). In line, E12.5 embryos of TPH-1 knock-out mice show a smaller brain size and a diminished number of mitotic cells in the developing cortex (Côté *et al.*, 2007). DL-P-chlorophenylalanine methyl ester hydrochloride (PCPA) inhibits TPH and by injection into pregnant dams, allows a precise depletion of serotonin during the fetal development (Vitalis *et al.*, 2007a). PCPA-treated animals support the findings of TPH1-KO mouse and display a decreased number of dividing cells in E16.5 embryos (Vitalis et al., 2007). E17.5 mouse embryos lacking MAOA and B, the enzyme responsible for the degradation of serotonin, showed a surprised decline in neuronal progenitor cells in the subventricular zone (Cheng *et al.*, 2010). The authors of the study identified that high levels of serotonin cause a reduction of symmetric divisions of intermediate progenitors (Cheng *et al.*, 2010).

Neurospheres of murine cells of the VZ and SVZ showed an increased growth upon exposure to 10 and 100 ng/ml serotonin while an excess of serotonin caused a decrease in size (Cheng *et al.*, 2010).

Serotonin is also associated with the migration and positioning of neurons as it was already shown in PCPA treated mice (Vitalis *et al.*, 2007a, 2007b). This is supported by a study focusing on the migration of interneurons derived from the caudal ganglionic eminence (Murthy *et al.*, 2014; Frazer, Otomo and Dayer, 2015). In rodents, serotonin facilitates the neuronal migration and controls the positioning of the cells via the receptor 5-HT_{3A} (Murthy *et al.*, 2014; Frazer, Otomo and Dayer, 2015). Moreover, two additional rodent studies showed that an excess of serotonin diminishes migration speed in interneurons and pyramidal neurons mediated by the 5-HT_{6A} (Riccio et al., 2009, 2011). Cajal-Retzius cells are among the first generated neurons and form the marginal zone, which gives rise to the layer I of the cortex. They release the glycoprotein reelin which has been shown to be a crucial player for neuronal migration, positioning and maturation. The release is reduced upon the activation of their 5-HT_{3A} which leads to an increased complexity of apical dendrites of cortical layer II/III pyramidal neurons (Janusonis, Gluncic and Rakic, 2004; Chameau *et al.*, 2009).

Interfering with the brain serotonin levels at later stages by knocking out TPH2, does not show gross alterations in the brain structure or brain size reduction (Migliarini *et al.*, 2013). However, more than 50% of the TPH2 KO mice do not survive the first thirty day of life and show a reduced body size (Alenina et al., 2009; Pelosi et al., 2015). Additionally, they show impaired thermoregulation, altered sleep pattern, decreased heart rate as well as behavior changes (Alenina et al., 2009).

Unfortunately, just a limited number of studies focused on the human brain development, though highlighted the role of basal radial glia cells (bRGs). Using human fetal slices, Mayer and colleagues validated the expression of 5-HT_{2A} on bRGs, which activation they associated with bRG fiber organization and morphology (Mayer *et al.*, 2019). This is supported by a second study where they observed an increase of bRG processes due to serotonin (Xing *et al.*, 2020). The latter study identifies a serotonin induced increase of bRG proliferation which is not found by the other group (Mayer *et al.*, 2019; Xing *et al.*, 2020).

The incontrovertible involvement of serotonin in the brain development makes it an interesting candidate for developmental psychiatric disorders, including attention deficit / hyperactivity disorder (ADHD) and most prominently autism spectrum disorder (ASD) (Azmitia, 2001; Quist *et al.*, 2003; Zafeiriou, Ververi and Vargiami, 2009). ASD is a very heterogeneous disease and although with a high degree of heritability, the genetic architecture is complex including rare and common variants and hundreds of reported genes (Rose'meyer, 2013; Tick *et al.*, 2016). Hyperserotonemia is present in approximately 30% of ASD patients and is determined the most often and best replicated biological manifestation in ASD (Veenstra-VanderWeele *et al.*, 2012; Pourhamzeh *et al.*, 2022). It describes

elevated serotonin levels in blood platelets in young patients and is discussed as potential biomarker (Yang *et al.*, 2015). Although it was already reported 60 years ago and validated in several studies since, the circumstances and how it contributes to the disease's onset is still not understood Abdulamir, 2018), (Schain and Freedman, 1961; Gabriele, Sacco and Persico, 2014). Conversely, additional findings point to a reduced serotonin availability in the brain (hyposerotonin) (Sato, 2013; Pourhamzeh *et al.*, 2022). Chugani and colleagues reported a decrease in brain serotonin synthesis in young ASD patients compared to their healthy siblings (Chugani *et al.*, 1999). This is further supported by a tryptophan depletion study, in which symptoms of ASD patients worsened (McDougle *et al.*, 1996). Genetic variations studies identified several genes with ASD, most prominently, the SERT encoding gene SLC6A4. The polymorphism within the promoter region of SLC6A4 (short and long variant) was subject for countless studies, however, yielded in ambiguous results with no clear association with ASD (Coutinho *et al.*, 2004; Garbarino *et al.*, 2019). Rare gene variants concerning SLC6A4 are more consistent, as they point to a gain of function and are more prevalent in ASD patients (Sutcliffe *et al.*, 2005; Muller, Anacker and Veenstra-VanderWeele, 2016). The most common rare variant Ala56 was also verified in animal models (Veenstra-VanderWeele *et al.*, 2012). Developmental abnormalities found in ASD patients like increased neuronal density and mispositioned neurons might be explainable by disturbed serotonin signaling (Boylan, Blue and Hohmann, 2007).

To further study in depth the relation between serotonin, human corticogenesis and developmental aberrations, proper model systems are missing.

1.5 Stem cells and derived organoids

Stem cells are the raw material of any developing multicellular organism and are characterized by two distinct capabilities: proliferation and differentiation. Dependent on the grade of those features, the cells are classified as toto-, pluri-, multi- and unipotent. The fertilized egg represents a totipotent state and descend to pluripotency, once the blastocyst is formed. A multipotent cell can differentiate in several, however closely related cell types and an unipotent cell can basically just give rise to one somatic cell type. Pluripotent stem cells can be isolated from embryos and cultured as embryonic stem cells (ESCs) *in vitro* (Evans and Kaufman, 1981; Thomson *et al.*, 1998). While maintained in the dish, ESCs preserve their abilities to differentiate to various different cells of all three germ layers (Watanabe et al., 2005). Moreover, due to their proliferation capacities, they offer and nearly endless supply of human material for differentiations and experiments.

The forced expression of transcription factors OCT4, KLF4, SOX2 and c-MYC overwrites the cell fate of differentiated somatic cells to a pluripotent state, which originated the term induced pluripotent stem cell (iPSC) (Takahashi and Yamanaka, 2006). Since their first discovery in 2006, a broad range of somatic

cells have been successfully reprogrammed to iPSCs including, fibroblasts, keratinocytes and peripheral blood cells (Takahashi *et al.*, 2007; Aasen and Belmonte, 2010; Staerk *et al.*, 2010). Although the pluripotency is induced, iPSCs display extensive proliferation and were shown to develop a large variety of cell types. Moreover, the iPSC technology overcomes ethical concerns associated with embryonic stem cells.

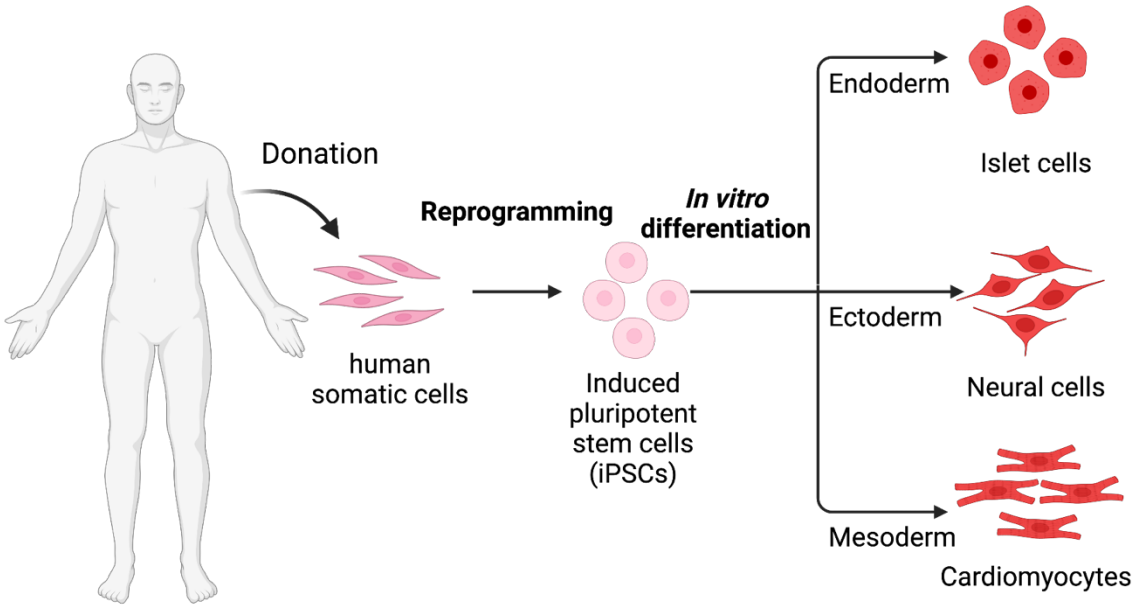

Figure 6: Schematic overview of human induced pluripotent stem cells.

Donated somatic cells, like fibroblasts, keratinocytes and peripheral blood cells can be reprogrammed by forced expression of the transcription factors OCT4, KLF4, SOX2 and c-MYC. Thus, the cells acquire a pluripotent state which gave rise to the term "induced pluripotent stem cells". Subsequently, iPSCs can be differentiated in a large variety of cell types of all three germ layers, including neural cells of the ectoderm.

The activation or inactivation of well described signaling pathways involved in the *in vivo* development allowed to differentiate PSCs to all three-germ layer, for instance the neuroectoderm (McComish and Caldwell, 2018). The inhibition of SMAD signaling, for example via the small molecules A83-01 and LDN193189 mediates a TGF-ß and BMP repression and thus blocks the differentiation towards meso- and endodermal germ layer (Chambers *et al.*, 2009). Moreover, it facilitates the neuroectodermal fate and serves as foundation for many neuronal cell type differentiations, like cortical, serotonergic and motor neurons (Dimos *et al.*, 2008; Lu *et al.*, 2016; McComish and Caldwell, 2018). Thus, iPSCs allowed modeling of the human neurodevelopment in a dish (Brennand *et al.*, 2011; Wen, 2017).

Given the retention of the donor's genetic identity during the reprogramming, the technology grants the generation of patient specific lines. Together with the advancement in gene editing methods,

allows the modelling of genetic contribution to the various diseases in a human context (Lin, Lachman and Zheng, 2016; Wen, 2017; de Masi *et al.*, 2020).

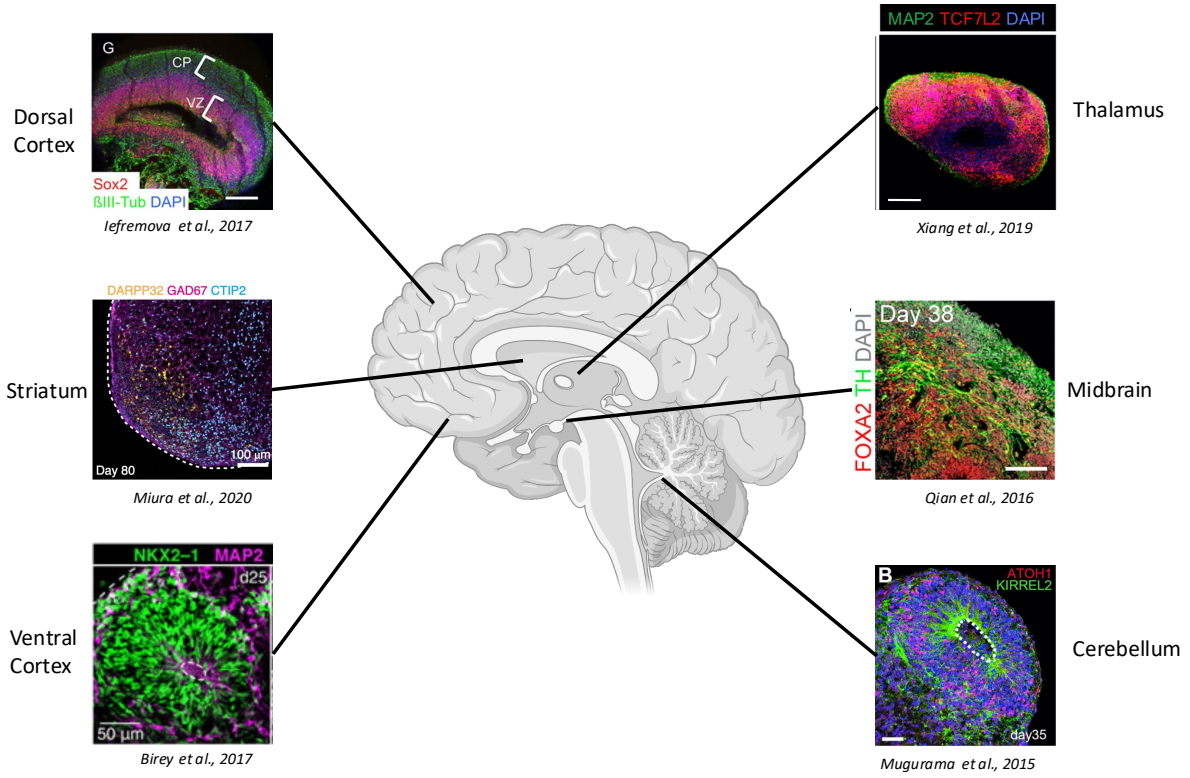

Figure 7: Schematic overview of published regional organoids

IPSCs are able to self-organize in three-dimensional structures and to recapitulate organogenesis. The so-called organoids can mimic the development of different organs including the brain's development. The application of certain morphogens even allows the precise formation of distinct brain areas, including midbrain, striatum and thalamus.

Pluripotent stem cells have demonstrated to have also other remarkable capabilities. The self-organizing to three-dimensional neuronal objects was first revealed by Eiraku and colleagues using ESCs in 2008 (Eiraku *et al.*, 2008). The so-called organoids mimic aspects of embryonic development processes and reflect certain structural or functional properties of their *in vivo* counterpart. Several approaches targeting different organs have been published, including lung, intestines and liver organogenesis (Spence *et al.*, 2011; Longmire *et al.*, 2012; Takebe *et al.*, 2013; Clevers, 2016). The term cerebral organoid was first introduced by Lancaster and colleagues when demonstrating organoids recapitulating parts of the human brain development (Lancaster *et al.*, 2013). The development of structural features like the ventricular zone, subventricular zone as well as the cortical plate could be now recapitulated *in vitro* (Lancaster *et al.*, 2013, 2017). The protocol is based on aggregating ESCs or IPSCs into spherical embryonic bodies (EBs) which are cultivated in suspension. After a neural induction, EBs are developing ventricular-like zones, which are loop-shaped structures consisting of

NES. Subsequently, the developing organoid gives rise to an apical-basal polarization and different neuronal precursor populations for instance apical and basal radial glia cells as well as intermediate progenitors which organize in the different proliferative zones (Watanabe *et al.*, 2017). The neurogenesis results in the formation of the cortical plate representing different neuronal layers (Qian *et al.*, 2020). Single cell RNA sequencing experiments found remarkable gene expression similarities between cerebral organoids and human fetal tissue (Camp *et al.*, 2015; Kelava and Lancaster, 2016). Apart of the described dorsal cortical structures, cerebral organoids develop also cell clusters representing other distinct brain areas like ventral cortex, retina and choroid plexus (Lancaster *et al.*, 2013; Quadrato *et al.*, 2017; Pașca *et al.*, 2022). In order to facilitate the development of individual specific brain regions, regionalized organoids were introduced (Tanaka and Park, 2021; Rosebrock et al., 2022; Figure 7). For this purpose, signaling pathways known to be fundamental for the regional identity of brain regions are utilized to recapitulate their development *in vitro*. For instance, the dual SMAD inhibition combined with the inhibition of WNT signaling using XAV939, allowed the generation of organoids representing dorsal cortical organoids (Huang *et al.*, 2009; Qian *et al.*, 2016; Iefremova *et al.*, 2017; Rosebrock *et al.*, 2022). Similarly, several protocols emerged targeting specific brain areas, among others midbrain, choroid plexus and cerebellum (Muguruma *et al.*, 2015; Jo *et al.*, 2016; Qian *et al.*, 2016; Pellegrini *et al.*, 2020). The brain organoid models have been broadly applied and proven to be robust and reliable (Velasco *et al.*, 2019; Yoon *et al.*, 2019).

The research field of brain organoids is still young, nevertheless it is rapidly developing and improved already our understanding of neurodevelopment and evolution (Li *et al.*, 2017; Karzbrun *et al.*, 2018; Pollen *et al.*, 2019). For instance, the use of brain organoids identified androgens as cause for differences in brain sizes between male and females (Kelava *et al.*, 2022). The comparison brain organoids of humans and great apes, allowed conclusions regarding the evolution of the human brain. Namely, in human brain organoids compared to great apes, the transition of NESs to radial glia cells is delayed, allowing an extended NES proliferation period (Benito-Kwiecinski *et al.*, 2021).

Given that brain organoids can be differentiated from PSPs of any donor, they retain disease relevant genetic alterations and thus, allows to model the disease in a three-dimensional human context. The unique structural abilities of brain organoids facilitate the modeling of malformations associated with corticogenesis (Szebényi *et al.*, 2021; Jabali *et al.*, 2022). Thus, brain organoids demonstrated various causes for micro- and macrocephaly as well as ceased gyrification (Lancaster *et al.*, 2013; Bershteyn *et al.*, 2017; Qian *et al.*, 2017; Zhang *et al.*, 2019). Moreover, the culture system proofed sensitive enough to display different disease grades rooting in LIS1 mutations (Rossetti *et al.*, 2022).

Brain organoids might be even able to answer the need for proper models for neuropsychiatric diseases (Quadrato, Brown and Arlotta, 2016; Dixon and Muotri, 2022). Specifically have brain

organoids proven valuable to foster our understanding of autism spectrum disorder (ASD). Several ASD-related genes have been associated with altered neurogenesis particularly of interneurons (Urresti *et al.*, 2021; Paulsen *et al.*, 2022).

Regionalized organoids opened the possibility to study also the distinct interaction between brain areas, which led to the introduction of assembloids (Bagley *et al.*, 2017; Andersen *et al.*, 2020; Miura *et al.*, 2020; Xiang, Cakir and Park, 2021). Specifically, organoids representing the dorsal cortex and the thalamus formed reciprocal connections when assembled, recapitulating the *in vivo* thalamocortical and corticothalamic projections (Xiang *et al.*, 2019). Assembled ventral and dorsal cortical organoids display the migration of interneurons and were capable do demonstrate deficiencies associated with timothy syndrome (Birey *et al.*, 2017). Moreover, this model system identified a distinct guidance function of serotonin on the interneuronal migration behavior (Bajaj *et al.*, 2021).

HiPSC-derived brain organoids offer the possibility to partially model the effect of serotonin on the human corticogenesis. However, this model system has been barely utilized yet. Two studies have been reported on organoids in the context of psychedelics and depression while two additional studies attempted to generate brainstem organoids (Dakic et al., 2017; Eura et al., 2020; Valiulahi et al., 2021; Wang et al., 2021).

1.6 Aim of the project

This thesis focused on the serotonergic system and its role during human corticogenesis. Published data using rodent models point to an important function of serotonin during brain development, in particular progenitor proliferation. However, many questions are left unanswered regarding the human system. Recent advancement in iPSC-technology made this topic approachable in the human context. In the first part, human iPSC-derived 2D cultures and 3D cortical organoids shall be utilized, to constitute a model for the human corticogenesis. Thus, raise the possibility to analyze the proliferative behavior of apical, intermediate and basal progenitors in response to serotonin.

Regionalized organoids helped studying various brain areas and were even utilized to mimic brain region interactions. Serotonergic neurons arise from the raphe nuclei, which have not been modeled successfully as organoid yet. Therefore, the second part of this project shall aim to do so and provide a full-characterization. This newly developed raphe organoid could then be used to model human serotonergic innervation. By fusing raphe organoids with cortical organoids, RO-CO would be achieved, which would then allow to study serotonergic innervation on human corticogenesis.

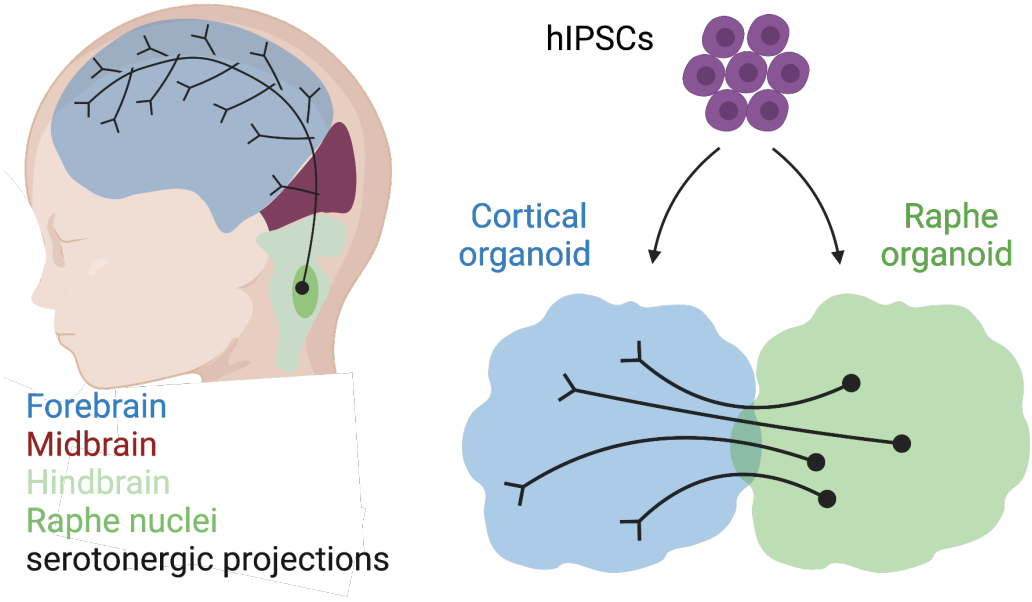

Figure 8: Schematic overview of the project aim to model serotonergic innervation on human corticogenesis

4 Materials

4.1 Cell culture

4.1.1 Cell lines

The induced pluripotent stem cell lines used in this study are listed in Table 2. All of them have been reprogrammed and fully characterized prior in the groups of Julia Ladewig or Philipp Koch.

Table 2: List of human iPSC lines used in this thesis

Cell line	Clone	Gender	Age	Origin
028	1	Female	44	Dermal fibroblasts reprogrammed using Sendai virus
028	4	Female	44	"
112	2	Female	19	"

4.1.2 Cell culture reagents

Table 3: List of commercial cell culture base media and ready-to-use supplements

Medium / Compound	Cat. number	Distributor	Headquarter
2-Mercaptoethanol	31350-010	Thermo Fisher Scientific	Waltham, USA
Advanced DMEM/F12	12634010	Thermo Fisher Scientific	Waltham, USA
Advanced MEM	12492013	Thermo Fisher Scientific	Waltham, USA
B-27 supplement	17504-044	Thermo Fisher Scientific	Waltham, USA
Bovine albumin fraction V (7.5%)	15260037	Thermo Fisher Scientific	Waltham, USA
DMEM with GlutaMAX	10566016	Thermo Fisher Scientific Thermo Fisher Scientific	Waltham, USA
DMEM/F12 with glutamine	11320033	Thermo Fisher Scientific	Waltham, USA
DMEM/F12 with glutamine and HEPES	11330057	Thermo Fisher Scientific	Waltham, USA
DNase I	10104159001	Sigma-Aldrich	Darmstadt, Germany
DPBS + $MgCl_2$ and $CaCl_2$	D8662	Sigma-Aldrich	St. Louis, USA
EDTA 0.5 M, pH 8.0 UltraPure™	15575020	Thermo Fisher Scientific	Waltham, USA
FBS	10270106	Thermo Fisher Scientific	Waltham, USA

Geltrex™, hESC-qualified	A1413302	Thermo Fisher Scientific	Waltham, USA
GlutaMAX supplement	35050038	Thermo Fisher Scientific	Waltham, USA
KnockOut™ Serum Replacement	10828028	Thermo Fisher Scientific	Waltham, USA
Laminin	23017015	Thermo Fisher Scientific	Waltham, USA
MEM-Non-essential amino acids	11140035	Thermo Fisher Scientific	Waltham, USA
Neurobasal™	21103049	Thermo Fisher Scientific	Waltham, USA
PBS	D8537-500ML	Thermo Fisher Scientific	Waltham, USA
Penicillin/Streptomycin	15140122	Thermo Fisher Scientific	Waltham, USA
Sodium pyruvate	11360039	Thermo Fisher Scientific	Waltham, USA
Trypan blue	17-942E	Lonza	Basel, Switzerland
TrypLE™ Express	12605-028	Thermo Fisher Scientific	Waltham, USA
Trypsin-EDTA (10X)	15400054	Thermo Fisher Scientific	Waltham, USA

Table 4: Small molecules and chemicals for cell culture

Compound	solvent	Cat	Company	headquarter
A83-01	DMSO	2939	Tocris	Bristol, UK
Amphotericin B	"-	15290-018	Thermo Fisher Scientific	Waltham, USA
BW 723C86	DMSO	70090	Cayman Chemical	Ann Arbor, USA
$CaCl_2$	H_2O	HN04.1	Carl Roth	Karlsruhe, Germany
CHIR99021	DMSO	SM13	Cell Guidance Systems	Cambridge, UK
Chloroquine diphosphate	H_2O	4106	Cell Guidance Systems	Cambridge, UK
CP809101	DMSO	CBS-FC64988	Biozol	Eching, Germany
D(+)-Glucose	H_2O	HN06.2	Carl Roth	Karlsruhe, Germany
DAPT	DMSO	SM15	Cell Guidance Systems	Cambridge, UK
DMSO	"-	D5879	Sigma-Aldrich	St. Louis, USA
Ethanol	°-	32205	Sigma-Aldrich	St. Louis, USA

FGF2-154	0.1 % BSA in H2O	GFH28	Cell Guidance Systems	Cambridge, UK
FGF4	0.1 % BSA in H2O	GFH31	Cell Guidance Systems	Cambridge, UK
GDNF	0.1 % BSA in H2O	GFH2	Cell Guidance Systems	Cambridge, UK
Heparin sodium salt	PBS	H3149	Sigma-Aldrich	St. Louis, USA
HEPES	H_2O	9105.4	Carl Roth	Karlsruhe, Germany
Insulin	10 mM NaOH	91077C	Sigma-Aldrich	St. Louis, USA
Ipsapirone	DMSO	22075	Cayman Chemical	Ann Arbor, USA
KCl	H_2O	A3582	Sigma-Aldrich	St. Louis, USA
Ketanserin	DMSO	B2248	ApexBio Technologies	Houston, USA
L-ascorbic acid	H_2O	A4544	Sigma-Aldrich	St. Louis, USA
L-ascorbic acid phosphate	H_2O	A8960	Sigma-Aldrich	St. Louis, USA
L-Tryptophan	H_2O	T0254-100G	Sigma-Aldrich	St. Louis, USA
LDN193189	DMSO	72148	Stemcell Technologies	Vancouver, Canada
LM22A	DMSO	SML0848-25MG	Sigma-Aldrich	St. Louis, USA
LM22B	DMSO	6037	Tocris Bioscience	Bristol, UK
$MgCl_2$	H_2O	105833	Merck Millipore	Darmstadt, Germany
NaCl	H_2O	31434	Sigma-Aldrich	St. Louis, USA
Pluronic F-127	H_2O	P2443	Sigma-Aldrich	St. Louis, USA
Poly-L-Lysine hydrobromide	H_2O	P2636	Sigma-Aldrich	St. Louis, USA
Progesterone	Ethanol	P8783	Sigma-Aldrich	St. Louis, USA
Purmorphamine	DMSO	SM30	Cell Guidance Systems	Cambridge, UK
Putrescine	H_2O	51799	Sigma-Aldrich	St. Louis, USA
S-WAY 100135	DMSO	sc-361330	Santa Cruz	Dallas, USA
SAG	H_2O	AG-CR1-3585-M005	Adipogen	San Diego, USA
SB 242084 hydrochloride	DMSO	sc-351848	Santa Cruz	Dallas, USA
Serotonin hydrochloride	H_2O	H9623	Sigma-Aldrich	St. Louis, USA
Sodium selenite	H_2O	A8960	Sigma-Aldrich	St. Louis, USA
TCB2	DMSO	2592	Tocris Bioscience	Bristol, UK
TGF-β1	0.1 % BSA in PBS	GFH39	Cell Guidance Systems	Cambridge, UK

TGF-β3	H_2O	GFH109	Cell Guidance Systems	Cambridge, UK
Transferrin	H_2O	T3705	Sigma-Aldrich	St. Louis, USA
Trypan blue	-	17-942E	Lonza	Basel, CH
XAV939	DMSO	13596	Cayman Chemical	Ann Arbor, USA
Y-27632	H_2O	SM02	Cell Guidance Systems	Cambridge, UK
γ-Aminobutyric acid (GABA)	H_2O	A5835- 337	Sigma-Aldrich	St. Louis, USA

4.1.3 Cell culture Media composition

Table 5: Self-made supplements and buffer solutions

Supplement/ buffer solution	Compound	Final concentration
D-Glucose solution	H_2O D-Glucose	 400 mg/ml
Imaging buffer	H_2O HEPES pH 7.4 NaCl KCl $CaCl_2$ $MgCl_2$ D-Glucose	 20 mM 140 mM 2.5 mM 1.8 mM 1 mM 10 mM
Low melting agarose solution	Slicing media Low melting agarose	 4% (w/v)
N2-Base	DMEM/F12 with Glutamine B27-Supplement N2-Supplement 2-Mercaptoethanol D-Glucose GlutaMAX Non-essential amino acids Pen/Strep	 1 % (v/v) 0.5 % (v/v) 50 µM 8 µg/ml 1 % (v/v) 1 % (v/v) 1 % (v/v)
N2-Supplement	DMEM/F-12 with Glutamine Insulin Progesterone Putrescine Sodium Selenite Transferrin	 0.5 %/ml 630 ng/ml 1.612 mg/ml 520 ng/ml 10 mg/ml
Pluronic coating solution	DPBS Pluronic F-127	 50 mg/ml

Table 6: Media composition

Medium	Components	Final concentration

Wash media	DMEM/F12 with GlutaMAX Pen/Strep	 1% (v/v)
Essential 8 (E8)	DMEM/F12 with glutamine and HEPES Pen/Strep LAAP Sodium selenite Insulin Transferrin FGF-2 (154) TGF–β1	 1% (v/v) 64 µg/ml 14 ng/ml 20 µg/ml 11 µg/ml 200 ng/ml 2 ng/ml
iPSC freezing medium	KnockOUT™ Serum Replacement Essential 8 DMSO Y-27632	50% (v/v) 40% (v/v) 10% (v/v) 20 µM
aPC induction medium	N2-base A83-01 LDN193189 XAV939	 500 nM 200 nM 500 nM
bPC proliferation boost medium	DMEM/F12 with glutamine Pen/Strep GlutaMAX supplement N2-supplement Non-essential amino acids Glucose 2-Mercaptoethanol FGF-2 (154)	 1% (v/v) 1% (v/v) 0.5% (v/v) 1% (v/v) 8 µg/ml 50 µM 20 ng/ml
NPC medium, phase 1	Advanced DMEM/F12 Pen/Strep GlutaMAX supplement B-27 supplement SB431542 LDN193189 XAV939	 1% (v/v) 1% (v/v) 1% (v/v) 10 µM 1 µM 2 µM
NPC medium, phase 2	Advanced DMEM/F12 Pen/Strep GlutaMAX supplement B-27 supplement LDN193189 XAV939	 1% (v/v) 1% (v/v) 1% (v/v) 200 nM 2 µM
Neuronal differentiation medium, phase 1	DMEM/F12 with glutamine Pen/Strep GlutaMAX supplement N2-supplement	 1% (v/v) 1% (v/v) 0.5% (v/v)

	B-27 supplement	1% (v/v)
	NEAA	1% (v/v)
	Glucose	1.6 mg/ml
	$CaCl_2$	1.8 mM
	Ascorbic acid	200 µM
	LM22A	1µM
	LM22B	1µM
	PD-0332991	2µM
	DAPT	5 µM
Neuronal differentiation medium, phase 2	Neurobasal™	
	Pen/Strep	1% (v/v)
	GlutaMAX supplement	1% (v/v)
	B-27 supplement	2% (v/v)
	Glucose	5 mg/ml
	Ascorbic acid	200 µM
	LM22A	1µM
	LM22B	1µM
	PD-0332991	2µM
	DAPT	5 µM
	CHIR99021	3 µM
	Forskolin	10 µM
	GABA	300 µM
Neuronal differentiation medium, phase 3	Neurobasal™	
	Pen/Strep	1% (v/v)
	GlutaMAX supplement	1% (v/v)
	B-27 supplement	2% (v/v)
	Glucose	5 mg/ml
	Ascorbic acid	200 µM
	LM22A	1µM
	LM22B	1µM
	PD-0332991	2µM
	CHIR99021	3 µM
Neuronal differentiation medium, phase 4	Neurobasal™	
	Pen/Strep	1% (v/v)
	GlutaMAX supplement	1% (v/v)
	B-27 supplement	2% (v/v)
	Glucose	5 mg/ml
	Ascorbic acid	200 µM
	LM22A	1µM
	LM22B	1µM
	PD-0332991	2µM
Cortical induction medium	N2-base	
	A83-01	500 nM
	LDN193189	200 nM
	XAV939	500 nM

	KnockOut™ Serum Replacement Heparin	2 % (v/v)
Cortical differentiation medium	N2-base KnockOut™ Serum Replacement Insulin	 2% (v/v) 2.5 µg/ml
Cortical maturation medium	N2-Base L-Ascorbic Acid GDNF Geltrex™ Insulin LM22A LM22B	 200 µM 10 ng/ml 30 µg/ml 2.5 µg/ml 1 µM 1 µM
Caudalization medium	N2-Base FGF2-154 Insulin A83-01 LDN	 50 ng/ml 7 µg/ml 500 nM 200 nM
Ventralization medium	N2-Base FGF2-154 Insulin A83-01 LDN Purmorphamine SAG	 50 ng/ml 7µg/ml 500 nM 200 nM 125 nM 250 nM
Specification medium	N2-Base A83-01 LDN Purmorphamine SAG FGF-4	 500 nM 200 nM 125 nM 250 nM 10 ng/ml
RO maturation medium	Neurobasal™ N2 Supplement B27 Supplement GlutaMAX Pen/Strep 2-Mercaptoethanol Glucose TGF-ß3 Insulin L-Ascorbic acid L-Tryptophan GDNF LM22A	 0.5% (v/v) 1% (v/v) 1% (v/v) 1% (v/v) 50 µM 8 µg/ml 1 ng/ml 2.5 µg/ml 200 µM 100 µM 10 ng/ml 1 µM

	LM22B DAPT	1 µM 2.5 µM
Functionality boost medium	Advanced MEM N2 Supplement B27 Supplement GlutaMAX Pen/Strep 2-Mercaptoethanol Glucose Insulin L-Ascorbic acid L-Tryptophan GDNF LM22A LM22B	 0.5% (v/v) 2% (v/v) 1% (v/v) 1% (v/v) 50 µM 8 µg/ml 2.5 µg/ml 200 µM 100 µM 10 ng/ml 1 µM 1 µM
HEK-293T medium	DMEM/F12 with GlutaMAX Non-essential amino acids Sodium pyruvate FBS	 1% (v/v) 1% (v/v) 10% (v/v)
Slicing media	DMEM/F12 with GlutaMAX Pen/Strep HEPES **Amphotericin B**	 1% (v/v) 15 mM 250 ng/ml

Selective serotonin receptor agonists and antagonists are listed in Table 7. To guarantee full receptor activation or inhibition without causing of target effects, concentrations were based on reported EC and IC50 values. Final concentrations were calculated by multiplying EC50 values with 20 and IC50 with 40 for agonists and antagonists respectively.

Table 7: List of selective serotonin receptor agonist and antagonists

Substance	EC or IC 50	Reference	Final concentration
BW723C86	18 nM	Kelly and Sharif, 2006	360 nM
CP 809101 hydrochloride	0.11 nM	Manufacturer	2.2 nM
Ipsapirone	56 nM	Schoeffter and Hoyer, 1988	1.12 µM
Ketanserin	6.3 nM	Manufacturer	252 nM
SB 242084 hydrochloride	0.28 nM	Eshleman et al., 2013	11.2 nM
TCB2	36 nM	Manufacturer	720 nM

1.1. Molecular biology

Table 8: List of reagents and chemicals used for molecular biology

Reagent	Cat. number	Distributor	Headquarter
100 bp marker, Quick-Load®	N0467S	New England Biolabs	Ipswich, USA
2-Propanol	1157	Th. Geyer	Renningen, Germany
50% Polyethylene glycol (PEG) - 6000 solution	101443-484	VWR	Radnor, USA
Acetic acid	33209	Sigma-Aldrich	St. Louis, USA
Ampicillin	A9518	Sigma-Aldrich	St. Louis, USA
Bacto-Tryptone	211705	BD Biosciences	Franklin Lakes, USA
Bovine serum albumin (BSA)	A3294	Sigma-Aldrich	St. Louis, USA
Bromophenol blue	B-8026	Sigma-Aldrich	St. Louis, USA
Chloroform	32211	Sigma-Aldrich	St. Louis, USA
DABCO	0718.2	Carl Roth	Karlsruhe, Germany
DAPI	422801	Biolegend	San Diego, USA
DEPC	K028.1	Carl Roth	Karlsruhe, Germany
DMSO	D5879	Sigma-Aldrich	St. Louis, USA
dNTPs	SL-Set-L-dNTPs	Steinbrenner	Wiesenbach, Germany Laborsysteme
Glycerol	15523	Sigma-Aldrich	St. Louis, USA
Glycine	10070150	Thermo Fisher Scientific	Waltham, USA
GoTaq® DNA Polymerase	M780B	Promega	Madison, USA
HEPES buffered saline (2x HBSS)	S0874	Takara Bio	Tokyo, Japan
KCl	1632	Th. Geyer	Renningen, Germany
KH_2PO_4	1648	Th. Geyer	Renningen, Germany
LB medium powder	X968.4	Carl Roth	Karlsruhe, Germany
Low melting agarose	6351.5	Carl Roth	Karlsruhe, Germany
Methanol	0082.1	Carl Roth	Karlsruhe, Germany
$MgCl_2$	A351B	Promega	Madison, USA
$MgSO_4$	105886	Merck Millipore	Darmstadt, Germany
Mowiol 4-88	81381	Sigma-Aldrich	St. Louis, USA
Na_2HPO_4	8622	Th. Geyer	Renningen, Germany
NaCl	1367	Th. Geyer	Renningen, Germany
Paraformaldehyde (PFA)	P6148	Sigma-Aldrich	St. Louis, USA
PCR Reaction buffer	331610	Biozym	Hessisch Oldendorf, Germany
peqGREEN DNA/RNA binding dye	peql37-5010	VWR	Radnor, USA

Polybrene Infection Reagent	TR-1003-G	Merck Millipore	Darmstadt, Germany
Reaction buffer	M890A	Promega	Madison, USA
Rori®-Liquid Barrier Marker	AN92.1	Carl Roth	Karlsruhe, Germany
RNA-Solv reagent	R6830-02	VWR	Radnor, USA
RNase AWAY	10666421	Thermo Fisher Scientific (Waltham, USA)	Waltham, USA
ROX	A351513	GENAXXON	Ulm, Germany
SDS, pellets	CN30.1	Carl Roth	Karlsruhe, Germany
Sodium hydroxide, pellets	6771.2	Carl Roth	Karlsruhe, Germany
Sucrose	S9378	Sigma-Aldrich	St. Louis, USA
Syber® Green I	S9430	Sigma-Aldrich	St. Louis, USA
Taq DNA Polymerase	331610	Biozym	Hessisch Oldendorf, Germany
Tissue-Tek O.C.T.™ Compound	4583	Sakura Finetek	Torrance, USA
TriFastTM, peqGOLD	30-2010,	VWR	Radnor, USA
Tris-HCl pH 8.5	4855.5	Carl Roth	Karlsruhe, Germany
Triton X-100	1.08603.1000	Merck Millipore	Darmstadt, Germany
Yeast Extract	212750	BD Biosciences	Franklin Lakes, USA

1.1.1. Bacteria

Amplification of plasmid DNA was performed in *Escherichia coli* DH5a purchased from New England Biolabs, USA (Cat. # C2987H).

Table 9: Bacteria cultivation media

Name	Compound	Final concentration
LB medium	LB medium powder Ampicillin	20% (w/v) 100 µg/ml
SOC medium	Bacto-Tryptone Yeast Extract NaCl KCl MgCl2 MgSO4 Glucose	2% (w/v) 0.5% (w/v) 10 mM 2.5 mM 10 mM 10 mM 200 mM

1.1.2. Plasmids

Table 10: List of plasmids

Plasmid	Cat. Number	Source	Headquater

psPAX2	12260	Addgene	Watertown, USA
pMD2.G	12259	Addgene	Watertown, USA
pLVX-EF1α-sDarken	gift	Massek Lab, University of Bremen	Bremen, Germany

1.1.3. PCR components

All primers were purchased from Integrated DNA Technologies, Inc., Coralville, USA and were reconstituted in nuclease free H_2O to a concentration of 100 µM by incubating 30 min at 37°C and 400 rpm.

Table 11: List of primers used in PCR and qPCR experiments

Primer name	Sequence (5'-3')
18S rRNA-for	AAACGGCTACCACATCCAAG
18S rRNA-rev	CCTCCAATGGATCCTCGTTA
EN1-for	GACTCGCAGCAGCCTCTC
EN1-rev	GCCTGGAACTCCGCCTTG
HOXA2-for	TTCAGCAAAATGCCCTCTCT
HOXA2-rev	TAGGCCAGCTCCACAGTTCT
HOXA3-for	CCAGAATCGCCGCATGAAGTACAA
HOXA3-rev	GGGCTCATACGGGACGCTGTTGA
HOXA4-for	TGTCAGCGCCGTTAACCC
HOXA4-rev	AGACAAACAGAGCGTGTGGG
HTR2A-for	TTGGGCTACAGGACGATT
HTR2A-rev	GAAGAAAGGGCACCACATC
HTR2C-for	GGAGCGAAAAGAGCCAAACC
HTR2C-rev	AGCTGATAACCCACTAGCGTC
GBX2-for	CAGGCTTCGCTCGTCGG
GBX2-rev	AGCTGTAGTCCACATCGCTC
NKX2.2-for	TGCCTCTCCTTCTGAACCTTGG
NKX2.2-rev	GCGAAATCTGCCACCAGTTG
FOXA2-for	CCACCACCAACCCCACAAAATG
FOXA2-rev	TGCAACACCGTCTCCCCAAAGT
Mycoplasma-for	GGGAGCAAACAGGATTAGATACCCT
Mycoplasma-rev	TGCACCATCTGTCACTCTGTTAACCTC

Table 12: Reaction mix for RT-PCR & qPCR

Mix	Component	Final concentration
RT-PCR reaction mix	PCR reaction buffer	1X
	dNTPs	200 µM each
	Primers	400 nM each
	Taq DNA Polymerase	0.625 U
	cDNA / genomic DNA	10 ng / 200 ng

	DMSO (for genomic DNA only)	1% (v/v)
RT-qPCR reaction mix	qPCR reaction buffer $MgCl_2$ dNTPs Primers DMSO Syber® Green I ROX GoTaq® DNA Polyermase cDNA	1x 2.5 mM 200 µM each 200 nM each 4% (v/v) 1X 25 nM 0.75 U 10 ng
iScript™ reaction mix	Nuclease free water 5 x iScript™ reaction mix iScript™ reverse transcriptase RNA template	To 20 µl 4 µl 1 µl Variable (500 ng)

1.1.4. Antibodies

Primary antibodies are listed in Table 13 and were diluted in DPBS with 10 % BSA and the respective Triton X-100 concentration to achieve permeabilization. Secondary antibodies are listed in Table 14 and were diluted accordingly to the used corresponding primary antibody.

Table 13: List of primary antibodies

Antigen	Host	Dilution	Triton X-100 concentration	Cat. #	Distributor	Headquarter
cFOS	rabbit	1:300	0.5 %	2250S	Cell Signaling Technology	Cambridge, UK
CHAT	goat	1:300	0.5 %	ab254118	Abcam	Cambridge, UK
EMX1	rabbit	1:50	0.5 %	HPA006421	Atlas Antibodies	Bromma, Sweden
FOXA2	goat	1:500	0.5 %	AF2400	R&D Systems	Minneapolis, USA
GAD65	mouse	1:500	0.1 %	844502	Biolegend	San Diego, USA
HOMER	guinea pig	1:400	-	160004	Synaptic Systems	Göttingen, Germany
HOXA2	rabbit	1:100	0.5 %	PA5-67492	Thermo Fisher Scientific	Waltham, USA
HOXB2	mouse	1:50	0.5 %	PCRP-HOXB2-1F2	Developmental studies Hybridoma Bank	Iowa City, USA
5-HT_{2A}	mouse	1:2500	-	sc-166775	Santa Cruz	Dallas, USA
5-HT_{2C}	mouse	1:1000	-	sc-17797	Santa Cruz	Dallas, USA

HuC/D	mouse	1:500	0.1 %	A-21271	Thermo Fisher Scientific	Waltham, USA
ITGB5	mouse		-	sc-398214	Santa Cruz	Dallas, USA
KI67	rabbit	1:500	0.5 %	9129S	Cell Signaling Technology	Cambridge, UK
LMX1	rabbit	1:500	0.5 %	AB10533	Merck	Darmstadt, Germany
MAP2	chicken	1:2500	0.1 %	822501	Biolegend	San Diego, USA
Nestin	mouse	1:500	0.1 %	MAB1259	R&D Systems	Minneapolis, USA
NKX2.2	mouse	1:250	0.5 %	74.5A5	Developmental studies Hybridoma Bank	Iowa City, USA
NKX6.1	rabbit	1:500	0.5 %	HPA036774	Atlas Antibodies	Bromma, Sweden
OLIG2	goat	1:500	0.5 %	sc-19969	Santa Cruz	Dallas, USA
OTX2	goat	1:500	0.5 %	AF1979	R&D Systems	Minneapolis, USA
PAX6	rabbit	1:500	0.5 %	901301	Biolegend	San Diego, USA
pH3	mouse	1:2000	0.5 %	9706S	Cell Signaling Technology	Danvers, USA
PHOX2B	rabbit	1:500	0.5 %	HPA074325	R&D Systems	Minneapolis, USA
PSD95	mouse	1:200	0.1 %	810401	Biolegend	San Diego, USA
PTPRZ1	rabbit	1:2500	-	HPA015103	Atlas Antibodies	Bromma, Sweden
SATB2	mouse	1:500	0.5 %	ab51502	Abcam	Cambridge, UK
Serotonin	goat	1:1000	0.1 %	AB66047	Abcam	Cambridge, UK
Serotonin	rabbit	1:10000	0.1 %	S5545	R&D Systems	Minneapolis, USA
SOX2	rabbit	1:500	0.5 %	3579	Cell Signaling Technology	Danvers, USA
SOX2	mouse	1:500	0.5 %	Sc-365823	Santa Cruz	Dallas, USA
Synapsin I/II/III	mouse	1:500	0.1 %	853701	Biolegend	San Diego, USA
TAU	guinea pig	1:1000	0.1 %	314004	Synaptic Systems	Göttingen, Germany
TBR1	rabbit	1:500	0.5 %	ab31940	Abcam	Cambridge, UK

TBR2	rabbit	1:500	0.5 %	ab23345	Abcam	Cambridge, UK
TH	mouse	1:500	0.1 %	818002	Biolegend	San Diego, USA
TPH2	rabbit	1:500	0.1 %	NB100-74555	Novus USA Biologicals	Centennial, USA
TUBB3	mouse	1:2000	0.1 %	801202	Biolegend	San Diego, USA
VGLUT1	guinea pig	1:200	0.1 %	135304	Synaptic Systems	Göttingen, Germany
VMAT2	rabbit	1:500	0.1 %	138302	Synaptic Systems	Göttingen, Germany

Table 14: List of secondary antibodies

Antigen	Host species	Concentration	Cat. #	Distributor	Headquarter
anti-chicken IgY Alexa Fluor-488	goat	1:1000	A11039	Thermo Fisher Scientific	Waltham, USA
anti-goat IgG Alexa Fluor 555	donkey	1:1000	A21432	Thermo Fisher Scientific	Waltham, USA
anti-guinea pig IgG Alexa Fluor 647	donkey	1:1000	A21450	Thermo Fisher Scientific	Waltham, USA
anti-mouse igG Alexa Fluor 488	donkey	1:1000	A21202	Thermo Fisher Scientific	Waltham, USA
anti-mouse IgG Alexa Fluor-488	goat	1:1000	A11001	Thermo Fisher Scientific	Waltham, USA
anti-mouse IgG Alexa Fluor-568	goat	1:1000	A11004	Thermo Fisher Scientific	Waltham, USA
anti-mouse IgG Alexa Fluor-647	goat	1:1000	A21236	Thermo Fisher Scientific	Waltham, USA
anti-rabbit IgG Alexa Fluor-488	goat	1:1000	A11008	Thermo Fisher Scientific	Waltham, USA
anti-rabbit IgG Alexa Fluor-555	goat	1:1000	A21428	Thermo Fisher Scientific	Waltham, USA
anti-rabbit igG Alexa Fluor 488	donkey	1:1000	A21206	Thermo Fisher Scientific	Waltham, USA

1.1.5. Buffers

Table 15: List of buffers and solutions

Buffer / Solution	Component	Final concentration
1 X PBS	H_2O NaCl	 137 mM

	KCl Na_2HPO_4 KH_2PO_4	2.7 mM 10 mM 1.8 mM
10 X DNA loading buffer	H_2O Tris-HCl pH 7.6 Glycerol Bromophenol blue	 50 mM 60% (v/v) 0.25% (w/v)
4% PFA solution	PBS PFA adjusted pH to 7.2	 4% (w/v)
DAPI staining solution	PBS DAPI	 300 nM
DEPC-H_2O	H_2O DEPC	 0.1% (v/v)
DNA isolation lysis buffer	Tris-HCl, pH 8.5 EDTA SDS NaCl	100 mM 5 mM 0.2% (w/v) 200 mM
Embedding solution	PBS Sucrose Gelatine	 10% (w/v) 7.5% (w/v)
Mounting solution	H_2O Tris-HCl pH 8.5 Glycerol Mowiol 4-88 DABCO	 100 mM 25% (v/v) 10% (w/v) 0.6% (w/v)
Sucrose solution	PBS Sucrose	 30% (w/v)
TAE (1X)	H_2O Tris, pH 8.0 EDTA Acetic acid	 40 mM 20 mM 1 mM
Triton X-100 stock solution	PBS Triton X-100	 10% (v/v)

1.1.6. Kits

Table 16: List of commercial kits

Kit	Cat. number	Distributor	Headquarter
ExtractMe® Genomic DNA Kit	EM13-050	BLIRT S.A.	Gdańsk, Poland
iScript™ cDNA synthesis kit	17088991BUN	Bio-Rad Laboratories	Hercules, USA
peqGOLD Gel extraction kit	12-2501-01	VWR	Radnor, USA
peqGOLD Plasmid miniprep kit	732-2780	VWR	Radnor, USA

PureLink™ HiPure Plasmid Filter Midiprep Kit	K210015	Thermo Fisher Scientific	Waltham, USA
Qubit RNA BR Assay-Kit	Q10210	Thermo Fisher Scientific	Waltham, USA
RNA 6000 Nano kit	5067-1511	Agilent Technologies	Santa Clara, USA

1.2. Consumables

Table 17: List of consumables used in cell culture and molecular biology

Consumable	Cat #	Manufacturer	Headquarter
24-well plate, TC Cell+	833.3923.300	Sarstedt	Nümbrecht, Germany
3.5 cm dish with polymer coverslip bottom	81156	ibidi	Gräfelfing, Germany
3.5 cm O dish, standard	83,39	Sarstedt	Nümbrecht, Germany
6 cm dish	833.901.300	Sarstedt	Nümbrecht, Germany
6-well plate, standard	833.920.005	Sarstedt	Nümbrecht, Germany
96-well plate, U-bottom	83.3925.500	Sarstedt	Nümbrecht, Germany
Bottle top filter, 500 ml	15983307	Thermo Fisher	Waltham, USA
Cell scraper, Ultra Cruz	sc-395251	Santa Cruz	Dallas, USA
Cover slips, 12 mm	631-1579	VWR	Radnor, USA
Cryotubes, conical bottom, 1 ml	123280	Greiner Bio-One	Frickenhausen, Germany
Cell culture inserts	PICM02050	Merck	Darmstadt, Germany
Microscope slides, glass	H868.1	Carl Roth	Karlsruhe, Germany
Pasteur pipette	7691061	Th. Geyer	Renningen, Germany
PCR strip tubes, 0.2 ml	710971	Biozym	Hessisch Oldendorf, Germany
Petri dish, 10 cm O	633180	Greiner Bio-One	Frickenhausen, Germany
Pipette tips, 10 µl	70,113	Sarstedt	Nümbrecht, Germany
Pipette tips, 1250 µl	701,186	Sarstedt	Nümbrecht, Germany
Pipette tips, 200 µl	70.760.002	Sarstedt	Nümbrecht, Germany
qPCR plate seal	4ti-0500	Steinbrenner Laborsysteme	Wiesenbach, Germany
qPCR plate, 96-well	4ti-0910/C	Steinbrenner Laborsysteme	Wiesenbach, Germany
Reaction tube, 0.2 ml	73.737.002	Sarstedt	Nümbrecht, Germany
Reaction tube, 0.5 ml	72,699	Sarstedt	Nümbrecht, Germany
Reaction tube, 1.5 ml	72.690.001	Sarstedt	Nümbrecht, Germany
Reaction tube, 2 ml	72.695.200	Sarstedt	Nümbrecht, Germany
Screw cap tube, 15 ml	62.554.502	Sarstedt	Nümbrecht, Germany
Screw cap tube, 50 ml	62.547.254	Sarstedt	Nümbrecht, Germany
Serological pipettes, 10 ml	861.254.001	Sarstedt	Nümbrecht, Germany

Serological pipettes, 25 ml	861.685.001	Sarstedt	Nümbrecht, Germany
Serological pipettes, 5 ml	861.253.001	Sarstedt	Nümbrecht, Germany
Serological pipettes, 50 ml	7695555	Th. Geyer	Renningen, Germany
Syringe 50 ml	946.077.137	Sarstedt	Nümbrecht, Germany
Syringe filter, 0.2 µm	831.826.001	Sarstedt	Nümbrecht, Germany
Syringe filter, 0.4 µm	SLHV033R	Merck Millipore	Darmstadt, Germany

1.3. Technical Equipment

Table 18: List of technical equipment

Appliance	**Name**	**Manufacturer**	**Headquarter**
Automated Cell Counter	Luna ™	Logos Biosystems	Anyang, South Korea
Block Heater	Thermomixer comfort	Eppendorf	Hamburg, Germany
Centrifuge	Z 366	Hermle	Gosheim, Germany
Centrifuge	5415 D	Eppendorf	Hamburg, Germany
Centrifuge (cooled)	Z216MK	Hermle	Gosheim, Germany
Centrifuge (plate)	5810	Eppendorf	Hamburg, Germany
Centrifuge	C1301-230V	Corning	Corning, USA
Cryostat	NX50	Cryostar	Hésingue, France
Electrophoresis RNA quality control	Bioanalyzer 2100	Agilent Technologies	Santa Clara, USA
Freezer -150°C	VIP plus	Hermle	Gosheim, Germany
Freezer -80°C	UF V 700	Hermle	Gosheim, Germany
Freezing container	Mr. Frosty ™	Thermo Fisher Scientific	Waltham, USA
Imaging system	GelStick Touch	iNTAS Science Imaging Instruments	Göttingen, Germany
Incubator	HERAcell 150i	Thermo Fisher Scientific	Waltham, USA
	C170 E3	Binder	Tuttlingen, Germany
Micro-Spectrophotometer	Nanodrop ®	Thermo Fisher	Waltham, USA
Microscope, brightfield	DMIL LED	Leica	Wetzlar, Germany
Microscope, confocal	TCS SP5 II	Leica	Wetzlar, Germany
Microscope, epifluorescence	DM6 B	Leica	Wetzlar, Germany
Microscope, live cell imaging	Celldiscoverer 7	Carl Zeiss	Oberkochen, Germany
Shaker	Celltron	Infors HT	Bottmingen, Swiss
PCR cycler	PTC-200	Bio-Rad Laboratories	Hercules, USA
pH-meter	pH 597	WTW	Weilheim in Oberbayern, Germany
Pipette-boy	Pipet Filler S1	Thermo Fisher	Waltham, USA

qPCR cycler	QuantStudio 7 Flex	Thermo Fisher	Waltham, USA
RNA quantification	Qubit 4 Fluorometer	Thermo Fisher	Waltham, USA
Sterile laminar flow hood	NU-540 Class II Type A2	Nuaire	Plymouth, USA
	Biosafety Cabinet Scanlaf Mars	Labogene	Lillerod, Denmark
Syringe pump	KDS 100 Legacy	KD Scientific	Holliston, USA
Tissue-Tek Cryomold, 10x10 mm	4565	Sakura Finetek	Torrance, USA
Tissue-Tek Cryomold, 25x20mm	4557	Sakura Finetek	Torrance, USA
Vacuum pump	FTA-1	Thermo Fisher	Waltham, USA
Vibratome	VT1000S	Lecia	Wetzlar, Germany
Water conditioner	Milli-Q Q-POD	EMD Millipore	Burlington, USA
Water purifier	Milli-Q® Integral 5	Merck KGaA	Darmstadt, Germany

1.4. Data processing & Software

Table 19: List of software solutions and digital resources

Software	Supplier	Headquarter
ApE - A plasmid editor	M. Wayne Davis	-
Biorender.com	Biorender	Toronto, Canada
Cellprofiler	Broad Institute	Boston, USA
ImageJ (FIJI)	NIH	Rockville, USA
Leica Application Suite AF	Leica	Wetzlar, Germany
Leica Application Suite X	Leica	Wetzlar, Germany
Mendeley reference manager	Mendeley Ltd.	London, UK
Office 2019	Microsoft	Redmond, USA
Prism5	Graph Pad Software	San Diego, USA
QuantStudio qPCR software	Thermo Fisher Scientific	Waltham, USA
Rstudio	Rstudio	Boston, USA
ZEN	Carl Zeiss	Oberkochen, Germany

5 Methods

5.1 Cell culture

All cultures were kept in a humidified incubator at 37 °C and an atmosphere of ambivalent O2 and 5% CO2. The cultures and medias were handled under sterile conditions. The media and buffers mentioned in the chapter can be found in Table 3, Table 5 and Table 6.

5.1.1 Maintenance of human induced pluripotent stem cells (hiPSCs)

The hiPSC lines used in this study can be found in Table 2. The cultures were maintained in daily renewed E8 media on 6-well plates which have been coated overnight at 4°C with Geltrex™ diluted 1:100 in wash media. Geltrex™-coating was re-used up to four times. Once the colonies reached a confluency above 70 %, the cultures were passaged using 500 µM EDTA diluted in DPBS. EDTA weakens cell-cell interactions and the attachment to the plate by removing bivalent CA^{2+} and Mg^{2+} ions. The cultures were washed twice and subsequently incubated with the EDTA solution for 3-5 min at room temperature. After removing the EDTA solution, the colonies were carefully harvested in E8 supplemented with 5 µM Y-27632 ROCK inhibitor and transferred to a new Geltrex™-coated plate in a 1:6-20 ratio. The ROCK inhibitor was removed on the following day.

In order to cryopreserve hiPSCs, nearly confluent cultures were incubated with TrypLE for 4-5 min at 37 °C. The cells were collected in wash media and spun down at 800 x g for 4 min. After removing the supernatant, the pellet was resuspended in 200 µl Cytobuffer and 300 µl KOSR and transferred to a cryovial. A mixture of 100 µl DMSO and 400 µl KOSR were then dropwise added and mixed by carefully inverting the vial. The cells underwent a gradual freezing to -80°C in a Mr. Frosty™ freezing container and were then transferred to -150°C.

Cryopreserved hiPSCs were quickly thawed at 37°C and transferred to a screw cap tube with 10 ml of wash media before pelleting at 800 x g for 4 min. The cells were resuspended in E8 complete supplemented with 10 µM Y-27632 and plated on a Geltrex™-coated plate.

5.1.2 Differentiation and treatment of apical neural progenitor cells derived from hiPSCs

In order to achieve a neural fate, the mesodermal and endodermal lineage was blocked by inhibiting BMP and TGF-ß signaling, using the dual-SMAD inhibition approach (Chambers *et al.*, 2009). Therefore, the media of a confluent well is changed to neural induction media and refreshed daily. For expanding the cultures, cells were split every 3-5 days in a ratio of 1:1,5 to 1:2: By incubating the cells for 4-5 min with TrypLE at 37°C the cells were detached and collected in 4-fold volume of wash media before spun

down at 1000 x g for 4 min. After resuspending the cells in aPC induction media supplemented with 5 µM ROCK inhibitor, cells were plated on Geltrex™-coated 6-well plates. The dorsal forebrain progenitor identity is achieved after 10 days of patterning.

For following immunofluorescent stainings or treatments, aPCs were detached using TrypLE, palleted and cell number was determined using trypan blue and an automated cell counter (Luna™). 250,000 cells were seeded per coverslip in apical induction medium supplemented with 5 µM Y-27632. Prior to coating, coverslips were pre-treated with 37% hydrochloric acid for 1-2 hours at RT with gentle shaking. After multiple washing steps with H_2O and ethanol coverslips were air-dried and autoclaved. Finally, coverslips have been coated overnight at 4°C with Geltrex™ diluted 1:100 in wash media.

ROCK inhibitor was removed from the media the following day, before initiating treatment the day after. The concentrations of the used substances are listed in Table 7. In co-treatment condition with serotonin and an inhibitor, the latter was applied 30 min prior adding serotonin to the cultures. The media and the treatments were renewed every day. After three days of treatment, cells were harvested, washed with PBS and fixed with 4 % PFA for 10 minutes.

5.1.3 Generation of cortical neurons

First, iPSCs were subject for neural induction, therefore cells were exposed with NPC medium phase 1 for 8 days with a 1:2 split after 4 days. On day 8, cells were split again and were cultivated for another 8 days in NPC medium phase 2. On day 16, cells were passaged using TrypLE as described above. The differentiation protocol for the generation of cortical neurons was based on previously published work by others (Kemp et al., 2016; Telezhkin et al., 2016). Thereby, neuronal differentiation is initiated by inhibition of Notch signaling and forced cell-cycle exit in the presence of elevated Ca^{2+} levels. Activation of TrkB and Wnt signaling at later stages of the protocol enhances synaptogenesis and network formation. At day zero, cortical precursors were detached using TrypLE, pelleted and counted using Trypan blue. One million cells were seeded per Geltrex™-coated 3.5 cm dish with polymer coverslip bottom in neuronal differentiation medium phase 1 supplemented with 5 µM Y-27632 which was removed the day after. On day 3, media was switched to neuronal differentiation medium phase 2. On day 10, medium was changed to neuronal differentiation medium phase 3 and from day 17 cells were cultured in neuronal differentiation medium phase 4.

5.1.4 Generation of basal radial glia cells

The differentiation of basal progenitors was developed and performed by Ammar Jabali, Andrea Rossetti and Annasara Artioli of the group of Julia Ladewig. Briefly, iPSCs were differentiated to apical progenitor cells using apical progenitor induction media as described above. Resulting aPCs were

subject for neuronal differentiation during a period of five weeks in N2 base media. Next, proliferation boost media was applied for a period of four weeks. The included mitogen FGF2 enhances the residing proliferative capacities in the culture. Resulting bPCs expanded over time until subsequently homogenous population emerged.

In order to initiate a treatment, cells were detached, counted and seeded on coverslips as described before. The following day, ROCK inhibitor and FGF2 were removed before treatment conditions were applied the day after. Concentrations of used substances are listed in Table 7. Samples were treated and fixed as reported above.

5.1.5 Generation and treatment of cortical organoids

The cortical organoid differentiation protocol was published by the group of Julia Ladewig and was slightly adapted (Iefremova *et al.*, 2017; Krefft *et al.*, 2018; Jabali *et al.*, 2022).

HiPSC cultures were singularized prior reaching >90% confluency and counted as described above. Depending on the cell line, 6,000 to 9,000 cells were then seeded in 150 µl E8 complete supplemented with 50 µM ROCK inhibitor per well of a 96-well plate. In order to foster the aggregation of the cells and to prevent the attachment to the well, U-bottom type wells were used which have been treated with Pluronic coating solution for 20 min at room temperature.

ROCK inhibitor was removed and E8 media was renewed on day 2 and day 4. To achieve a dorsal cortical identity, the formed embryonic bodies were exposed to cortical induction media which contains the dual SMAD inhibitors LDN, A83 as well as the Wnt-antagonist XAV939. This media was renewed every other day. On day 10, the EBs were embedded in a Geltrex™-cortical induction medium solution (2:1 ratio) to foster the structural development. Therefore, up to 18 EBs were collected in 66.6 µl cortical induction media and carefully mixed with 100 µl Geltrex™. The solution was then equally spread on a Pluronic-coated 6 cm culture dish and solidified at 37 °C for 30 min before adding carefully cortical differentiation media. After 24 hours the dish was placed on an orbital shaker set at 70 rpm and the media was renewed the day later. Thenceforth, the media was changed twice a week. From day 35 onwards, the media was switched to cortical maturation media. This media includes the TrK A and B receptor agonists LM22A and B, GDNF, ascorbic acid and insulin to help neuronal maturation. Furthermore, Geltrex™ was added to support structural development.

5.1.6 Generation of raphe organoids

Embryonic bodies were formed as described above. At day 2, the media was replaced with caudalizing medium which includes dual SMAD inhibition as well as insulin and FGF-2. This combination has been shown to posteriorize the cell's identity effectively and was utilized here to achieve a hindbrain identity

(Muguruma *et al.*, 2010, 2015). During the patterning phase, the media was changed every other day. At day 12, the EBs are transferred to a Pluronic-coated 6 cm dish with ventralization medium and kept on an orbital shaker at 70 rpm. Ventralization medium includes the sonic hedgehog pathway activating agents Puromorphamine and Smoothend agonist (SAG) which are ventralizing the cell's identity in order to mimic the ventral P3-domain. At day 17, the media was switched to specification medium which finalizes the patterning period by upregulating the expression of the transcription factor FOXA2 which inhibits the pro-motor neuronal transcription factor PHOX2b.

After the patterning period, the media is switched to RO maturation. This media stimulates neuronal differentiation by inhibiting Notch signaling and fosters neuronal maturation by adding neurotrophic factors. To foster functionality of RO, medium was replaced by functionality boost after 14 days.

5.1.7 RO outgrowth assay

3.5 cm dishes with polymer coverslip bottom were coated with Geltrex™ diluted 1:50 in wash media over night at 4°C. The following day, mature RO were carefully seeded on the coated dish, before adding RO maturation media carefully to the dish 5 minutes later. Half-media changes were done every other day cautiously. After five days in culture, samples were fixed similar to 2D cultures as described in 5.2.1. However, every pipetting step had to be done very slowly and carefully to avoid detaching of the cultures.

5.1.8 Organoid dissociation

Three D24 raphe organoids were selected per dissociation and transferred to a 15 ml screw cap tube. After washing the organoids once with PBS, pre-warmed 1X EDTA-Trypsin in PBS and was added. During the following incubation for 10 min at 37 °C, screw cap tube was mixed regularly. Next, 1 ml of N2 base was added and samples were mechanically dissociated. Therefore, solution was pipetted slowly 20 times up and down using a P1000 pipette. If there were still organoid fragments visible, solution was allowed to settle briefly and supernatant including the single cells was transferred to a second screw cap tube. Cells were spun down at 300 x g for 4 min and cell pellet was resuspended in 1 ml of RO maturation medium. Cell number was determined using an automated counting system in combination with trypan blue. 1,000,000 cells were seeded per Geltrex™-coated 3.5 cm dish with a polymer coverslip bottom in RO maturation supplemented with 5 µM Y-27632 ROCK inhibitor. During the course of maturation, 1:1,000 laminin was applied if necessary.

5.1.9 Slicing and assembly of organoids

In order to improve long term cultures of organoids and allow assembloids, organoids were sliced using a vibratome between day 35 and 45.

Up to 10 mature organoids were harvested with a cut plastic P1000 pipette tip and embedded in 4 % low melting agarose gel in embedding molds. After solidifying on ice for approximately 15 min, a block with the embedded organoids was cut out from the mold and glued on the vibratome table. As soon as the glue hardened, the sample was processed with the vibratome and subsequently collected in ice cold slicing media. 200 µm slices were cut for viral transfections and assemblies. For treatments, 400 µm slices of the same organoid were collected in separate dishes to allow different treatment conditions of the same organoid.

Slices were kept off the shaker overnight and depending on the designed experiment, either transferred to the shaker for culturing, infected with a lentivirus for live cell imaging or seeded on a membrane to form assemblies on the following day.

5.2 Molecular biology

5.2.1 Fixation and cryo-sectioning

Cells or organoids were washed once with PBS, followed by a fixation with 4 % PFA cells for 10 min and organoids up to 15 min depending on their size at RT. After removing the PFA, the samples were washed three times with PBS. Organoids were then transferred to a 30 % sucrose solution for de-hydrolyzation for at least 12 h at 4°C. Afterwards, organoids were embedded in galantine solution and frozen using an ethanol/dry ice freezing bath with a temperature of about -40°C. Samples could then be stored at -80°C or directly processed with a cryostat. 20µm slices were collected on microscope slides.

5.2.2 Immunocytochemistry

First, samples were transferred to a wet chamber in which the entire procedure was performed. Cryosectioned organoid slices were delaminated using a liquid barrier and washed once with PBS. Samples were blocked and permeabilized in PBS and 10 % FBS and Triton X-100 for 1 hour at RT. The concentration of Triton X-100 was dependent on the antibody used in the staining. Primary antibodies were diluted in DPS + 10% FBS with the appropriated Triton X-100 concentration as listed in Table 13 and applied overnight at 4°C. The following day, antibody solutions was removed and samples were washed three times before incubated with fluorescently-labeled secondary antibodies in DPBS + 10% FBS with the corresponding concentration of Triton X-100 for 1 hour at RT (Table 14). After removing the secondary antibody, samples were washed with PBS and counterstained with DAPI (300 nM in PBS) for 5 min, before washing them again with PBS. The samples were then mounted using Mowiol solution.

Images of stained samples were acquired using Leica DM6 B microscope and for higher magnification Leica confocal TCS SP5 II microscope was applied. RO-outgrowth assay was imaged using Zeiss Celldiscoverer 7.

5.2.3 DNA isolation and Mycoplasma detection

As a measure for cell culture quality control, cultures were regularly tested for potential mycoplasma contamination (Ossewaarde *et al.*, 1996). Therefore, cells were harvested, washed with PBS and lysed by applying a lysis buffer for 1 hour at 37°C and 400 rpm. Afterwards, Proteinase K was inactivated by 10 min incubation at 95°C before adding 105 µl 2-propanol for 30 min at RT to precipitate the DNA. 10 min centrifugation at 12,000 x g pelleted the DNA, which was then washed twice with 75% (v/v) ethanol in ddH_2O followed by air-drying. The DNA pellet was resuspended in 100 µl ddH_2O and the concentration was measured using a spectrometer.

Mycoplasma screening was regularly performed by Helene Schamber.

5.2.4 RNA isolation and cDNA synthesis

RNA isolation was performed under a chemical hood and the workspace as well as pipettes were cleaned with RNase AWAY. At least three organoids were pooled per sample and transferred to a 1.5 ml reaction tube with ice cold DPBS. 2D cultures were washed with ice cold DPBS as well. 1 ml RNA-Solv reagent was applied to the samples and lysed by pipetting. Detaching of 2D cultures was facilitated using a cell scraper and transferred to 1.5 ml reaction tubes. Samples were either stored at -80°C for later processing or incubated for 5 min at RT directly. Next, 100 µl chloroform was added and samples were vortexed for 15 sec. Followed by a 10 min incubation at RT, samples were centrifuged at 12,000 x g for 5 min at RT to allow phase separation. The upper aqueous phase, containing RNA and DNA was transferred to a new 1.5 ml reaction tube. 500 µl 2-propanol was added per sample, carefully mixed and incubated at -20°C overnight. After allowing nucleic acid precipitation, samples were centrifuged at 12,000 x g for 15 min at 4°C. Resulting pellet was subject for two washing steps with 1 ml 75% ethanol (v / v in DEPC H_2O) and centrifugation steps at 12,000 x g for 10 min at 4°C. Before resuspending with 10 µl DEPC-H_2O at 37°C for 15 and 400 rpm rocking, pellets were air-dried. In order to remove genomic DNA, 2.5 µl DNase I and 2.5 µl 10 x reaction buffer were added and incubated for 15 min at RT. Afterwards, reaction was stopped by adding 2.5 µl stop-solution and incubated for 10 min at 70°C. Finally, RNA concentration was determined using a NanoDrop™ spectrophotometer and samples were stored at -80°C.

Synthesis of cDNA was done using the iScript™ cDNA synthesis kit. The procedure was carried out as instructed by the manufacture and the reaction mix is listed in Table 12 and the thermos cycler program in Table 20. Resulting cDNA was diluted in 1:5 in nuclease-free H_2O.

Table 20: Thermocycler program for cDNA synthesis

Step	Temperature	Duration
Priming	25°C	5 min
Reverse transcription	46°C	20 min
Enzyme inactivation	95°C	1 min
	4°C	∞

5.2.5 Qualitative real time PCR

SYBR Green-based qPCR analysis was performed using a QuantStudio 7 Flex system. A GoTaq® DNA Polymerase was used for amplification. All substances used for qPCR, as well as their final concentrations in the reaction mixture, are listed in Table 12 and all primers are listed in Table 11. The threshold cycle (Ct) values and melting curves were calculated using the QuantStudio software. The ΔΔCt method was applied to determine fold changes (Livak & Schmittgen, 2001) and gene expression was normalized to 18S rRNA.

Table 21: Standard qPCR program

Steps	Temperature	Duration	Cycles
Hold stage	50°C 95°C	2 min 10 min	
PCR stage	95°C 60°C 72°C	15 sec 15 sec 30 sec	40
Melt curve stage	95°C 60°C 95°C	15 sec 1 min 15 sec	

5.2.6 Polymerase Chain Reaction (PCR)

Table 12 lists the RT PCR reaction mix, including all the substances and concentrations. Amplification of target amplicons from cDNA or gDNA was performed using the RT-PCR cycling program specified in Table 22. Annealing temperature and elongation time was adjusted based on primers and expected amplicon size. All primers used in this thesis can be found in Table 11.

Table 22: Standard RT-PCR program

Step	Temperature	Duration	Cycles
Initial denaturation	95°C	5 min	
Denaturation Annealing	95°C 60°C	20 sec 20 sec	 35

Elongation	72°C	1 min/500 bp	
Final elongation	72°C	10 min	
	4°C	∞	

To test for mycoplasma contaminations in cultures, whole genomic DNA (see 5.2.3) was subject for PCR amplification for mycoplasma specific 16S rRNA gene. The used primers, concentrations and cycler program can be found in Table 11, Table 12 and Table 23, respectively. Subsequently, PCR products were analyzed by 1% agarose gel electrophoresis. If present, a mycoplasma contamination was detectable by a 270 bp band.

Table 23: PCR program for mycoplasma detection

Step	Temperature	Duration	Cycles
Initial denaturation	95°C	1 min	
Denaturation Annealing Elongation	95°C 50°C 72°C	15 sec 15 sec 10 sec	35
Final elongation	72°C	3 min	
	4°C	∞	

5.2.7 Agarose gel electrophoresis of amplified DNA

PCR amplicons were mixed with 10x DNA sample buffer and separated by 1 or 2% (w/v) agarose gel electrophoresis in TAE buffer. Gels contained 1:15,000 peqGREEN DNA detection reagent. A 100 bp DNA marker was included on gels as a reference for DNA fragment size. DNA was resolved for 50 min at 80 V and gels were imaged on a GelStick Touch imaging system.

5.2.8 RNA quality control for bulk sequencing

For RNA bulk sequencing experiments, RNA of three biological replicates of aPCs were isolated as described above. The concentration was determined using a Qubit 4 Fluorometer with the Qubit RNA BR Assay-Kit according to the manufacturer's instructions. To assess the RNA integrity, samples were prepared using the RNA 6000 Nano kit and were subsequently analyzed using a Bioanalyzer 2100 according to the manufacturer's instructions.

5.2.9 RNA bulk sequencing

All samples passed the quality control with RIN values ≥ 9.2 assessed using the RNA 6000 Nano kit on a Bioanalyzer 2100 (Agilent Technologies 5067-1511) and were sent to the High Throughput Sequencing Unit of the Genomics & Proteomics Core Facility, German Cancer Research Center (DKFZ) to be processed. Libraries were prepared with the TruSeq Stranded protocol (Illumina) and sequenced

to 50 bp paired end reads on a SP flowcell on the Illumina NovaSeq 6K platform. Sequencing data was run through an RNAseq processing workflow by the Omics IT and Data Management Core Facility, German Cancer Research Center (DKFZ). Total counts per feature were imported to R and analyzed.

RNA bulk sequencing data analysis was performed in collaboration with Anne Hoffrichter.

5.2.10 Single cell sequencing analysis

Single cell sequencing data mentioned in this thesis have been previously generated by Olivia Krefft and Ammar Jabali. FastQC was used for general sequencing quality control and data analysis was performed using the Seurat v4.1.0 package in R (Andrews, 2010; Hao *et al.*, 2021)

Re-analyzing of single cell sequencing data sets was performed in collaboration with Anne Hoffrichter.

The data were normalized using sctransform. Dimensional reduction was performed using UMAP with dims = 1:30. Shared nearest-neighbor graph was constructed with dims = 1:30. Clusters were generated with resolution = 0.4. Cells were defined by interpreting expression of known marker genes.

5.2.11 Plasmid isolation

In order to trace serotonergic binding and thus serotonergic activity, we utilized sDarken, a genetically encoded serotonin sensor based on the 5-HT_{1A} receptor. sDarken was developed and integrated in a pLVX-backbone by Martin Kubitschke (Figure 9)(Kubitschke *et al.*, 2022). The construct was then amplified in chemically component *E. coli* DH5α. Therefore, bacteria were thawed on ice for 5 min before 50-500 ng of plasmid DNA were added. After mixing the solution by flicking the reaction tube 2-3 times and an incubation of 30 min on ice, the uptake of DNA into the bacteria was fostered by heat shock at 42°C for 42 s. Next, bacteria were allowed to recover on ice for 3 min and 250 µl SOC media were added followed by an incubation at 37°C for 1 h and 400 rpm. The suspension was them used to inoculate midi cultures and grown over night at 37 °C in the presence of 100 µg/ml ampicillin. The following days, the plasmid DNA was isolated using the PureLink™ HiPure Plasmid Filter Midiprep Kit according to manufacturer's instruction. The concentration of the resulting DNA was measured using a NanoDrop™ spectrophotometer.

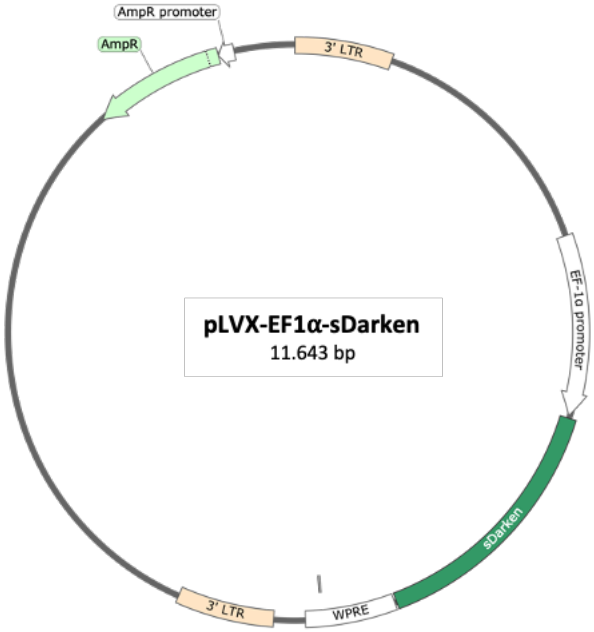

Figure 9: Plasmid map of pLVX-EF1α-sDarken.

The pLVX-EF1α-sDarken plasmid contains the serotonin sensor sDarken under the EF1-α promotor as well as a resistance against ampamycin. The plasmid was generated by Martin Kubitschke.

5.2.12 Virus generation

All lentivirus related work was performed according to Laboratory Biosafety Level (BSL) 2. When HEK293T cells cultures reached around 70% confluency, cells were exposed to 25 µM chloroquine diphosphate for at least 1 h. Chloroquine inhibits the lysosomal degradation of DNA and thus facilitates the transfection. Plasmids were transfected into HEK-293T cells via calcium phosphate transfection. Therefore, 7.9 µg of a psPAX2 lentiviral packaging plasmid, 3.5 µg envelope expressing plasmid pMS2.G VSV-G and 10 µg of pLVX-EF1α-sDarken plasmid were mixed in 100mM $CaCl_2$ and 75 mM Sodium Chloride in ddH_2O to a total volume of 1 ml. A second screw cap tube was prepared with 1ml 5 mM HEPES buffered saline (HBSS) solution. Using a 5 ml serological pipette, air was blown into HBSS solution, while plasmid mix was carefully added. Following a 30 min incubation at RT, the solution was added dropwise to the HEK-293T cells.

The medium was renewed after 8-12 h and virus containing supernatant was collected after 24 and 48 h later. The collected media was then centrifuged for 5 min at 1200 x g and the supernatant was then filtered using a 0.45 µm filter to remove any cells or cell debris. In order to purify the lentivirus, polyethylene glycol (PEG)-6000 precipitation was performed. Therefore, supernatant was mixed with 8.7 % (vol/vol) PEG-6000, 296 mM NaCl in DPBS (without $MgCl_2$ and $CaCl_2$) and incubated for 90 min at 4°C, while mixing it every 30 min. After centrifugating the solution at 4600 rpm for 30 min at 4°C,

the supernatant was removed and the pellet air-dried. The virus was then resuspended in DPBS (+$MgCl_2$ and $CaCl_2$), aliquoted and stored at -80°C.

5.2.13 Viral infection

Single cell cultures, namely dissociated RO and cortical progenitors were infected during the seeding. Therefore, single cell suspension was achieved by either TrypLE or Trypsin-EDTA as described above. After pelleting the cells and counting, 1 million cells were transferred in a separate screw cap tube supplemented with 5 µM Y-27632 in the appropriate media. Next, 10 µl of pLVX-EF1α-sDarken was added to the suspension and carefully mixed. Finally, cells were seeded homogenously on 3.5 cm dishes with polymer coverslip bottom. After 12 hours, the media was renewed to remove the virus and ROCK inhibitor.

200 µm RO and CO slices were transfected with pLVX-EF1α-sDarken the day after slicing. Therefore, selected slices were transferred to a 1.5 ml reaction tube with 120 µl of the respective media. The media was further supplemented with 10 µg/ml polybrene in order to increase the efficiency (Davis, 2002). Next, 10 µl of pLVX-EF1α-sDarken was added to the media and carefully mixed. After 24 hours, 240 µl of respective media was added and a full media change occurred 48 hours after the infection.

5.2.14 Live cell imaging

Live imaging of dissociated RO, RO slice cultures as well as assembloids were performed using Celldiscoverer7 at 37°C and 4% CO_2. Media of samples was changed to imaging buffer prior imaging. Images were acquired every 0.5 seconds over a five min period.

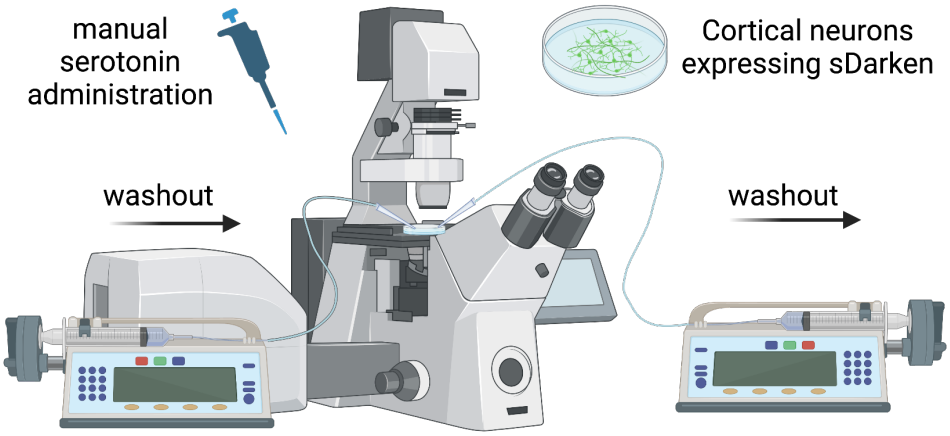

Figure 10: Live imaging set up to analyze sDarken sensitivity in hiPSC-derived cortical neurons.

sDarken was applied to cortical progenitors before neuronal differentiation and maturation, cultured in 3.5 cm dishes with polymer coverslip bottom. Live imaging was performed in imaging buffer using confocal microscope TCS SP5 II. After measurement 1 min baseline, according serotonin concentration was applied (1:1000) manually. Washout with imaging buffer was initiated 30 secs later with a rate of 2 ml/min for at least 3.5 mins.

Live imaging of hiPSCs-derived cortical neurons was performed using the TCS SP5 II. The set-up is illustrated in *Figure 10*. Briefly, dishes containing cortical neurons expressing sDarken was arranged on microscope table. Glass pipette to the left were connected to syringe filled with imaging buffer, while glass pipette to the right was connected to a syringe for media aspiration. Both syringes were installed in automatic syringe pumps set at 2 ml / min. Prior to the imaging, serotonin was diluted to 100X of target concentration and stored on ice. Medium of the neurons was changed to imaging buffer. Baseline was recorded for 1 min before administrating serotonin manually carefully to the dish. After 30 seconds, washout was initiated by activating both pumps. Images were acquired every 0.5 seconds using a 63X oil immersion objective. Total measurement lasted five minutes per condition with an extended washout period if needed.

5.3 Image and data analysis

Images were processed using ImageJ (Fiji) or Cellprofiler. Quantifications were performed with Cellprofiler with individually adjusted pipelines (Stirling *et al.*, 2021). Number of pH3- and TBR2-positive cells were counted manually using ImageJ.

Recordings of sDarken were analyzed by Lutz Wallhorn from the Massek lab of the University of Bremen.

5.4 Generation of schemes

All Schemes have been created with the help of Biorender.com.

5.5 Statistical analysis

Data for quantitative analysis are based on at least three independent biological replicates. Replicates are displayed as means with standard error of the mean (SEM). Significance was assessed either by Man-Whitney-U testing two groups or Kruskal-Vallis (with Dunn's post hoc test) for multiple groups using GraphPad Prism 5. The exact numbers and the applied statistical test can be found in the individual figure legends. Significances were displayed as not significant (ns) >0.05, * $p < 0.05$, ** $p < 0.01$ and *** $p < 0.001$.

6 Results

6.1 Investigating the effect of serotonin on proliferation in human stem cell derived progenitor populations

Induced pluripotent stem cells opened the possibility to study the human neural system in the dish. The human brain development and in particular the role of serotonin is of interested in this study. So far, most studies have been performed using rodent models and to answer open question in the human context, human iPSCs from healthy donors were utilized. As targeting single progenitor types remains difficult, progenitor types were clustered as follows: Progenitors which develop at early stages during development and divide at the ventricular lining including apical radial glia cells, apical intermediate progenitors and neural epithelial cells are summarized as apical progenitor cells (aPCs); TBR2-positive cells were defined as intermediate progenitors (IPs); and progenitors dividing in the SVZ and marked by PTPRZ1, were classified as basal progenitor cell (bPCs).

6.2 Apical progenitor cells displayed an increased proliferation upon 5-HT_{2C}-activation

In a first set of experiments, apical neural progenitor cells (aPCs) were targeted by utilizing a differentiation protocol previously established in the group of Julia Ladewig (Figure 11 A). Therefore, iPSC monolayers were exposed to a dual SMAD inhibition and thus, prevented to achieve a mesodermal or endodermal identity, instead facilitated a neuroectodermal fate (Chambers, 2009). A complementary prohibition of Wnt signaling ensured an anterior cell identity (Huang, 2009). The resulting aPCs were characterized by immunofluorescent stainings which revealed a high expression of pan-progenitor markers like SOX2 and Nestin (Figure 11 B). Additional markers as KI67 were indicating great proliferative capacities. Analysis of regional specific transcription factors like OTX2, PAX6 and the absence of HOXB2 indicated an anterior-dorsal identity of the majority of cells. A small subset of cells expressed TBR2, which indicates IPs (Cappello *et al.*, 2006). The same holds true for basal radial glia marker PTPRZ1 (Pollen *et al.*, 2015).

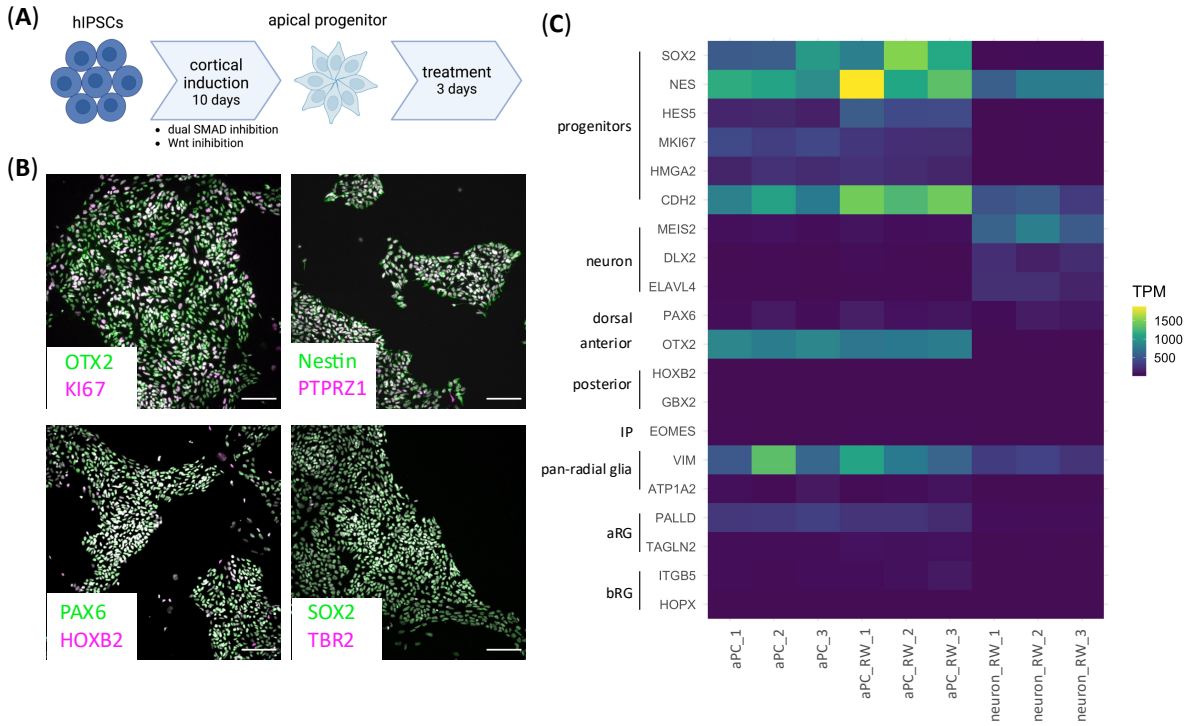

Figure 11: Characterization of apical progenitors.

(A) Scheme of the aPC differentiation protocol. (B) Representative immunostainings for pan-progenitor (SOX2, KI67, Nestin), regional (OTX2, HOXB2) and additional cell type specific markers to exclude bPCs (PTPRZ1) and IPs (TBR2). Scale bars: 100 µm (C) RNA bulk sequencing data of three independent aPC differentiations in comparison with aPCs and D5 neurons from Wilkens et al, 2022 to further characterize aPCs.

To further define the cells, a RNA bulk sequencing experiment was performed. To that end, aPCs were harvested, RNA isolated and after passing several quality control steps, gene expression of characteristic genes was analyzed. To validated the cultures, the expression profile was compared to a previously published RNA bulk sequencing data set (Wilkens *et al.*, 2022). The data set includes this cell type, as well as young cortical neurons. Here, broad expressions of neural progenitor genes were detected, including SOX2, Nestin (NES) and HES5 (Figure 11 C). Proliferative activity was demonstrated by the expression of HMGA2, HES5 and MKI67 (KI67). Additionally, pro-neuronal genes MEIS2, DLX2 and ELAV4 (HuD) were not transcribed. The bulk sequencing detected high levels of CDH2 which is encoding N-cadherin. N-cadherin is the main component of the adherent junctions between progenitors at the apical lining (Kadowaki et al., 2007). Next, the cultures were analyzed for radial glia markers. Pan-radial glia marker as VIM and ATP1A2, as well as apical radial glia cell markers like PALLD and TAGLN2 were detected, while basal radial glia markers, including ITGB5, HOPX remained low expressed (Pollen et al., 2015). EOMES, the gene encoding for TBR2, was not highly transcribed, thus, excluded intermediate progenitors in the cultures (Cappello *et al.*, 2006). In line with immunofluorescent data, expression pattern of regional defining genes including PAX6, OTX2, HOXB2

and GBX2 indicate a dorsal-anterior identity of the cultures. Therefore, the culture displayed a mixed population of apical progenitor cells, including neural epithelial and apical radial glia cells.

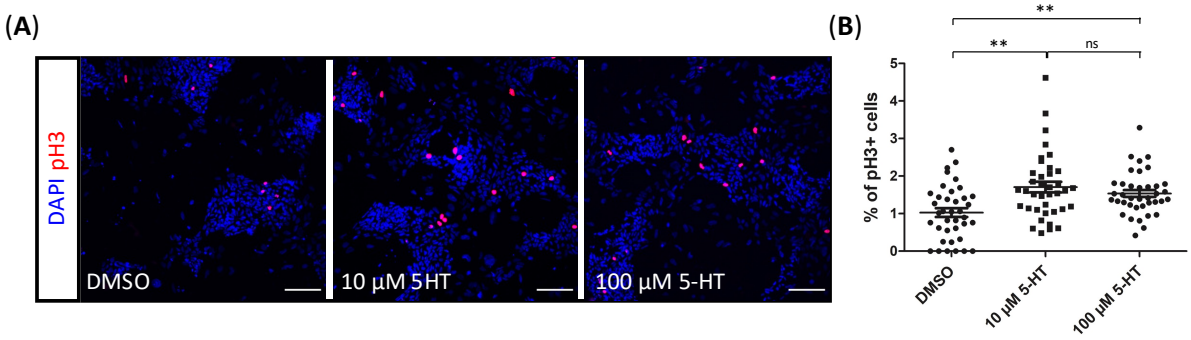

Figure 12: 10 and 100 µM serotonin increased the proliferation of aPC cultures.

(A) Representative immunofluorescent stainings of pH3 of aPCs after three days of exposure to DMSO, 10 or 100 µM serotonin. Scale bars: 100 µm. (B) Quantification of the proportion of pH3-positive cells of three independent differentiations showed a significant increase after three-days 10 and 100 µM serotonin exposure compared to the control. Data shown as mean ± SEM, Kruskal-Wallis test with Dunn's multiple Comparison test; ns - not significant, ** $p<0.01$.

To test the effect of serotonin on proliferation of aPCs, immunofluorescent analysis of phosphorylated histone 3 (pH3) of aPC cultures exposed to 10 or 100 µM serotonin were performed. Histone 3 is phosphorylated during the onset of mitosis and therefore, indicates proliferative events (Figure 12 A. After three days of exposure, the numbers of pH3 positive cells were quantified and normalized to the total cell number per image. Both, 10 µM (1.71 ± 0.14%) and 100 µM (1.54 ± 0.09%) serotonin increased significantly the proportion of mitotic events in aPC cultures compared to the control (1.03 ± 0.12%; Figure 12 B). Of note, there was no statistically difference between the two serotonergic conditions.

The serotonergic receptors are highly divers and represent with 14 subtypes the largest G-protein coupled neurotransmitter receptor class in the human system (Nichols and Nichols, 2008). To further decipher which receptor subtype might mediate the proliferation stimulation effect in aPCs, RNA bulk sequencing data set was analyzed for receptor expression levels. The receptor 5-HT_{2C} encoded by the gene HTR2C became of interest as it is highly upregulated compared to all other receptor subtypes (Figure 13 A). Furthermore, to investigate the serotonergic receptor expression in the course of neuronal development, RNA bulk sequencing data set from Wilkens *et al*. was exploited (Wilkens, 2022). Here, the HTR2C expression significantly decreased in all subsequent neuronal stages compared to aPCs (Figure 13 B).

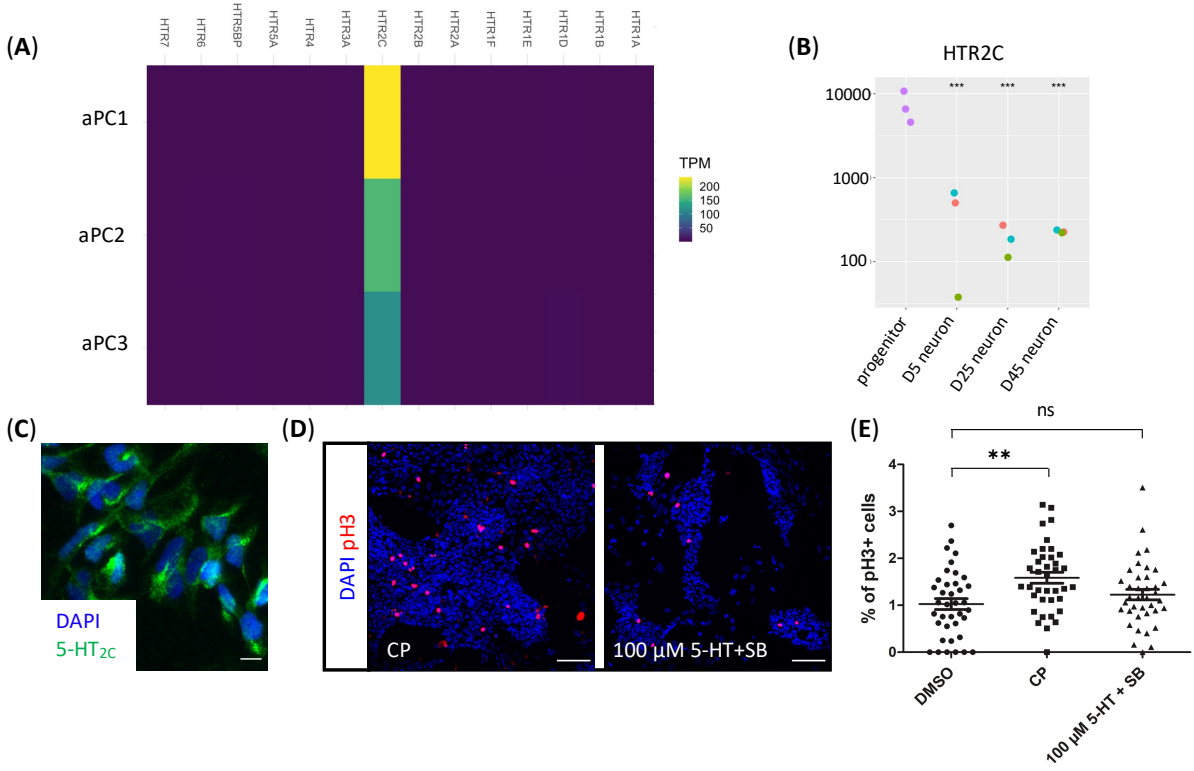

Figure 13: APCs express the receptor 5-HT2C which activation caused a proliferation increase.

(A) RNA bulk sequencing data comparison of three independent aPC differentiation for all serotonergic receptor genes. (B) RNA bulk sequencing data from Wilkens et al. indicated significant upregulation of HTR2C in aPCs compared to D5, D25 and D45 cortical neurons. (C) Representative analysis validated 5-HT_{2C} expression in aPC. (D) Representative images of immunofluorescent stainings of pH3 of aPCs after three days of exposure to 5-HT_{2C} agonist CP809101 (CP) or 5-HT_{2C} antagonist SB242084 (SB) together with serotonin. (E) Quantification of the proportion of pH3-positive cells in three independent differentiations reveal a significant increase upon CP exposure. Data shown as mean ± SEM, Kruskal-Wallis test with Dunn's multiple Comparison test; ns - not significant, ** p<0.01. Scale bars: (C) 10 µm, (D) 100 µm. Sequencing analysis was performed in collaboration with Anne Hoffrichter.

In line, immunofluorescence experiments showed a broad expression of the 5-HT_{2C} in aPCs (Figure 13 C). Based on these data, 5-HT_{2C} was targeted specifically by the agonist CP809101 (CP) as well as the antagonist SB 242084 (SB) together with 100 µM serotonin. Cell proliferation was determined based on pH3 immunofluorescence signal (Figure 13 D). A three-day exposure of CP resulted in a significant elevated proportion of mitotic events (1.58 ± 0.12%) compared to the control. Moreover, the presence of SB omitted the mitogenic effect of serotonin (1.23 ± 0.11%) (Figure 13 E).

6.3 Increased aPC proliferation also found in mature but not in young cortical organoids

Cortical organoids are capable to recapitulate human corticogenesis to a certain degree and have been used to address a large variety of associated questions. In contrast to 2D-monocultures, the three-dimensional structures of CO develop a broad range of progenitor populations, among others aPCs.

Thus, we utilized cortical organoids to investigate whether the observed mitogenic effect of serotonin holds true in this more complex model system. Therefore, iPSCs were allowed to self-aggregate to embryonic bodies (EBs) and suspect to an anterior-neuroectodermal induction, similar to the aPC differentiation protocol (Figure 14 A). When neuroectoderm was formed, noticeable as bright structure at the EB's surface, EBs were embedded in a membrane matrix (Geltrex^{TM}). This added structural component supports the development of ventricular zones visible as loop-shaped structures. Cortical ventricular zones harbor the apical progenitor pool and were characterized by regional markers for instance PAX6 and OTX2 which validate their cortical dorsal identity (Figure 14 B, C). Differentiated neurons are labeled by HuC/D and give rise to the cortical plate, whereby the development occurs inside-out: apical layers marked by TBR1 develop earlier than upper layer neurons labeled by SATB2 (Hevner et al., 2001; Britanova et al., 2008) (Figure 14 C, D).

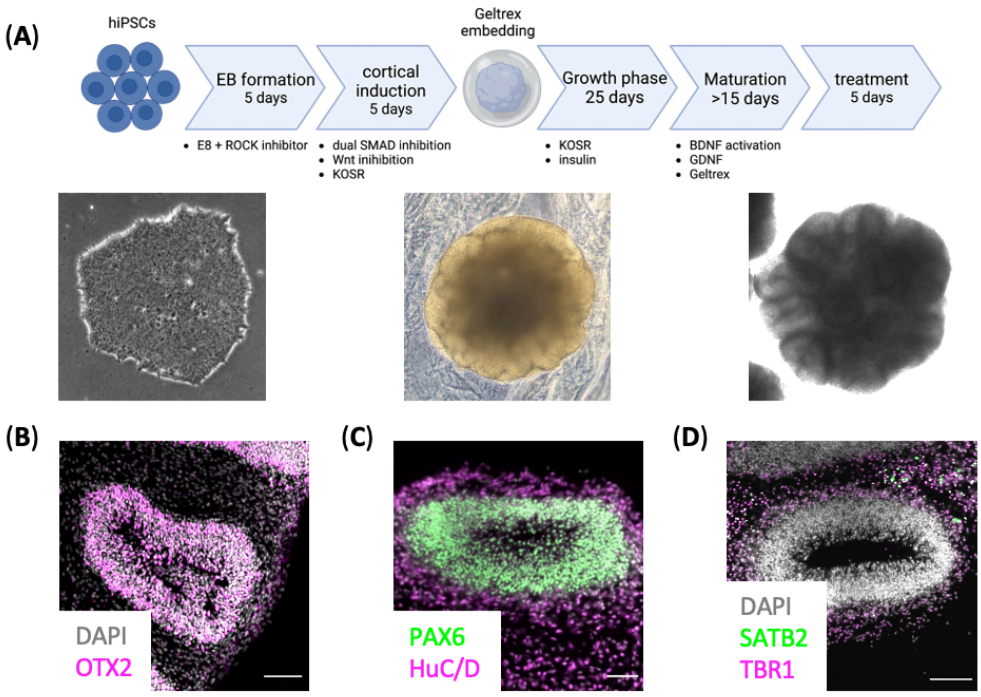

Figure 14: Characterization of cortical organoids.

(A) Scheme of the CO differentiation protocol with representative brightfield images of hiPSCs before starting the protocol, Geltrex^{TM}-embedded organoids (D10) and matured organoid with large ventricular areas. (B-D) Immunofluorescence characterization of mature CO. CO develop cortical ventricular structures which represent ventricles of the developing forebrain. Ventricular structures consist of progenitors and were marked by OTX2 and PAX6. Developing neurons are labeled by HuC/D and reside outside of VZ. The majority of neurons are allocated to the deeper cortical layers (TBR1-positive), while at later stages also neurons of the upper layers arise (SATB2-positive). Scale bars: 50 µm.

To test for a serotonergic mitogenic effect, D30 cortical organoids were exposed to 10 µM serotonin. As apical progenitor cells divide along the ventricular lining, immunofluorescent signal of pH3 at this

location was quantified. Interestingly, after a five-day period, the proliferation of aPCs (22.61 ± 2.85) in serotonin exposed samples was similar compared to the control (22.32 ± 2.54; Figure 15 A).

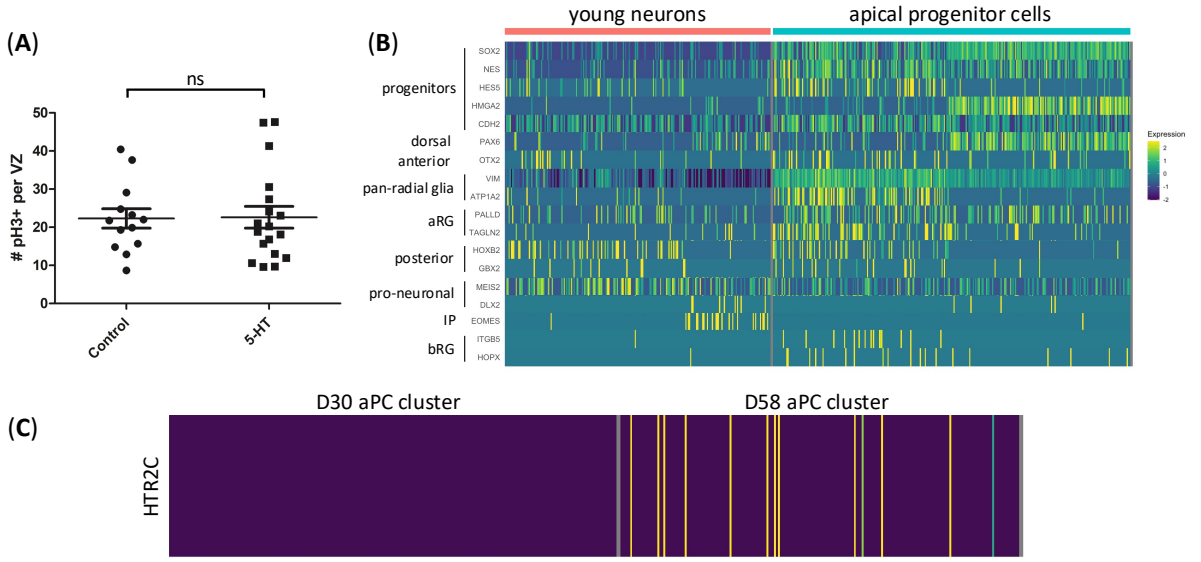

Figure 15: D30 CO did not show altered proliferation upon serotonin exposure and displayed no expression of HTR2C in contrast to D58 CO.

(A) Quantification of pH3 per VZ in D30 cortical organoids revealing no differences between control and five-days serotonin exposed CO. Data of two independent differentiations are shown as mean ± SEM. Mann Whitney test; ns - not significant (B) Comparison between two single cell sequencing data generated by Ammar Jabali and Olivia Krefft. COs have been generated from the same cell line as used in the experiment here. Cells have been allocated to cell types based on expression of selected genes (SOX2, NES, HES5, HMGA2, CDH2, PAX6, OTX2, VIM, ATP1A2, PALLD, TAGLN2) compared to others (MEIS2, DLX2, HOXB2, GBX2, EOMES, ITGB5, HOPX). Expression patterns of aPC cluster are shown vs young neuron cluster. (C) Expression of HTR2C of cells within apical progenitor cell cluster of D30 and D58 CO. Sequencing analysis was performed in collaboration with Anne Hoffrichter.

In order to understand the gene expression pattern of HTR2C during CO development, previously generated single cell RNA sequencing data sets were re-analyzed. The data sets consisted of D30 and D58 COs and have been previously performed by Ammar Jabali and Olivia Krefft, respectively. The organoids of both studies were generated from the same cell line as in this thesis and are therefore valuable as comparison. To specifically analyze the expression levels in apical progenitors, clusters representing different cell types were created depending on expression of sets of characteristic genes (Figure 15). Similar to 2D aPC characterization in Figure 12 B, SOX2, NES, HES5, HMGA2, SDH2, were analyzed to describe early progenitors, while regionality was defined by PAX6, OTX2, HOXB2 and GBX2. Expression of pan-radial glia marker as VIM and ATP1A2, as well as apical radial glia cell markers like PALLD and TAGLN2 indicate radial glia identity. While the low expression of ITGB5 and HOPX, as well as EOMES, MEIS2 and DLX exclude IPs, bRGs and neurons. Expression levels are shown in Figure 15 B in comparison to young neurons to help contextualizing data. Next, defined aPC clusters in D30 and

D58 organoids were analyzed regarding HTR2C expression (Figure 15 C). Interestingly, D30 organoids showed no HTR2C expression, while single cells in D58 CO indicated a fair HTR2C expression.

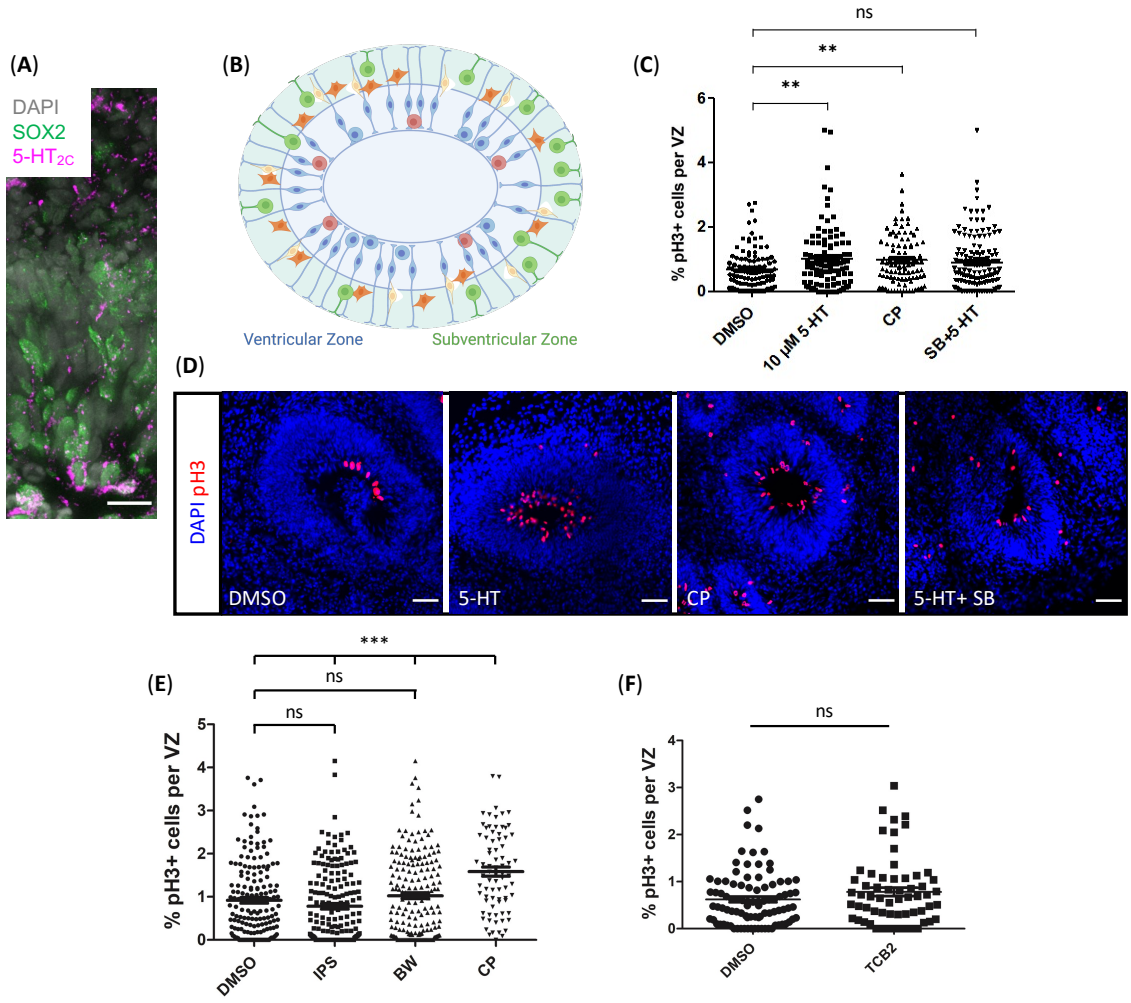

Figure 16: Activation of 5-HT$_{2C}$ increased the proliferation of aPC in mature cortical organoids.

(A) Representative immunofluorescent staining of 5-HT$_{2c}$ at the ventricular lining of mature D60 COs. (B) Schematic overview of ventricular zones and proliferative aPCs in red. (C, D) Immunofluorescent analysis of pH3-positive cells along the apical lining in different conditions targeting the 5-HT$_{2C}$ after five-days of exposure. Four independent batches were analyzed and number of pH3-positive cells were normalized to cells within the ventricular zone. (E) Quantification of immunofluorescent stainings of agonists targeting 5-HT$_{1A}$, 5HT$_{2B}$ and 5-HT$_{2C}$ of 4 independent batches. (F) Immunofluorescent analysis of the proportion pH3-positive cells normalized to the number of cells of the ventricular zone after five-days 5-HT$_{2A}$ agonist and antagonist exposure. Scale bars: (A) 15, (D) 50 µM. Data are shown as mean ± SEM; (C, E) Kruskal-Wallis test with Dunn's multiple Comparison test, (F) Mann Whitney test; ns - not significant, ** p<0.01, *** p<0.001.

In line to the gene expression data, immunofluorescence analysis of D60 CO indicated 5-HT$_{2C}$ expression of single cells along the apical lining (Figure 16 A). Subsequently, D60 CO were exploited to decipher the mitogenic effect of serotonin. Therefore, D60 CO were exposed to serotonin, CP or SB

together with serotonin for five days and pH3 positive cells along the ventricular lining were quantified (Figure 16 B). After normalization to the total number of cells in the VZ, significant differences were identified (Figure 16 C, D). More specifically, serotonin exposure significantly increased the proportion of mitotic events (1.02 $\pm$ 0.09%) compared to the control (0.67 $\pm$ 0.06%). This effect was omitted in the presence of the antagonist SB (0.89 $\pm$ 0.07%). Importantly, specific activation of 5-HT_{2C} by CP was sufficient to induce an amplified proliferation (0.97 $\pm$ 0.09%).

To further confirm the role of 5-HT_{2C}, other serotonergic receptors were targeted, which have been previously associated with proliferation. Therefore, D60 CO were treated for five days with specific agonists targeting 5-HT_{1A} (Ipsapirone; IPS), 5-HT_{2B} (BW-723C86; BW) and 5-HT_{2A} (TCB2). Neither IPS (0.78 $\pm$ 0.06% compared to 0.92 $\pm$ 0.67%), BW (1.02 $\pm$ 0.07% compared to .92 $\pm$ 0.67%), nor TCB2 (0.78 $\pm$ 0.09% compared to 0.62 $\pm$ 0.06%) caused a different aPC proliferation behavior (Figure 16 E, F). Moreover, CP was used as a positive control, validated previous results and showed a significant proliferation surge (1.58 $\pm$ 0.1%) compared to DMSO, BW and IPS.

In summary, 2D as well as 3D CO experiments demonstrated an mitogenic effect of serotonin on apical progenitor cells. This stimulation effect was due to the activation of 5-HT_{2C}.

6.4 Serotonin does not affect proliferation behavior of intermediate progenitors

Intermediate progenitor cells are characterized by the expression of TBR2 and reside within the subventricular zone (Cappello *et al.*, 2006). This proliferative neuronal precursor plays a crucial role during the cortical expansion for lissencephalic animals. To test whether the proliferative behavior of IPs is affected by serotonin, mature D60-65 cortical organoids were exposed to serotonin. After five days of treatment, the proportion of TBR2-pH3 double positive cells, mostly localized in the SVZ, were quantified (Figure 17, A, B). No significant differences were detected as 1.5 $\pm$ 0.16% of TBR2-positve cells were mitotic under serotonin exposure while the control showed 1.65 $\pm$ 0.15% mitotic IPs (Figure 17 C).

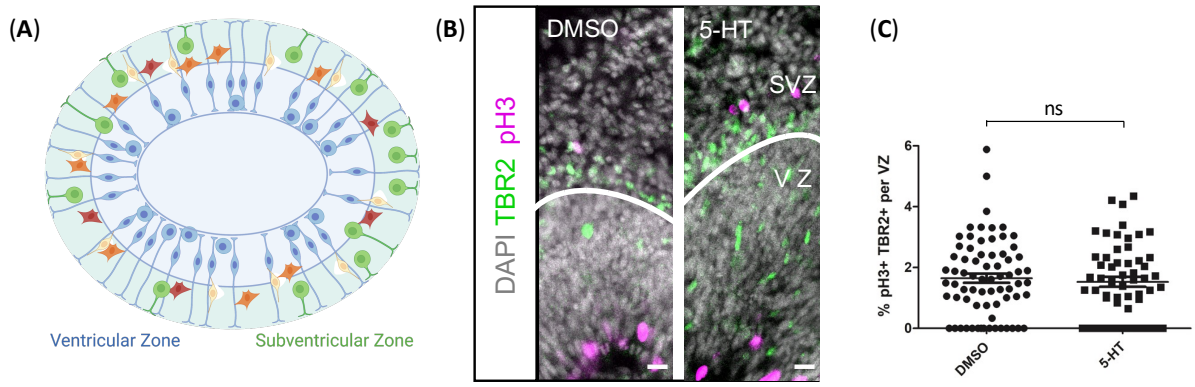

Figure 17: Serotonin does not affect IP proliferation behavior in mature COs.

(A) Schematic overview of ventricular and subventricular zone with mitotic IPs highlighted in red. (B) Representative images of immunofluorescent stainings of mature cortical organoids of TBR2 and pH3. Scale bars: 15 µm. (C) Quantification of the proportion of pH3-TBR2-positive cells per VZ revealed no effect after a five-day serotonin exposure. Three independent batches were analyzed and data are shown as mean ± SEM; Mann Whitney U test; ns - not significant.

In conclusion, serotonin does not affect the proliferative behavior of IPs in mature cortical organoids.

6.5 Serotonin induces proliferation in basal progenitor cells via 5-HT$_{2A}$-activation

In contrast to aPCs, basal progenitor cells divide in the subventricular zone. It is believed that bPCs, especially basal radial glia cells, give rise to the majority of neurons during human corticogenesis and thus responsible to the massive expansion of the human cortex.

To test whether serotonin influences the proliferative capabilities of bPCs, hiPSC-derived bPC cultures were employed. The differentiation protocol for this progenitor type was developed and performed in the group of Julia Ladewig by Ammar Jabali, Andrea Rossetti and Annasara Artioli. Briefly, iPSCs were differentiated to aPCs as described above and allowed to follow neuronal differentiation for four weeks (Figure 18 A). Residual proliferative capacity of bPCs was then upregulated by the addition of FGF-2. Subsequently, bPC culture purified over a time course of at least 4 weeks until they exhibit a broad expression of PTPRZ1 as well as ITGB5 (Figure 18 B).

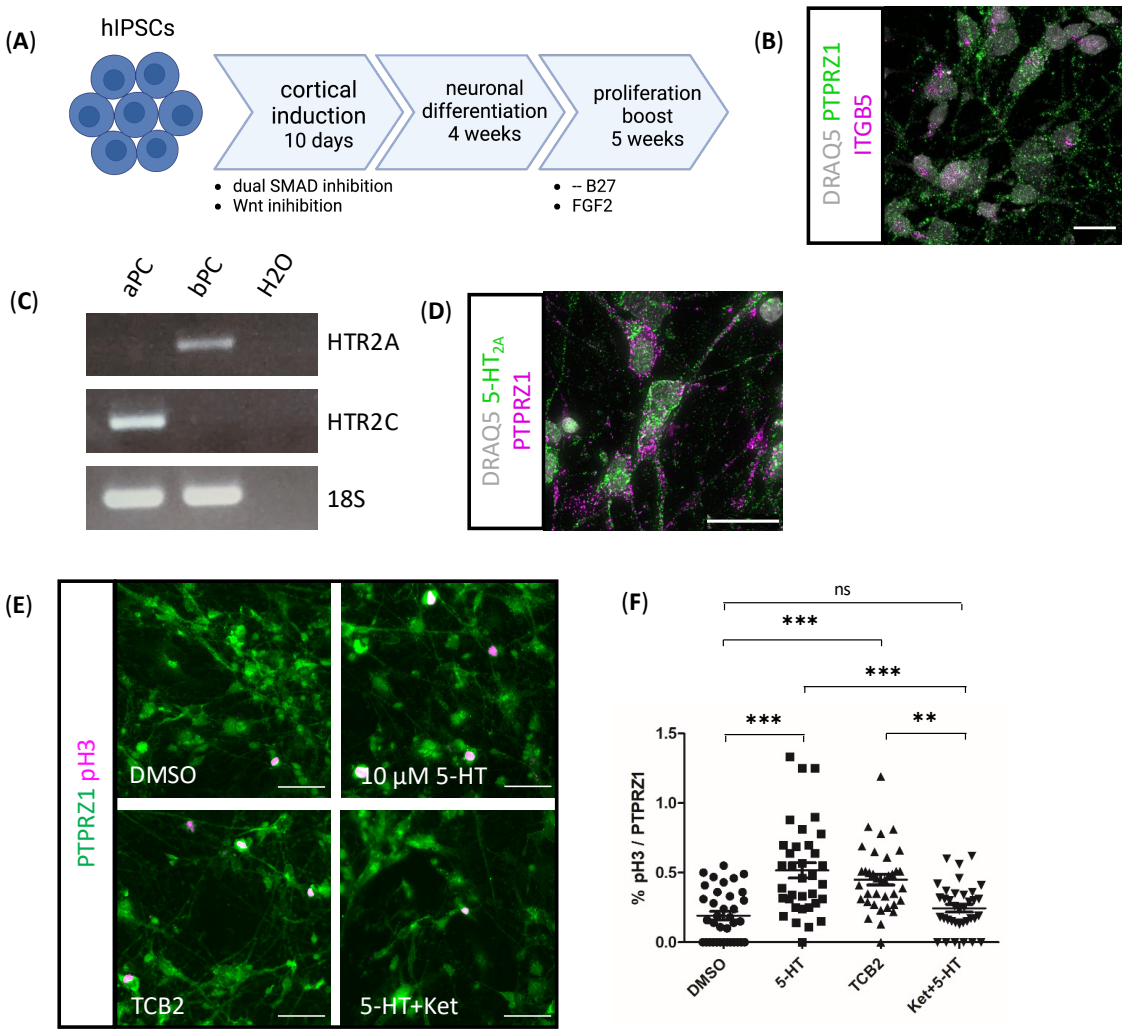

Figure 18: BPCs expressed 5-HT$_{2A}$ which activation caused an increase of mitotic events.

(A) Scheme of bPC differentiation protocol RT-PCR analysis of apical and basal progenitors which express different serotonergic receptors. The development of this protocol as well as it's execution was not part of the thesis. It was performed by Ammar Jabali, Annasara Artioli and Andrea Rosetti of the group of Julia Ladewig. (B) Representative immunofluorescent staining of bPCs of the characteristic markers PTPRZ1 and ITGB5. (C) RT-PCR analysis of serotonergic receptor gene expression in aPCs and bPCs. (D) Validation of 5-HT$_{2A}$ expression in bPC cultures via immunofluorensence. (E) Representative images of immunofluorescent stainings of bPC of PTPRZ1 and pH3. The cultures were exposed for three days to serotonin, the 5-HT$_{2A}$ agonist TCB2 or the 5-HT$_{2A}$ antagonist Ketanserine (Ket) together with serotonin. (F) Quantification of the proportion of pH3-PTPRZ1 double positive cells reveal a significant increase by both serotonin or TCB2. The experiment included three batches and are shown as mean ± SEM; Kruskal-Wallis test with Dunn's multiple Comparison test; ns - not significant, ** p<0.01, *** p<0.001. Scale bars: (B) 15, (D) 25, (E) 50 µm.

Previous studies associated on 5-HT$_{2A}$ as the only serotonergic receptor subtype with bPCs (Mayer *et al.*, 2019; Xing and Huttner, 2020; Xing *et al.*, 2020). Indeed, PCR experiments demonstrated the expression of encoding gene HTR2A in the bPC cultures in comparison to aPCs (Figure 18 C). Additionally, immunofluorescent analysis of 5-HT$_{2A}$ validated the presence of the receptor subtype in

the cultures (Figure 18 D). Next, bPCs proliferation behavior under the influence of serotonin was investigated, therefore the mitogen FGF2 was withdrawn from the cultures. To target 5-HT_{2A} specifically, agonist TCB2 and the antagonist Ketanserine (Ket) in a co-treatment with serotonin were included as additional conditions (Figure 18 E). Quantification of the proportion of pH3-PTPRZ1-double positive cells revealed a significant increase of mitotic bPCs after serotonin exposure to 0.52 $\pm$ 0.06% compared to the control (0.19 $\pm$ 0.03%) (Figure 18 F). A similar significant enhanced proliferation was detected in TCB2-treated bPCs (0.45 $\pm$ 0.04%). Moreover, no effect was observed when Ket was present as just 0.24 $\pm$ 0.03% of PTPRZ1-labeled cells were also positive for pH3.

6.6 Basal progenitor cells in CO repeated proliferation increase due to activation of 5-HT_{2A}

Basal progenitor cells emerge along the apical lining, from where they migrate basally. The subventricular zone grants a defined niche where they proliferate and later, give rise to neurons and astrocytes. The use of CO allows to include these cell type heterogeneity and structural component in the experimental design. COs have shown to develop bPCs around D50-55. Together with IPs, they give rise to a progenitor cluster of SOX2-positive cells in the SVZ basal to VZ (Figure 19 A). In line, SOX2-labeled cells showed also positive signal for PTPRZ1 (Figure 19 B). Additionally, overlapping immunofluorescent signal of PTPRZ1 and 5-HT_{2A} were identified (Figure 19 C). Hence, we employed mature D60-65 CO to test proliferative behavior of bPCs after serotonin exposure. To reduce variability in the experimental set up, CO were sliced and slices of the same organoid were assigned to different conditions as before: Control, 5-HT, TCB2 and Ket+5-HT (Figure 19 D).

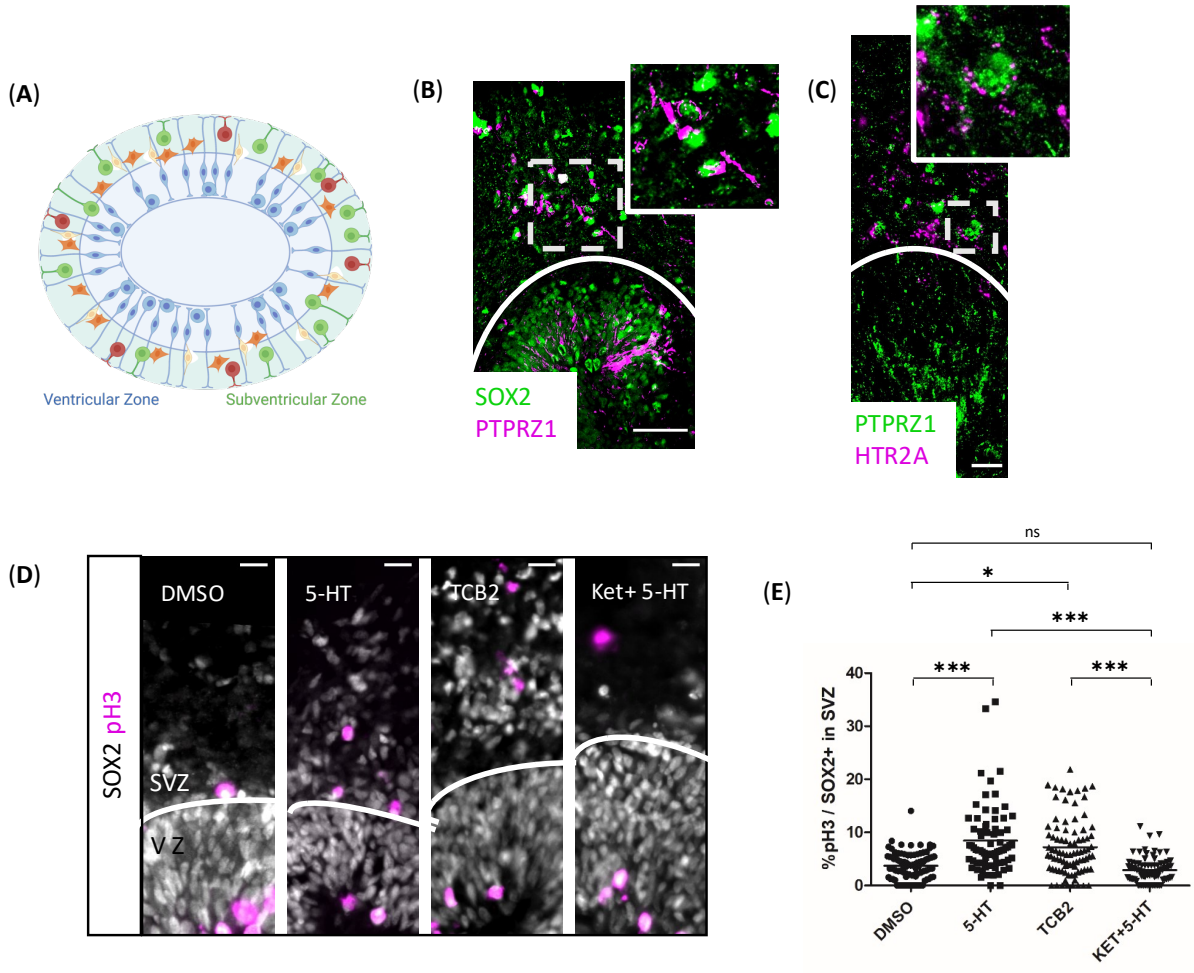

Figure 19: Serotonin increases the proliferation of bPCs in mature organoids via 5-HT$_{2A}$-activation.

(A) Schematic overview of ventricular and subventricular zone with mitotic bPCs highlighted in red. (B, C) Representative images of immunofluorescent stainings of mature cortical organoids. BPCs, marked by PTPRZ1 represent a SOX2-positive cell population in the SVZ and express the serotonergic receptor 5-HT$_{2A}$. (D) Immunofluorescent analysis of pH3 and SOX2 in the SVZ of mature CO. Representative images show CO exposed to serotonin, TCB2 or Ketanserin together with serotonin after five days. (E) Quantification of the proportion of pH3-SOX2-positive cells in the SVZ reveal a significant increase after serotonin or TCB2 exposure. Data are shown as mean ± SEM; Kruskal-Wallis test with Dunn's multiple comparison test; ns - not significant, ** p<0.01, *** p<0.001. Scale bars: (B) 25, (C) and (D) 15 µm.

When analyzing the proportion of SOX2-pH3-positive cells in the SVZ in CO, a significant increase was detected from 3.7 ± 0.28% to 8.44 ±0.73% in samples exposed to serotonin (Figure 19 E). This effect was omitted in the presence of Ket (2.89 ± 0.27%). In line, when activating 5-HT$_{2A}$ specifically by TCB2, the percentage of mitotic SOX2-postive cells in the SVZ was significantly elevated to 7.22 ± 0.58%.

Taken together, experiments with 2D cultures and complex cortical organoids highlight the stimulative effect of serotonin on basal progenitor proliferation. More specifically, activation of the bPC's 5-HT$_{2A}$ was sufficient and required to alter the progenitor dividing capabilities.

6.7 Introducing organoids representing raphe nuclei

In summary, pharmacological experiments revealed a mitogenic effect of serotonin on cortical progenitor populations. To achieve a closer representation of the *in vivo* situation, namely, serotonergic innervations, a new organoid protocol was developed reflecting the generation of the raphe nuclei. The protocol is based on different differentiation protocols aiming for 2D serotonergic neurons and cerebellar organoids (Muguruma *et al.*, 2015; Lu *et al.*, 2016; Vadodaria *et al.*, 2019).

6.7.1 Characterization of distinct stages during raphe organoid development

HIPSCs were allowed to form EBs in essential 8 for two days, before applying dual SMAD inhibition to prompt a neuroectodermal fate. As serotonergic progenitors emerge in the brainstem, different caudalizing compounds were tested. The capability of FGF2 to shift the cells' identity to a posterior fate has been demonstrated in multiple species and also insulin has shown to be an effective agent (Cox and Hemmati-Brivanlou, 1995; Wataya *et al.*, 2008; Hendrickx, Van and Leyns, 2009). The synergetic impact of the combination of FGF2 and insulin was first demonstrated by Muguruma and colleagues in 2010 and could even be proven in a cerebellar organoid model (Muguruma *et al.*, 2010, 2015). Titrating and adjusting the exposure time and concentration of the substances, resulted in a 10-day period with 50 ng/ml FGF2 and 7 µg/ml insulin in combination with an established dual SMAD inhibition (Figure 20 A). D12 RO consisted uniformly of SOX2-positive cells, indicating neuroectodermal progenitors (Figure 20 H). Further immunofluorescence analysis revealed the broad expression of characteristic markers of the hindbrain (Figure 20 B). Two cell lines showed 82.82 $\pm$ 3.38 % and 75.6 $\pm$ 2.76% HOXB2- positive cells and additional experiments demonstrated HOXA2 expression (Figure 20 C, D, E, I). OTX2, a regional marker for the fore- and midbrain remained expressed in a subset of cells (2.23 $\pm$ 1.0% and 3.4 $\pm$ 0.81%). In line, gene expression experiments of the hindbrain gene GBX2 revealed a significant upregulation by 53.44 $\pm$ 6.53 times compared to iPSCs (Figure 20 F). When analyzing expression pattern of HOX genes within the hindbrain, high levels of EN1 and HOXA2 were found, while modest expression of HOXA3 and HOXA4 was detected. Thus, analysis of the gene expression and protein level demonstrate a strong shift of the cells' identity towards the anterior hindbrain.

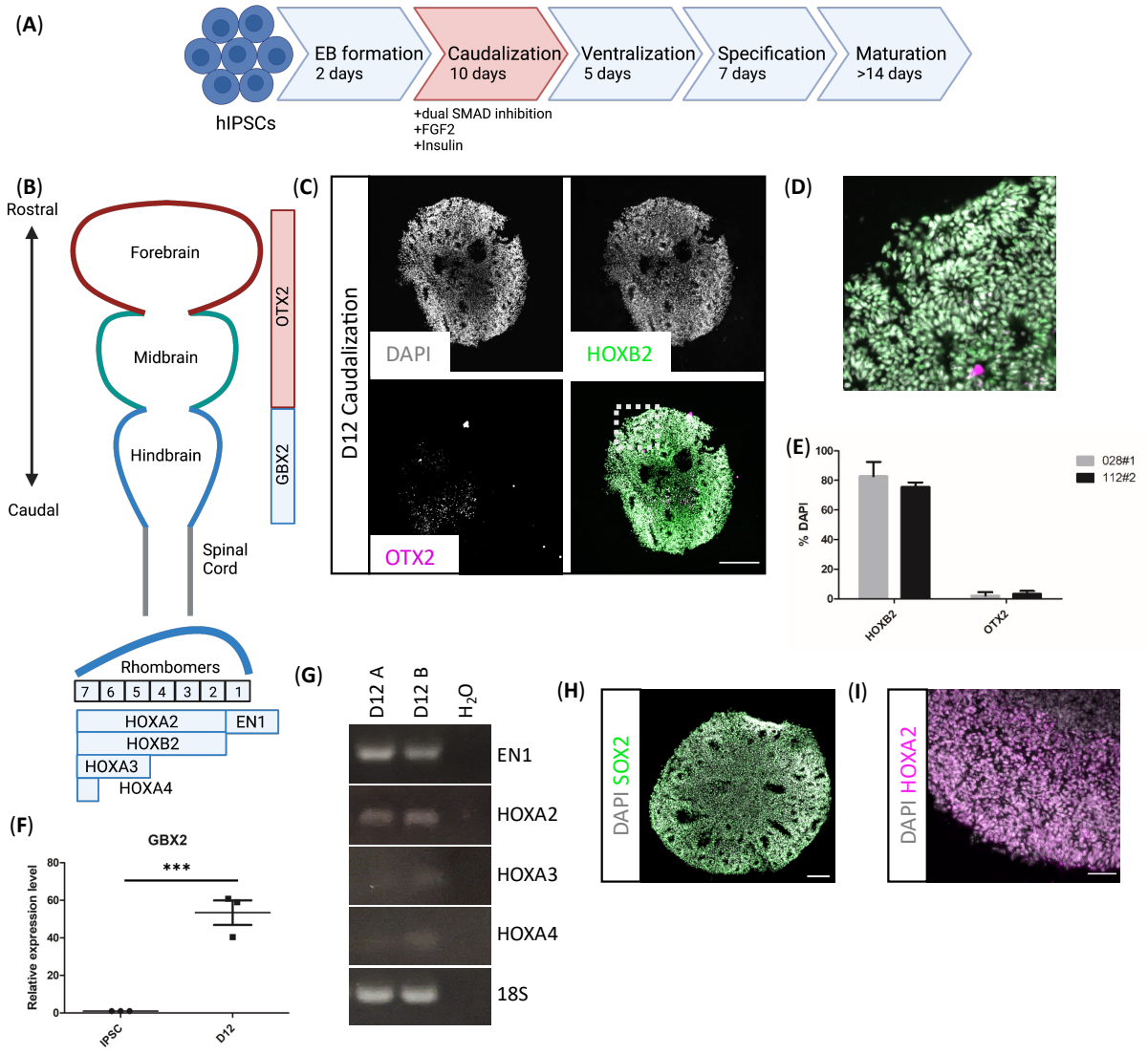

Figure 20: Characterization of casualized D12 Raphe organoids.

(A) Scheme of the raphe organoid differentiation protocol with indicated factors driving the caudalization. (B) Scheme indicating characteristic genes along the rostral-caudal axis in the developing brain and along rhombomers in the hindbrain. (C, D) Representative overview and close up images of fluorescence stainings of the hindbrain marker HOXB2 and the fore- and midbrain marker OTX2. (E) Quantification of three independent differentiations showed broad expression of HOXB2, while OTX2 was just present in a subset of cells. (F) RT-qPCR analysis of three independent differentiations indicating a significant upregulation of the hindbrain marker GBX2 in D12 RO compared to iPSCs. (G) RT-PCR analysis of D12 RO of two independent differentiations. (H,I) Representative images of immunofluorescent stainings of the precursor marker SOX2 and the hindbrain marker HOXA2. Data shown as mean ± SEM; Mann Whitney U test; *** $p<0.001$. Scale bars (C, H) 200, (I) 50 µm.

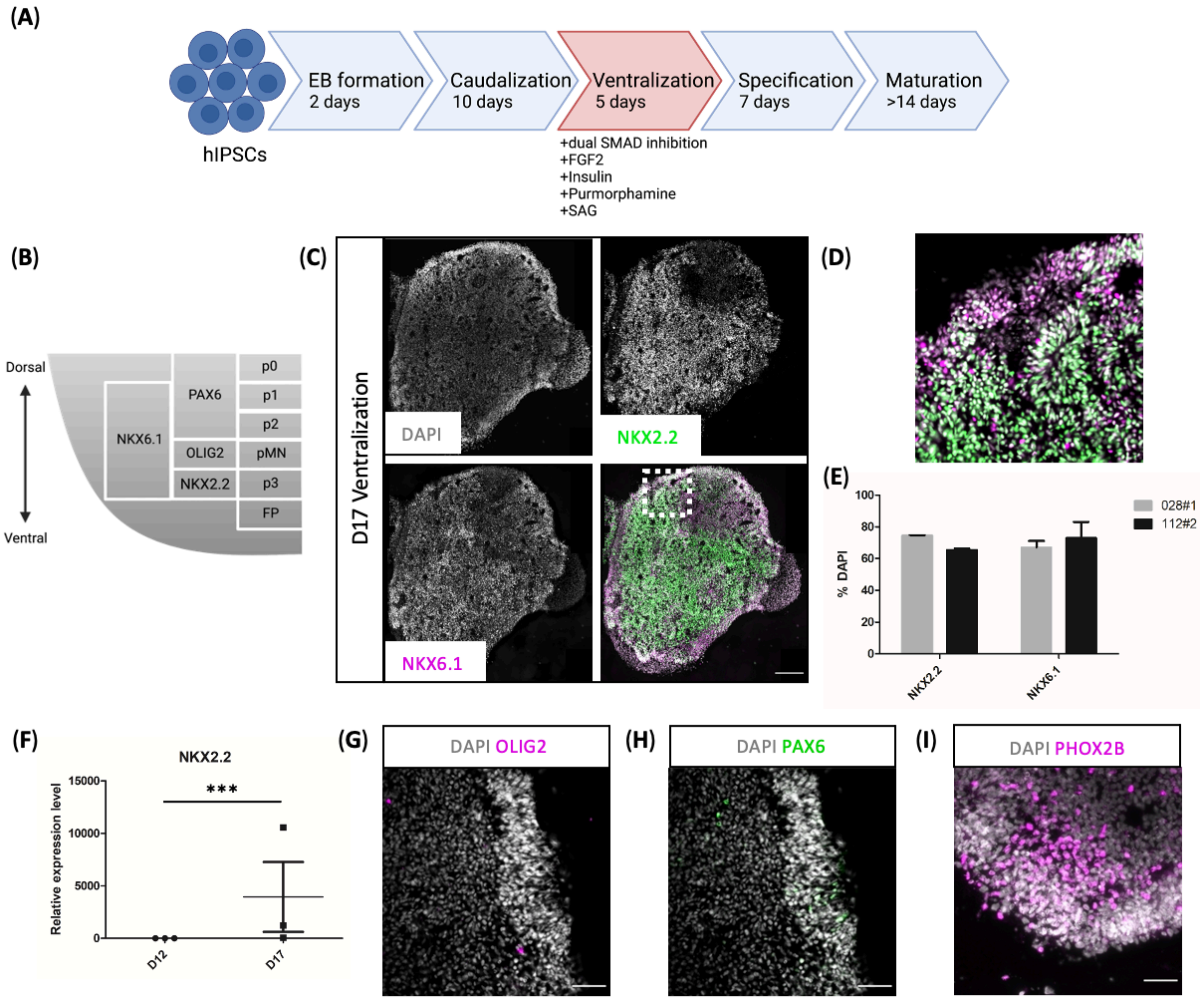

Figure 21: Characterization of ventralized D17 Raphe organoids.

(A) Scheme of the raphe organoid differentiation protocol with indicated factors for the ventralization. (B) Scheme of the expression profile of characteristic genes along the dorsal-ventral axis in the developing hindbrain. (C, D) Representative overview and close up images of fluorescence stainings of p3 domain markers NKX2.2 and NKX6.1. (E) Quantification of three independent differentiations show broad expression of both markers. (F) RT-qPCR analysis of three independent differentiations indicating a significant upregulation of NKX2.2 in D17 RO compared to D12 RO. (G, H, I) Representative images of immunofluorescent stainings of additional markers (OLIG2, PAX6 and PHOX2B). Data shown as mean ± SEM; Mann Whitney U test; *** $p<0.001$. Scale bars (C) 200, (G, H, I) 50 µm.

The dorsal-ventral axis in the developing organism is defined by the two opposing morphogens BMP and SHH, whereby SHH signaling is more important for the dorsal region. SHH is secreted by the notochord and floor plate and activates Ptc which then allows Smo to translocate from the membrane (Briscoe and Ericson, 1999; Taipale *et al.*, 2002). As serotonergic progenitors are located in the ventral P3 domain, the small molecules purmorphamine and smoothened agonist (SAG) were applied during the second phase of the protocol (Figure 21 A). Both agents activate efficiently Smo and stimulate SHH downstream signaling (Chen *et al.*, 2002; Sinha and Chen, 2006). Careful titration of exposure time and concentration of both molecules resulted in 125 nM Purmorphamine and 250 nM SAG for a five-day

period. Immunofluorescent analysis of D17 organoids revealed that 74.48 ± 2.22% and 65.37 ± 1.48% of the progenitor cells are positive for NKX2.2 while 66.95 ± 2.27% and 72.92 ± 4.21% are positive for NKX6.1, both distinct markers of the ventral p3 domain (Figure 21 B-E) (Ye *et al.*, 1998; Briscoe and Ericson, 1999; Briscoe *et al.*, 2000). Additional analysis of gene expression confirmed the significant upregulation of NKX2.2. RT-qPCR experiments showed that RO D17 had a 3945.34 ± 3324.40 times higher expression of NKX2.2 compared to D12 (Figure 21 F). OLIG2 is a characteristic marker for the pMN region, adjacent to the p3 area. Here, a subset of cells was identified expressing this transcription factor (Figure 21 G). The same was true for PAX6 which is characteristic by more ventral areas (Figure 21 H). Together, gene expression and immunofluorescent analysis demonstrated that the majority of progenitors within D17 RO had a comparable identity as precursors in the ventral p3 region where serotonergic neurons arise from.

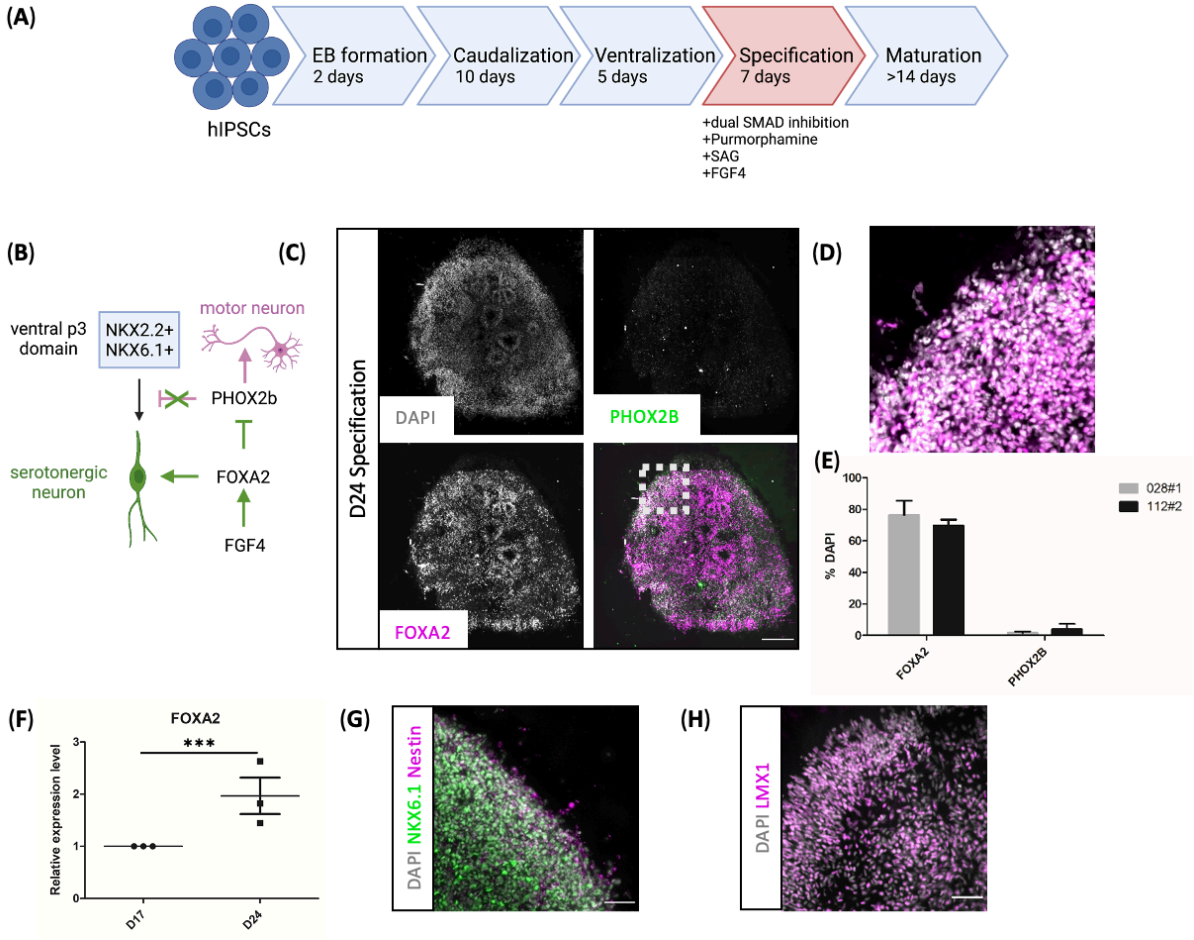

Figure 22: Characterization of D24 Raphe organoids after the specification.

(A) Scheme of the raphe organoid protocol with indicated factors facilitating the specification of serotonergic neurons. (B) Schematic overview of the effect of FGF4. FGF4 likely activates FOXA2, which inhibits PHOX2b and therefore, prohibits a motor neuronal fate. (C, D) Representative overview and close up images of fluorescence analysis of pro-motorneuronal marker PHOX2B and FOXA2. (E) Quantification of three independent differentiations show broad expression of FOXA2, while PHOX2b is just present in a subset of cells. (F) FOXA2 upregulation is validated by RT-qPCR analysis of three independent differentiations in D24 RO compared to D17. (G, H) Representative images of immunofluorescent stainings of p3-domain marker NKX6.1, pan-progenitor marker Nestin and LMX1, representing serotonergic differentiation cascade initiation. Data shown as mean ± SEM; Mann Whitney U test; *** $p<0.001$. Scale bars (C) 200, (E, H) 50 µm.

However, the ventral p3 domain gives rise to both, viscero-motor as well as serotonergic neurons (Pattyn *et al.*, 2003; Kiyasova and Gaspar, 2011)(Figure 22 B). The generation of the neuronal type is temporally controlled and the key player is forkhead transcription factor 2 (FOXA2) (Kittappa, Kehler and Barr, 2017; Deneris and Gaspar, 2018b). Its' expression activates a cascade of transcriptional factors directly involved in the development of serotonergic neurons (Okaty et al., 2015; Deneris and Gaspar, 2018b). FOXA2 is repressing PHOX2B, which is its counterplayer and acts as pro motor neuronal factor (Pattyn et al., 2000; Jacob et al., 2007b) (Figure 21 I). Here, fibroblast growth factor 4 (FGF4) was applied in the third phase of the differentiation protocol to upregulate FOXA2 in cultures

(Figure 22 A). In the developing brain, FGF4 is produced by the primitive streak from where it diffuses to cells (Alenina *et al.*, 2009). Previously, FGF4 was associated with the induction of serotonergic neurons *in vivo*, shown to diminish dopaminergic neurons, and was utilized for this purpose in 2D differentiation protocol for serotonergic neurons (Ye *et al.*, 1998; Kim *et al.*, 2002; Lu *et al.*, 2016; Vadodaria *et al.*, 2016). The quantification of immunostainings of RO at day 24 reveal a high expression of FOXA2 (Figure 22 C, D). 76.45 ± 3.42% and 69.59 ±1.34% of the progenitors are positive for FOXA2 (Figure 22 E). It's counterplayer PHOX2B was just detected in a small proportion of cells (1.73 ± 0.55% and 3.9 ± 0.76). This is also validated in RT-qPCR experiments in which FOXA2 is 1.97 ± 0.35 times higher expressed compared to D17 organoids (Figure 22 F). The expression of NKX6.1, NKX2.2 and FOXA2 marks the final defined serotonergic precursor. Together, they initiate the cascade of transcription factors leading to the differentiation towards serotonergic neurons (Cheng et al., 2003; Deneris and Gaspar, 2018b). LMX1b is the first element of this cascade which we could confirm the expression of LMX1 in our RO by immunostainings (Ding *et al.*, 2003) (Figure 22 H). This transcription factor is a crucial player in the network as it is initiating the expression of many serotonergic genes for instance FEV, TPH2 and VMAT2 (Ding *et al.*, 2003; Wylie *et al.*, 2010).

In conclusion, patterned RO consisting of progenitors displayed characteristic marker expression on gene and protein level similar to their *in vivo* counterparts on the verge to proceed the postmitotic serotonergic differentiation.

6.7.2 Mature raphe organoids developed functional serotonergic neurons

In the course of this project, several different compounds were tested specifically enhancing serotonergic differentiations and carefully integrated in the media composition (Figure 23 A). By switching to Neurobasal™, neurogenesis and survival was enhanced (Brewer *et al.*, 1993; Lu *et al.*, 2016). To facilitate the development of serotonergic neurons cultures were supplied with transforming growth factor beta 3 (TGFß-3) (Dias *et al.*, 2014), the tropomyosin kinase B (TrkB) agonists LM22A-4 and LM22B, mimicking the effect of brain derived neurotrophic factor (Rumajogee *et al.*, 2005; Massa *et al.*, 2010; Yang *et al.*, 2016), L-tryptophan (Höglund, Øverli and Winberg, 2019), glial cell-derived neurotrophic factor (GDNF) (Ducray *et al.*, 2006) and L-ascorbic acid (Shin *et al.*, 2004). To further foster neuronal differentiation, gamma-secretase was inhibited by DAPT (Crawford and Roelink, 2007). Resulting D45 mature RO displayed an enlarged population of serotonergic neurons, indicated by co-labeling HuC/D and serotonin (Figure 23 B, C). The serotonergic population make up 24.09 ± 4.43% and 15.78 ± 4.93% respectively, in two tested cell lines (Figure 23 D). Serotonergic neurons were further characterized by the expression of the rate limiting synthesis enzyme TPH2 and the vesicular monoamine transporter 2 (VMAT2), responsible for shuffling serotonin into vesicles (Figure 23 E, F).

Other smaller neuronal populations of GABAergic, glutamatergic, dopaminergic, noradrenalinergic as well as acetylcholinergic neurons were also detected (Figure 23 G-I).

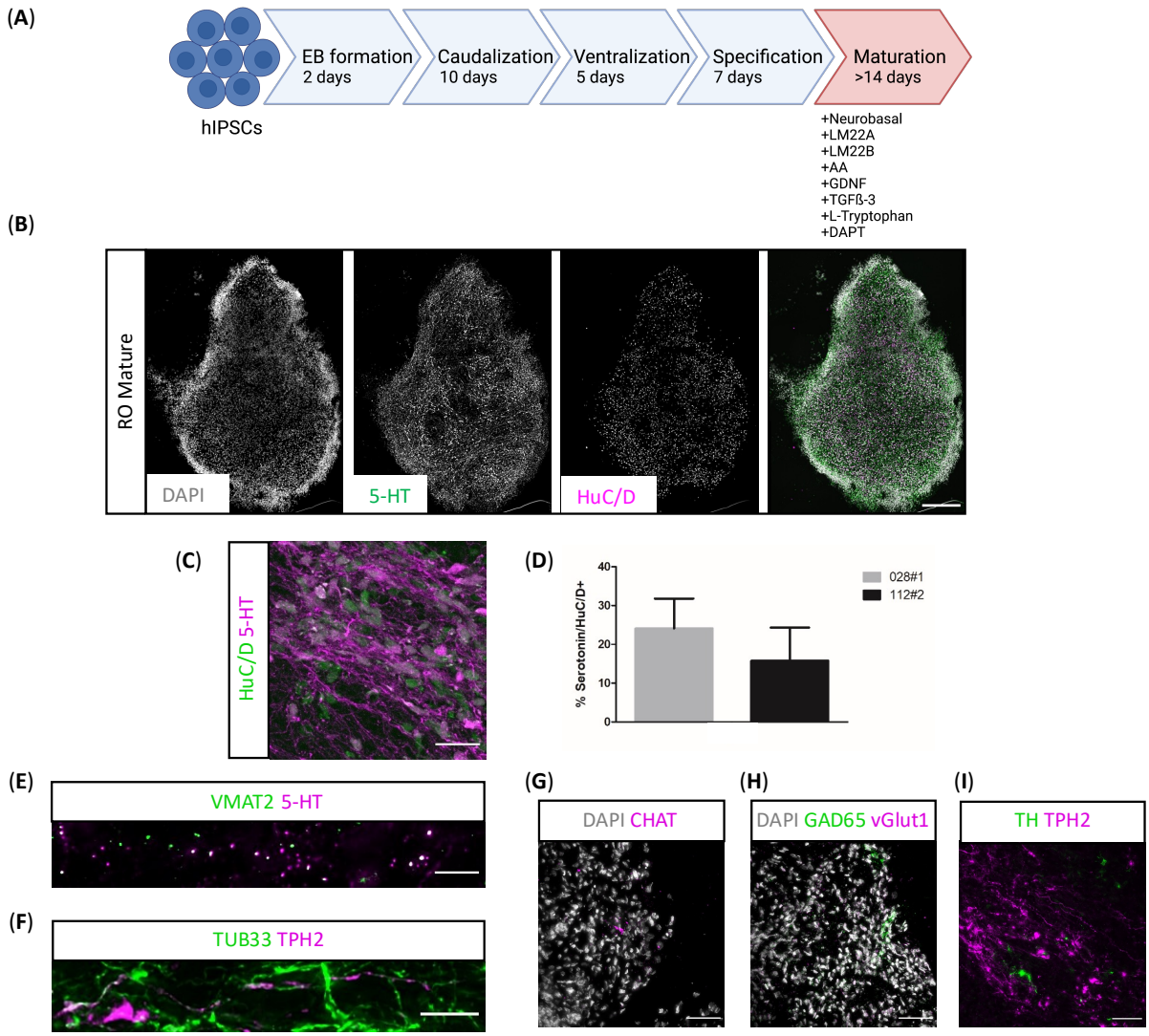

Figure 23: Characterization of mature raphe organoids at day 45.

(A) Scheme of the raphe organoid protocol with indicated maturation factors. (B, C) Representative overview and close up images of immunofluorescence stainings of pan-neuron marker HuC/D and serotonin. (D) Quantification of three independent differentiations reveal enlarged serotonergic population. (E, F) Representative images of immunofluorescence analysis of serotonergic marker. Double positive axons for serotonin and VMAT2; as well as pan-neuronal marker TUBB3 together with TPH2. (G-I) Additional immunofluorescent analysis of neuronal subtypes. Representative images of CHAT (motor neurons), GAD65 (GABAergic neurons), vGlut1 (glutamatergic neurons) and TH (dopaminergic neurons). Data shown as mean ± SEM. Scale bars (B) 250, (C) 25, (E, F) 10, (G, H, I) 50 µm.

In vivo, serotonergic neurons are capable to develop long projections throughout the entire brain and spinal cord. This feature needed to be fulfilled by RO-derived serotonergic neurons as they were required to expand towards cortical areas within the assembloid. Therefore, an outgrowth experiment was performed in which matured RO were seeded on Geltrex™-coated dishes to allow the

development of neurites (Figure 24 A). RO started to develop extensions after 24 hours and were analyzed after five days. Immunofluorescent stainings of βIII-tubulin (TUBB3) marked outgrowing neuronal processes. Double-labeling with serotonin exhibit serotonergic neurons (Figure 24 B). The observation allowed to conclude that RO-derived serotonergic neurons are indeed able to grow out which would provide the basis for the assembloid.

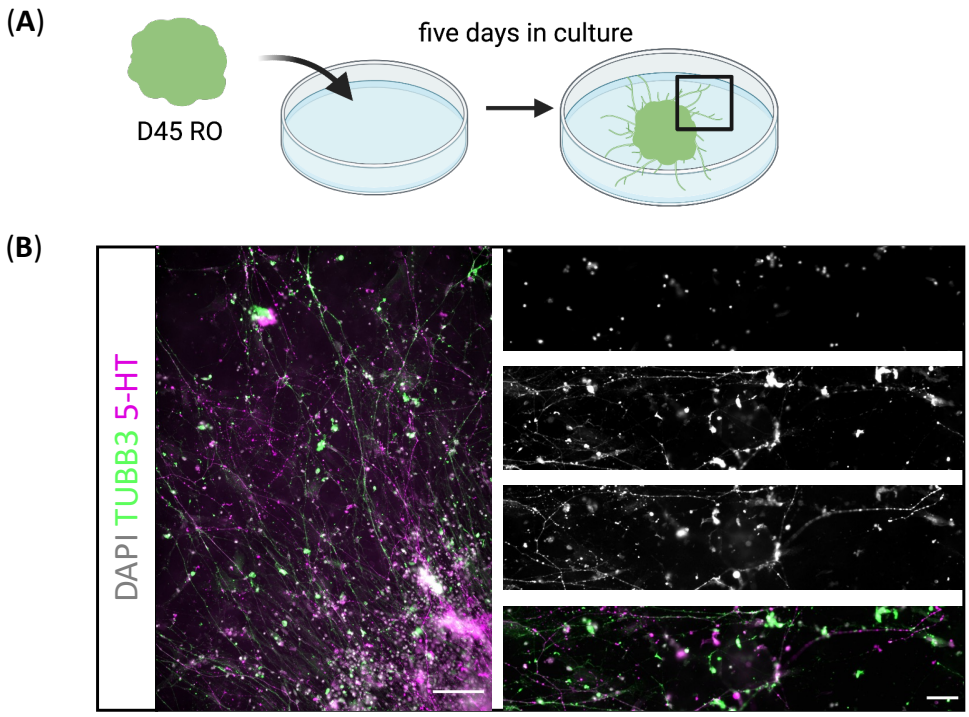

Figure 24: Outgrowth assay revealed great outgrowth potential of RO-derived serotonergic neurons.

(A) Schematic overview of experimental outline. RO were differentiated, plated on Geltrex™-coated dishes and processed after five days of culture. (B) Representative overview and close up images of immunofluorescent stainings of TUBB3 and serotonin.

In order to analyze the functionality of RO-derived serotonergic neurons, serotonin darkening 5-HT_{1A} receptor-based sensor (sDarken) was utilized (Kubitschke *et al.*, 2022). This genetically encoded serotonin sensor is based on the native 5-HT_{1A} receptor of which the third intracellular loop is replaced by a circularity permuted GFP (Figure 25 A). Upon binding of serotonin, the sensor's fluorescence is diminished and is restored after serotonin removal.

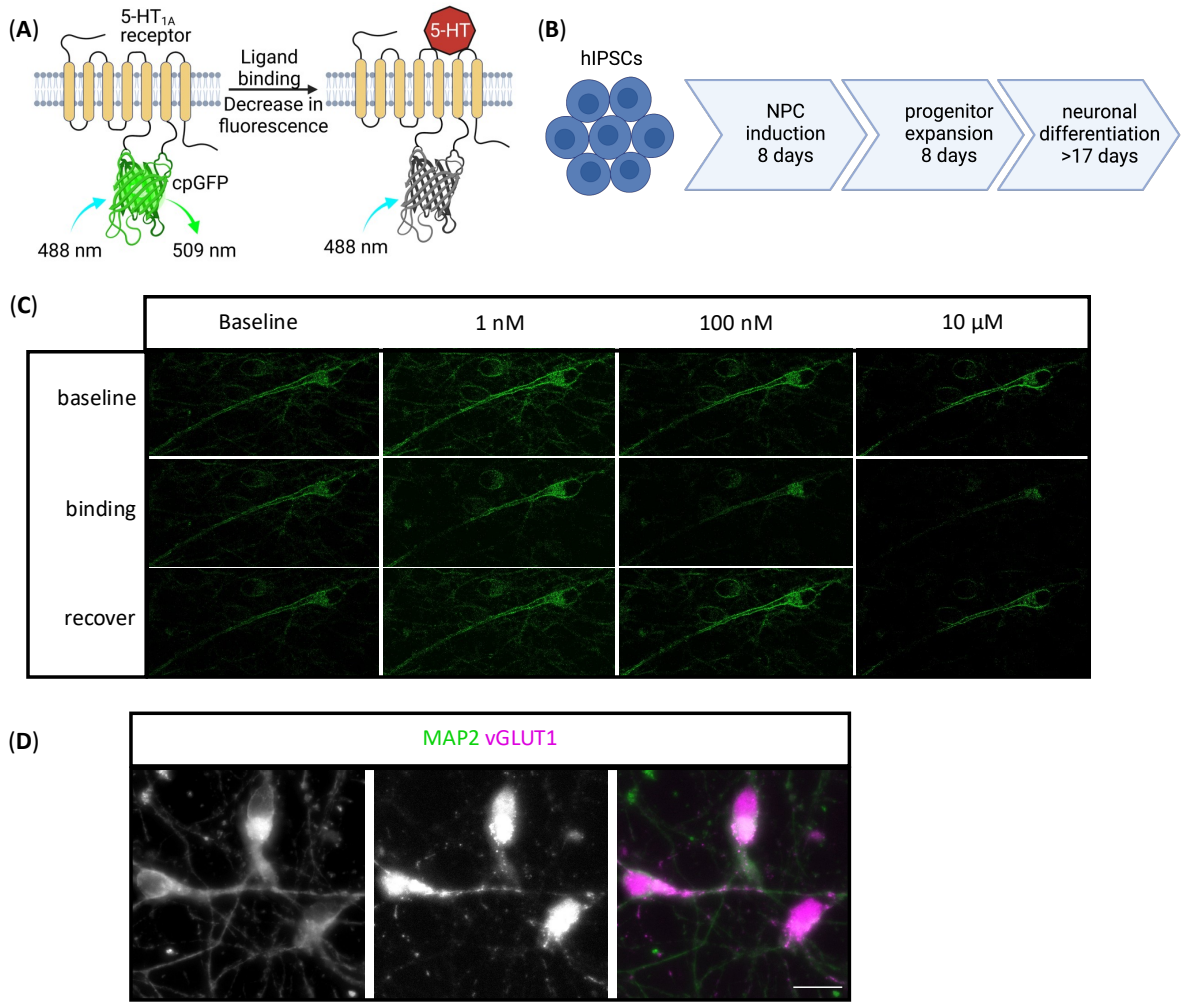

Figure 25: Characterization of sDarken using hiPSC-derived cortical neurons.

(A) Scheme of serotonin sensor sDarken. (B) Scheme of cortical neuron differentiation protocol. Cortical progenitors were infected with pLVX-EF1α-sDarken and subsequently differentiated to neurons. (C) Representative images of sDarken expressing neurons (baseline), after administration and binding of serotonin (binding) and after washout period (recovery). (D) Cortical neurons were validated by co-immunostainings for vGlut1 and MAP2 for glutamatergic neurons. Scale bar 15 µm.

As sDarken was not tested in the human context yet, functioning needed to be validated in the human system prior further experiments. Therefore, well-established cortical neuron protocol of the group from Philipp Koch was applied (Wilkens *et al.*, 2022). Briefly, hiPSC cultures were pushed towards neuroectodermal fate by an enhanced dual-SMAD inhibition combined with an inhibition of wnt-signaling (Figure 25 B). Resulting D17 progenitors were transfected with a lentivirus carrying sDarken overnight. Subsequently, cultures were subject for neuronal differentiation initiated by DAPT and forced cell cycle arrest. Cortical neuron differentiation was further fostered by a temporary exposure to gamma-aminobutyric acid (GABA) and elevated calcium chloride levels. Cortical neurons were validated by immunofluorescence analysis and expressed neuronal marker MAP2 and glutamatergic marker vGlut1 (Figure 25 D).

Live imaging of cortical neuron cultures showed a stable sDarken fluorescent signal and just upon administration of serotonin to the media, a rapid decline of the intensity was observed (Figure 25 C). The signal intensity persisted at lower levels and could be fully restored by a washout. These application and wash-out cycles could be repeated several times. In order to validate the sensitivity of sDarken, different serotonin concentrations were tested. sDarken displayed a slight reduction of signal intensity at 1 nM serotonin and a brief wash-out period to recover the baseline signal. Higher levels of serotonin as 100 nM and 10 µM caused a stronger declined and needed an extended wash-out phase. In conclusion, sDarken demonstrated functioning in the human system, was able to detect low and higher concentrations of serotonin reliable and proofed repeatability.

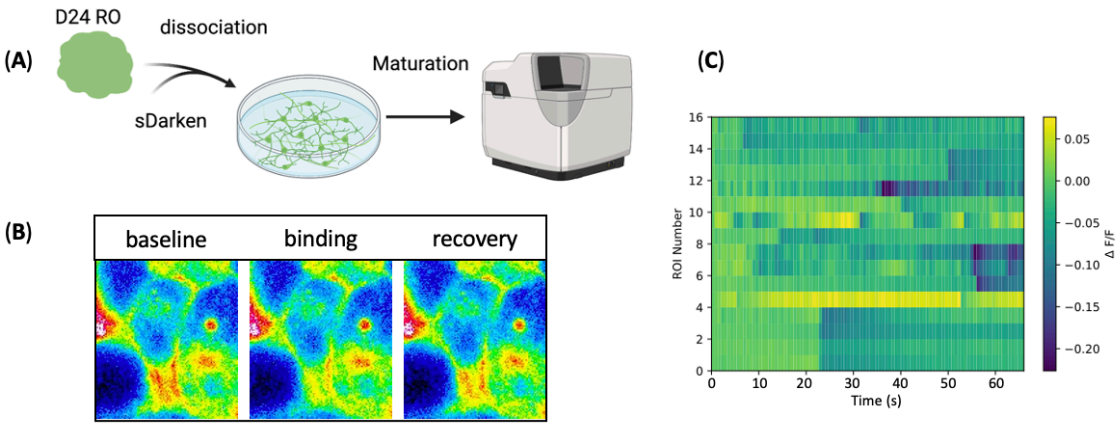

Figure 26: Characterization of sDarken using dissociated RO.

(A) Scheme of experimental outline. D24 RO were dissociated using Trypsin-EDTA and infected with pLVX-EF1α-sDarken. After plating cells on dishes with a polymer coverslip bottom, cultures were subject for maturation. (B). Representative images of sDarken expressing cells during baseline, serotonin binding and recovery. No exogenous serotonin was added to the cultures. (D) Heatmap of selected regions of interest (ROIs) show repeated decreasing and recovering sDarken signal, displayed as % Δ F/F. Signal intensity changes of sDarken was analyzed in collaboration with Lutz Wallhorn.

To test for functionality of sDarken in context of endogenous serotonergic innervation, dissociated RO-cultures were utilized. Therefore, D24 RO were dissociated using EDTA-Trypsin, transfected with pLVX-EF1α-sDarken and plated on Geltrex™-coated dishes (Figure 26 A). The majority of cells expressed sDarken and after a 14-day maturation period, live imaging was performed without any exogenous serotonin present. Cells displayed recurring rapid diminishing and recovering of the fluorescent signal of sDarken as seen in the exemplary trace heat maps (Figure 26 B, C).

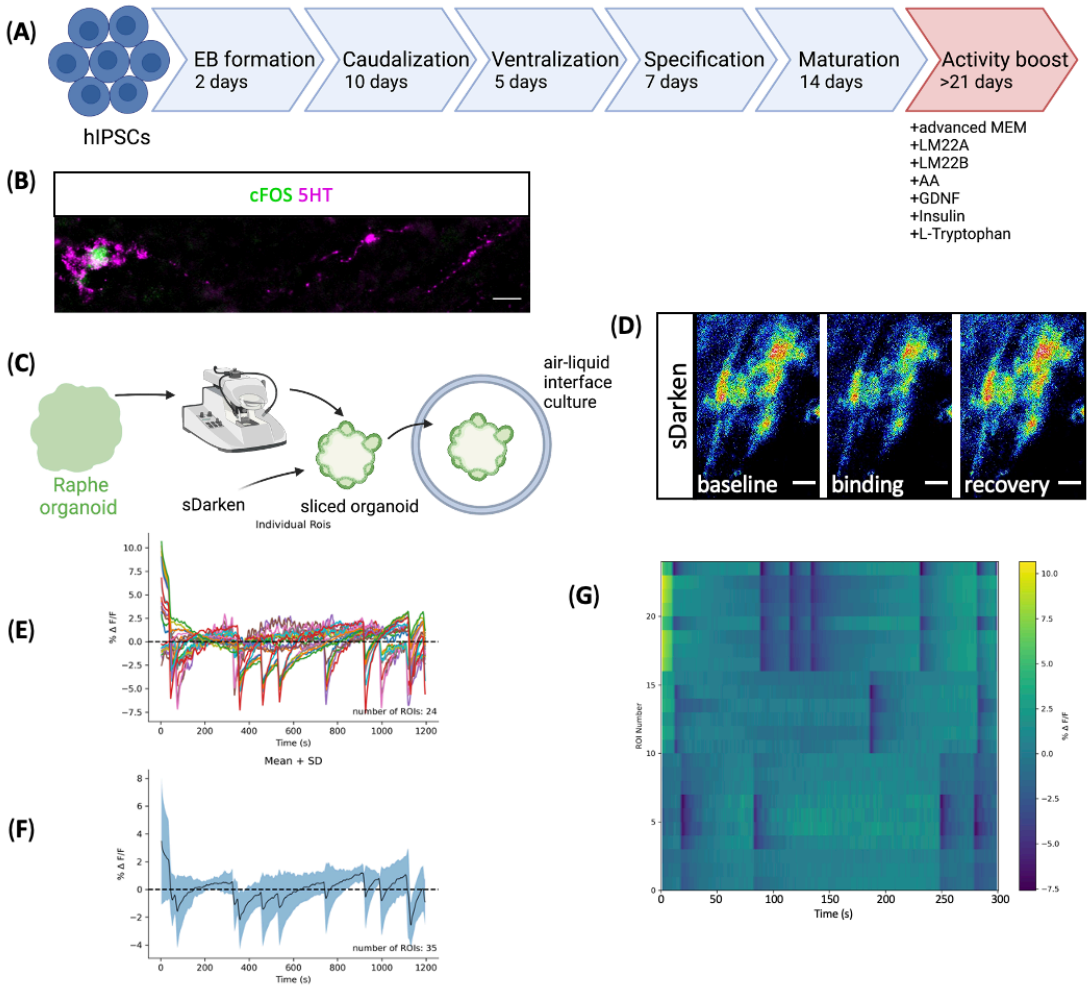

Figure 27: Validating serotonergic activity in sliced RO using sDarken.

(A) Schematic overview RO-differentiation protocol with highlighted activity boost phase. (B) Representative immunofluorescent staining of activity marker cFos and serotonin. (C) Scheme of experimental outline. RO were generated and sliced prior 200 µm slices were transfected with pLVX-EF1α-sDarken. (D) Representative images of neurons carrying sDarken during baseline, after binding of serotonin and after recovering. (E) RO were recorded for five minutes and analyzed. Fluorescent intensity changes of all selected ROIs are displayed as % Δ F/F. In total 24 ROIs of three independent differentiations were analyzed. (F) Mean intensity changes as mean + SD. (G) Heatmap indicating fluorescent intensity changes of sDarken in all ROIs. Scale bars: (A) 15, (D) 10 µm. Signal intensity changes of sDarken was analyzed in collaboration with Lutz Wallhorn.

After validating serotonergic activity and functionality of sDarken in dissociated cultures, serotonergic activity in RO was assessed. Therefore, D24 RO were sliced and pLVX-EF1α-sDarken was applied directly to 200 µm slices for 48 hours. Further maturation as described above was performed as air-liquid interface culture on cell culture inserts (Giandomenico *et al.*, 2019). When imaging RO after a three-weeks maturation period, no spontaneous activity was observed. Subsequently, the media composition was adjusted and tailored to foster functionality (Figure 27 A). Thus, advanced MEM was used as base media supplemented with insulin as well as GDNF, LM22A, LM22B, L-ascorbic acid and L-

tryptophan (Garcia *et al.*, 2008). After exposing RO slices to this media for additional 21 days, immunofluorescent analysis revealed c-FOS expression in serotonin-positive neurons, indicating neuronal activity (Figure 27 B). Subsequent experiments using sDarken on functionally matured RO were performed (Figure 27 C). Despite several improving measures, the efficiency of pLVX-EF1α-sDarken remained below 5% in RO slices. Live imaging of sDarken-expressing cells revealed rapid diminishing of sDarken fluorescent signal indicating spontaneous neuronal activity (Figure 27 D). Manually selected regions of interest (ROIs) of five-minute videos were analyzed and resulting trace heat maps showed repeating diminishing-recovery of sDarken signal across several cells (Figure 27 E-G).

Taken together, RO developed serotonergic neurons characterized by the expression of crucial proteins like TPH2, VMAT2 as well as serotonin itself. Moreover, by applying distinct media supplements, RO-derived serotonergic neurons proved functional activity validated by sDarken.

6.8 Cortical-raphe-assembloids displayed serotonergic innervation and induced proliferation

The assembloid model has shown to display certain features of the human brain by recapitulating interactions of different brain regions. This allowed modeling the migration of interneurons from ventral to the dorsal part of the cortex, the formation of reciprocal thalamocortical projections or even skeletal muscle contraction control of the cortex (Bagley *et al.*, 2017; Xiang *et al.*, 2017, 2019; Andersen *et al.*, 2020). The here described generation of organoids representing the raphe nuclei, allowed for the first time, by fusing them with cortical organoids, to create an assembloid focusing on the serotonergic function during corticogenesis.

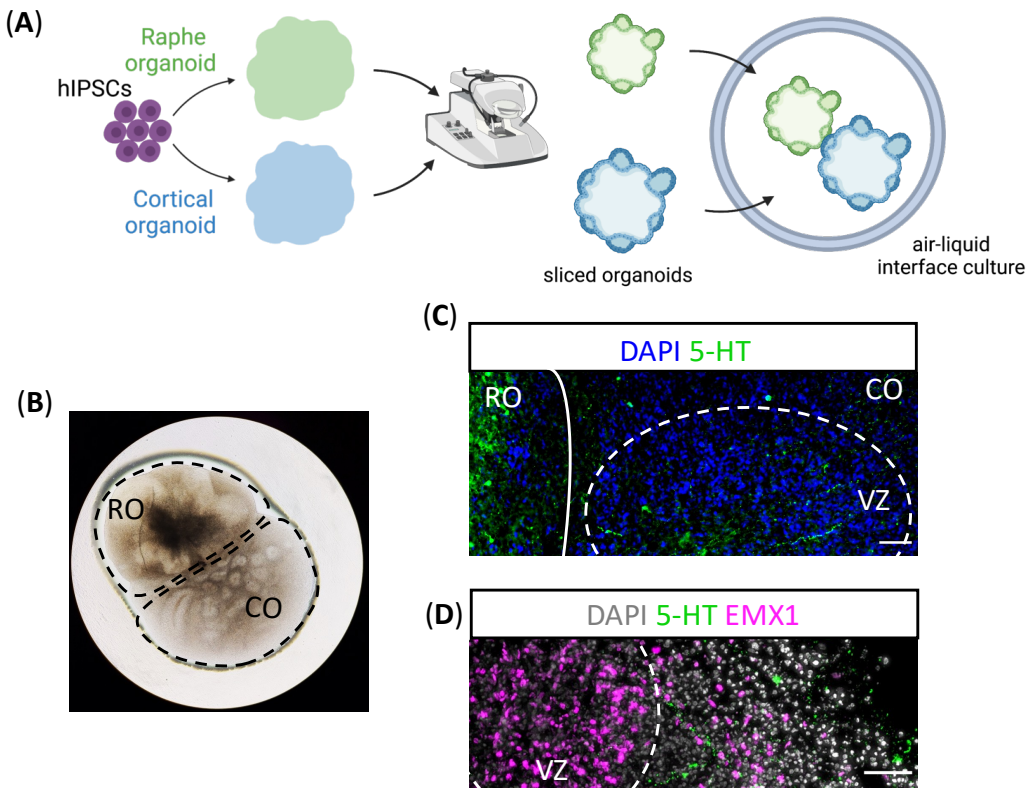

Figure 28: RO-CO assembloids displayed ingrowing RO-derived serotonergic neurons.

(A) Scheme showing the experimental outline and assembloid procedure. (B) Representative bright field image of RO-CO assembloid as air-liquid culture. (C) Representative image of immunofluorescent stainings of RO-CO assembloid displaying in growing serotonergic projections. (D) Representative image of immunofluorescent stainings showing serotonergic projections around EMX1-positive cortical VZ in assembloid. Scale bars: 50 µm.

To that end, RO and CO were differentiated separately according to their protocols and processed with a vibratome around D40. 200 µm slices of each organoid type were then placed on cell culture inserts in close proximity (Figure 28 A). The slices were kept as air-liquid interface and exposed to functional boost media for at least three weeks. After this period, slices were firmly attached, indicating strong interconnections (Figure 28 B). Indeed, immunofluorescent stainings reveal RO-derived serotonergic projections spanning broadly through assembled cortical organoid areas (Figure 28 C, D). Of note, somas of serotonergic neurons were restrained to raphe part of the assembly, indicating that serotonergic neurons are indeed develop projections and are not migrating.

Next, to validate the functionality of RO-CO-assembloids, immunofluorescent experiments focusing on synaptic connections were performed. Here, overlapping signal of serotonergic projections with synapsin and Homer were identified (Figure 29 A). Synapsin is a marker of the pre-synapse while Homer marks post synaptic structures. Coinciding signal of all three markers indicate synaptic structures between RO-derived serotonergic neurons and CO cells. As reported above, 5-HT_{2A} is expected to be

more abundantly expressed in the SVZ, immunofluorescent analysis of this receptor together with serotonin as well as Homer was performed (Figure 29 B). In line, we observed overlapping signal, indicating that RO-derived serotonergic neurons might indeed be able to innervate cells in assembled CO.

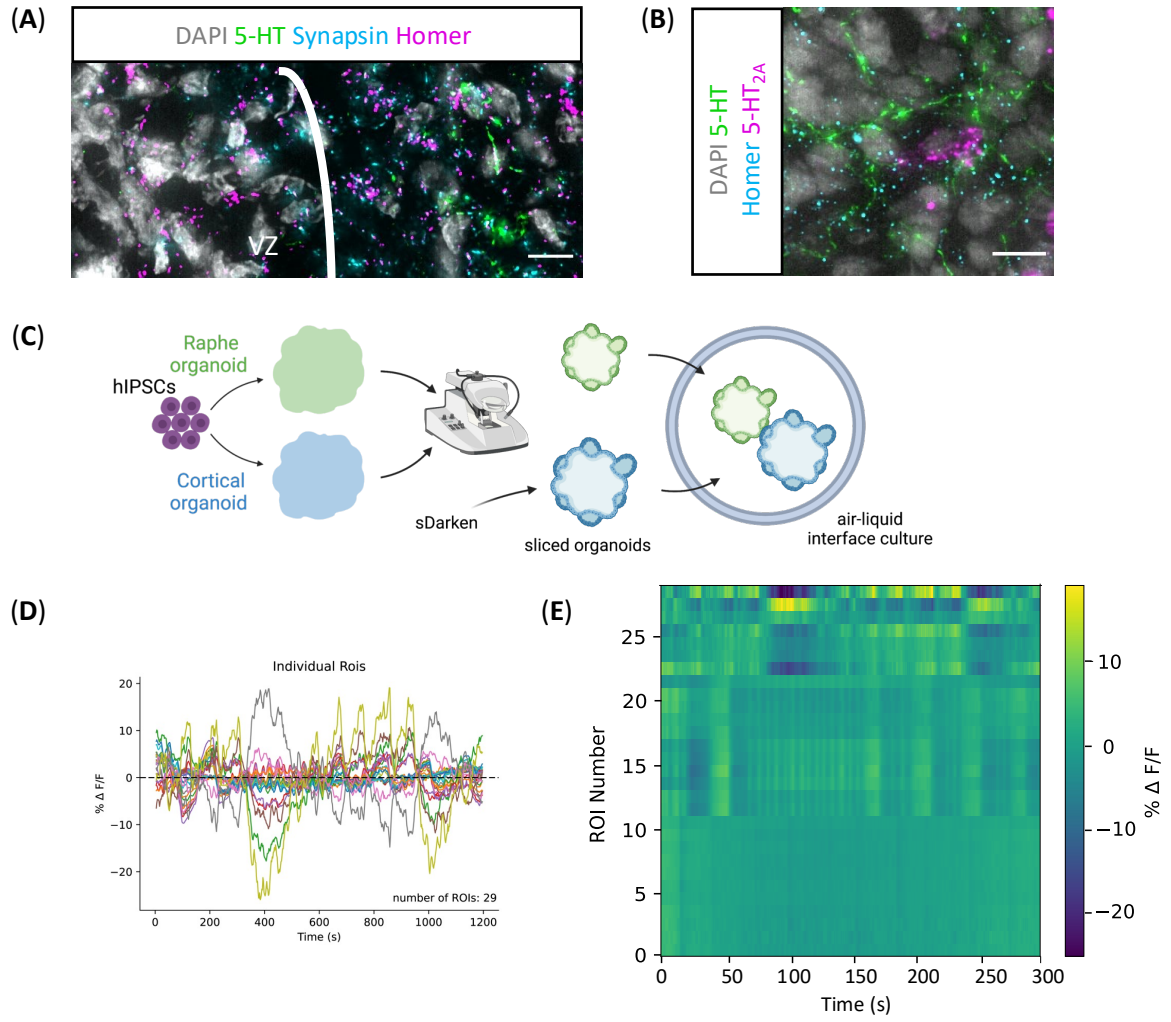

Figure 29: Introduction of sDarken to assembloids validated serotonergic innervation of assembled cortical organoids.

(A, B) Representative images of immunofluorescent analysis of synaptical markers in RO-CO assembloids. Overlapping signal of serotonergic projections and pre- (synapsin) and post- (Homer) synaptic markers as well as the serotonergic receptor 5-HT_{2A}. Scale bars: 10 µm. (C) Scheme of experimental outline. Organoids have been developed independently and sliced. 200 µm CO slices were infected with pLVX-EF1α-sDarken prior the assembly. (D) CO within the assemblies were recorded for five minutes and 29 ROIs in three independent differentiations were analyzed. Fluorescent intensity changes of all single ROIs are displayed as % Δ F/F. (E) Heatmap indicating fluorescent intensity changes as % Δ F/F of all ROIs. Signal intensity changes of sDarken was analyzed in collaboration with Lutz Wallhorn.

Thus, the structural component to allow innervation are present in the assembly, however, it remained open, whether RO was indeed innervating assembled CO. Therefore, pLVX-EF1α-sDarken was applied

to sliced CO for 48 hours before forming the assembloid as described above (Figure 29 C). Despite several improvement measures, the efficiency of the transfection remained inefficient with >1% of the cells showing a sDarken fluorescent signal after >7 days. Live imaging of expressed sDarken in assembled CO was performed after >21 days as air-liquid interface culture in functionality boost media. Trace heatmaps display rapid diminishing of sDarken fluorescent signal in manually selected ROIs in three independent assemblies (Figure 29 D, E). Thus, serotonergic innervation of CO can be concluded.

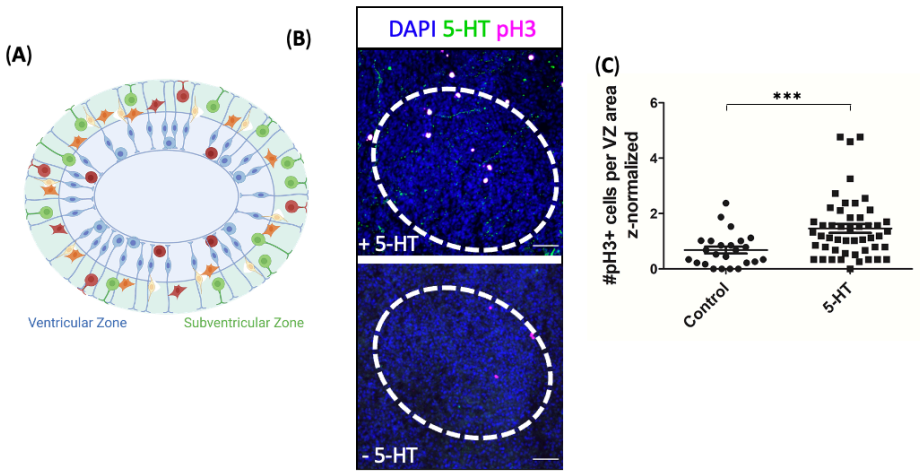

Figure 30: Serotonergic innervation increased proliferation in cortical VZ in RO-CO assembloids.

(A) Schematic overview of ventricular and subventricular structure. Cells which were quantified here are marked in red. (B) Representative images of immunofluorescent stainings for pH3 in cortical VZ and SVZ in assembloids. Mitotic cells were labeled with pH3 and occurred more frequently if serotonergic projections were nearby. Scale bars: 50 µm (C) Quantification of pH3 positive cells per cortical VZ and SVZ. Ventricular areas innervated by serotonergic projections showed a significant higher number of dividing cells. Three independent differentiations were analyzed and data are shown as mean ± SEM; Mann Whitney U test; *** p<0.001.

As demonstrated above, different progenitor populations within CO, namely apical progenitor cells as well as basal progenitor cells, showed an increased proliferation behavior upon serotonin exposure. Additionally, RO-derived serotonergic neurons were capable of growing into assembled CO and granted serotonergic innervation. Thus, an assembly model was provided which might be able to represent the mitogenic effect by serotonergic innervation. To test this hypothesis, mitotic events of all progenitor types in the VZ and SVZ of cortical ventricular structures were quantified (Figure 30 A). Thereby, ventricular structures were distinguished depending on whether or not they displayed in growing serotonergic neurons (Figure 30 B). The subsequent quantification revealed a significant increase in proliferation in cortical structures in presence of serotonergic projections (1.46 ± 0.16) compared to others (0.68 ± 0.13) (Figure 30 C).

Therefore, RO-CO assembloids were capable to develop projections and form connections where serotonergic innervation could be demonstrated. Moreover, RO-CO assembloids recapitulate the

proliferative stimulation effect of serotonin on cortical progenitor types which was previously identified in pharmacological experiments.

7 Discussion

The first part of this thesis described an mitogenic effect of serotonin on apical and basal progenitor cells via the receptor subtypes 5-HT_{2C} and 5-HT_{2A}, respectively. IPs were the only precursor type which did not show proliferation behavior changes. In the second part, a new organoid protocol was developed which resembles the human raphe nuclei. It recapitulated the identities of precursor stages and gave rise to functional serotonergic neurons. Combining RO with cortical organoids to form an assembloid, allowed serotonergic innervations of cortical cells and was sufficient to induce cortical progenitor proliferation.

7.1 HiPSCs and organoid development

The technology to re-program somatic cells to a pluripotent stem cell state, was an enormous milestone for the research field of neuroscience. As human material is otherwise challenging to obtain and very limited. Thus, for decades questions targeting the neuronal system had to be answered using animal models or human cancer cell lines which nevertheless, elevated our understanding tremendously. Fundamental differences to the human system became more and more evident which brought up the urgent need for improved human models. HiPSCs gave researchers the opportunity to routinely work with human neuronal cultures. Since the discovery, neuronal differentiation protocols using human iPSCs emerged, targeting different neuronal subtypes in greater efficiency and allowed studying human evolution, corticogenesis or associated diseases in a human system.

Ever since the first description, cerebral organoids have been continuously improved. A constant drawback of organoids is the lack of proper supply of nutrients and O2 to the inner organoid core (Lancaster *et al.*, 2013; Kelava and Lancaster, 2016; Qian *et al.*, 2017; Qian, Song and Ming, 2019). Reducing the volume by slicing the organoids helped significantly to overcome this issue (Giandomenico *et al.*, 2019; Qian *et al.*, 2020; Szebényi *et al.*, 2021). Adopted from murine brain slice cultures, air-liquid interface cultures have been introduced by culturing human organoid slices on cell culture inserts (Giandomenico *et al.*, 2019; Szebényi *et al.*, 2021). Those techniques have been introduced in this project and helped facilitate long term cultures. When possible, slices of the same organoid were assigned to different treatment conditions in order to reduce variability (Qian, Song and Ming, 2019). Sliced cultures also enabled the application of lentiviruses. Preliminary transfection experiments using whole organoids did not result in an expression of sDarken (data not shown). Just the administration of lentivirus on sliced cultures, resulted in a visible expression. ALI fostered neuronal projections and thus, improved assembloids significantly. Live imaging of organoids was just feasible utilizing ALI technique since organoids had a set position while remained optimal provided with nutrients.

Unfortunately, the organoid-field is still battling with protocol robustness and recent work highlighted the importance of the starting iPSC condition. Improved cultures were reported by either inhibiting FGF-2 or activating TGF-ß signaling (Ideno *et al.*, 2022; Watanabe *et al.*, 2022). Both studies demonstrate convincing results which may have improved organoid cultures and reduced variation and failed attempts. Unfortunately, both reports were published in October 2022 and could therefore not applied in this thesis.

7.2 Apical progenitors

Rodent models showed that serotonin has an effect on neural progenitor proliferation (Banasr *et al.*, 2004; Vitalis *et al.*, 2007a; Cheng *et al.*, 2010). To further decipher the mitogenic effect of serotonin in the human system, distinct progenitor populations were targeted as mono culture in 2D, as well as in cortical organoids.

Having differentiation protocols available not exclusively targeting post mitotic neurons, but focusing on different neuronal progenitor types, was crucial for this study. It allowed the standardized and reliable generation of larger quantities in short time periods. Apical progenitors used in this study can be kept stable over a brief time period of 2-3 passages before losing their proliferative capabilities. This rather short time window however, was sufficient to perform the experiments stated in this thesis. The immunofluorescent analysis and expression profile of the aPC cultures in the RNA bulk sequencing experiments helped characterizing the cultures. Moreover, the comparison of this to other datasets of the cell type previously generated in the Koch group, highlighted the robustness of the protocol (Wilkens *et al.*, 2022). While many genes are expressed by both NES and aRGs, the expression of OTX2, SOX2 or HES5 was reported to be more prevalent in NES, others, including VIM and PALLD are indicating radial glia characteristics (Pollen *et al.*, 2015; Shang *et al.*, 2018). Hence, the integrated term apical progenitor cells seemed justified.

Apical progenitor cells showed an increase in proliferation upon 5-HT_{2C} activation (Figure 13) which has been previously associated with proliferation in rodents (Banasr *et al.*, 2004). However, on the first glance, the results appear contrary to other reports using human material (Dakic *et al.*, 2017; Wang *et al.*, 2021). Wang and colleagues used NES cultures and cerebral organoids with respect to depressive behavior (Wang *et al.*, 2021). Interestingly, they identify 5-HT_6 highly expressed and reported an increase of proliferation upon receptor activation. However, given that their NES maintenance is achieved by two posteriorizing agents (10 ng/ml FGF-2 and 3 µM CHIR99021), the cells might have a more caudalized identity. Unfortunately, they fail to further define their targeted cell type (Wang *et al.*, 2021). This study highlights the complex role of serotonin and its highly divers network of receptors in different cell types (Nichols and Nichols, 2008).

Dakic and colleagues utilized human ESC-derived neural progenitor cells to study the effect of 5-methoxy-N,N-dimethyltryptamine (5-MeO-DMT) (Dakic *et al.*, 2017). This psychoactive substance acts via the serotonergic receptors 5-HT_{2A} and 5-HT_{2C} and is associated with neuroregenerative effects as well as neuroimmune communication (Fontanilla *et al.*, 2009; Szabo *et al.*, 2016). In contrast to this thesis, they do not identify 5-HT_{2C} expression in their progenitor culture (Dakic *et al.*, 2017). Their cultures were further defined in their previous work where 91.25 % of the cells stained positive for TBR2 (Dakic *et al.*, 2016). Thus, Dakic *et al.* seemed to work with a culture equating intermediate progenitors whereas this study focused on apical progenitor cells (Cappello et al., 2006; Dakic et al., 2016). Dakic *et al.* did not observe any changes after 5-MeO-DMT exposure on their IP-like cells which supports the outcome observed in this thesis after targeting IPs in CO (Figure 17) (Dakic *et al.*, 2017).

Apical progenitors are present in the ventricular zone but are restricted to the apical lining during mitosis and allowed identification of the cell type in cortical organoids. The expression of 5-HT_{2C} in cerebral organoids was already shown elsewhere and could be validated in this study (Dakic *et al.*, 2017). Interestingly, just a subset of cells in the ventricular zone of mature organoids showed a pertinent immunofluorescent signal (Figure 15 C). In line, relevant HTR2C expression was found scattered in single cell RNA sequencing experiments. In contrast, the same cell cluster of D30 COs did not show any HTR2C expression. Together, this indicates a heterogeneity within the ventricular zones in COs. One possibility would be a diverse cell composition of VZ. Apical progenitors comprise several subtypes, as neural epithelial cells, apical intermediate progenitors or apical radial glia cells (Florio and Huttner, 2014). That raises the possibility that one cell type, but not the others might express the receptor. Given that the expression was detected in later stage organoids, apical radial glia cells might be the sought-after type as they emerge later during corticogenesis.

Serotonin has shown to have concentration dependent effects. For instance, Cheng and colleagues observed an increase in proliferation after serotonin exposure and a reduction after serotonin excess (Cheng *et al.*, 2010). Furthermore, interneurons in the cortex showed a slowed migration in serotonin-depleted mice, while *in vitro* experiments demonstrated similar results after a serotonin excess. Here, no differences were detected after exposing cultures to 10 or 100 µM serotonin (Figure 12 B). These concentrations might indicate the range in which serotonin shows a stimulative effect. Based on the described literature, one shall expect a decline of the mitogenic effect or even a reduction in proliferation in higher concentrations.

The mitogenic effect of serotonin on aPCs seems to be exclusively via 5-HT_{2C}– activation. The activation of other receptors tested in this study, namely 5-HT_{1A}, 5-HT_{2A} and 5-HT_{2B} did not result in an effect on proliferation. Agonist and antagonist experiments were designed to ensure target receptor activation while unintended co-activation of additional receptors was avoided. Thus, agonist concentrations were

used in a low concentration at 20-times the EC50 value. For instance, 2.2 nM CP809101 guaranteed the full activation of 5-HT_{2C} (affinity 0.11 nM), while other receptors like 5-HT_{2A} and 5-HT_{2B} with reported affinities of 65.3 nM and 119 nM, respectively remained disregarded. To sufficiently inhibit receptors while sparing other subtypes, 40-times the IC50 concentration was used.

7.3 The role of bRGs during corticogenesis and serotonin's contribution

The second type of progenitor class addressed in this thesis were basal progenitors including basal radial glia cells. Basal progenitor cells were classified as PTPRZ1-positive precursor, localized and dividing in the subventricular zone, similarly as done elsewhere (Kalebic *et al.*, 2019). The group might contain some rare and not well define cell types like subapical progenitors, but the majority are likely basal radial glia cells (Betizeau *et al.*, 2013; Pilz *et al.*, 2013; Florio and Huttner, 2014). Those have been discovered in 2010 (Hansen, 2010) and subject of growing interest since. The relevance of this precursor for the human brain development is apparent by now, but many questions are still unsolved (Bershteyn *et al.*, 2017; Penisson *et al.*, 2019; Fischer *et al.*, 2022; Kaluthantrige Don and Kalebic, 2022). The amount of bRGs in cortical organoids does not reflect the quantity found i*n vivo* yet and is therefore subject for constant improvement (Watanabe *et al.*, 2017; Penisson *et al.*, 2019; Kaluthantrige Don and Kalebic, 2022). Hence, the application of the 2D culture offered the possibility for a homogeneous cell culture and allowed an easier readout in a large number of cells.

Here, 2D cultures and 3D cortical organoids revealed mitogenic effect of serotonin via 5-HT_{2A}-activation (Figure 13, 15). The expression of 5-HT_{2A} of basal radial glia cells was previously shown in two independent studies using human fetal tissue (Mayer *et al.*, 2019; Xing *et al.*, 2020). In line with the data of this thesis, Xiang and colleagues demonstrated that its activation upregulates bRGs proliferation (Xing *et al.*, 2020). Conversely, this effect was not observed in the second paper, rather an effect on bRG fibers (Mayer *et al.*, 2019) . During maintenance of bPC 2D cultures, proliferation is sustained by the addition of FGF2 which is known as strong mitogen (Jin, Hu and Feng, 2005; Bithell *et al.*, 2008). However, preliminary data acquired using the normal maintenance media including FGF2, showed a tendency but failed to reach statistical relevance. Just the withdrawal of the growth factor revealed significant differences induced by 5-HT_{2A} activation. This indicates that the potent mitogenic effect of FGF2 covered the shallower stimulation by serotonin. Concerns initiating bRG differentiation after FGF2 withdrawal could be reconciled, as >90% of the cells remained positive for PTPRZ1.

In this context, follow up experiments examining long lasting effects of serotonin exposure would be of interest. Upper layer neurons are mostly generated by bRGs *in vivo* which is likely also true in the organoid model (Watanabe *et al.*, 2017; Penisson *et al.*, 2019). Given that serotonin increased the bPC proliferation and thus, likely expanded the bRG pool in cortical organoids, it is reasonable to assume

that this might lead to a higher abundance of upper layer neurons (Kalebic *et al.*, 2019). Furthermore, both studies Mayer *et al.* and Xing *et al.* highlighted the role of serotonin for the fibers and morphology of bRGs which has not been addressed here. Follow up experiments utilizing the here described bRG 2D and organoid 3D model could target morphology changes after serotonin exposure (Mayer *et al.*, 2019; Xing *et al.*, 2020).

7.4 Raphe organoids and Assembloids

The here developed raphe organoid fills a hole in the compilation of established regional specific brain organoids including midbrain, cerebellum or thalamus (Muguruma *et al.*, 2015; Jo *et al.*, 2016; Xiang *et al.*, 2019; Kelley and Pașca, 2022). After balancing carefully potency and duration of the activation of distinct signaling pathways, RO displayed specific marker expression throughout different progenitor states and gave rise to functional serotonergic neurons (Figure 20-27).

The protocol was developed with one control cell line and validated in a second one. Although the second cell line also displayed fundamental precursor markers and serotonergic neurons, the efficiency was reduced. It is likely, that slight adaptations would elevate the results greatly. The sensitivity of the utilized signaling pathways are known to be cell line dependent. Specifically, Nolbrant and colleagues demonstrated that effective midbrain caudalaziation of different PSCs lines via Wnt agonist GSK3i varied significantly between 0.6 and 0.9 µM (Nolbrant *et al.*, 2017). Similar results were reported regarding an efficient ventralization where different stem cell lines needed various concentrations of activators (Nolbrant *et al.*, 2017). The optimal concentrations of molecules were tested for eight lines, just two of them proved similar concentrations demands (Nolbrant *et al.*, 2017). That different cell lines respond differently when exposed to a signaling pathway activator or inhibitor, is known to the research field. This might also be the reason why organoid publications often just use one cell line (Muguruma *et al.*, 2015; Bagley *et al.*, 2017; Pellegrini *et al.*, 2020) or just show data from one line (Jo *et al.*, 2016; Xiang *et al.*, 2017; Eura *et al.*, 2020).

FGF4 was used to promote a serotonergic fate, as previously indicated by 2D serotonergic differentiation protocols (Lu *et al.*, 2016; Vadodaria *et al.*, 2016, 2019). However, the precise mechanism is not yet understood (Gaspar and Nedelec, 2016). Recent evidence points to an upregulation of FOXA2 instead of a downregulation of PHOX2b. In an FGF4 induced murine heart organoid, unintended high levels of FOXA2 were detected (Lee *et al.*, 2020).

Published serotonergic 2D differentiation protocols achieved around 60-80 % serotonergic neurons (Lu *et al.*, 2016; Vadodaria *et al.*, 2019). This is significantly higher than the number of serotonergic neurons in this study. Similar differences were observed in the generation of dopaminergic neurons in 2D protocols and within midbrain organoids. While Tieng and colleagues reach 70-80 % dopaminergic

neurons in 2D, they achieve approximately 25 % in midbrain organoids, a value also reached by others (Tieng *et al.*, 2014; Jo *et al.*, 2016). Organoids seek to represent brain areas with a distinct identity which also includes other cell and neuron types. As the DRN and MRN have around 50 and 20 % serotonergic neurons, respectively, RO indeed reached comparable values (Descarries *et al.*, 1982; Sos *et al.*, 2017).

Several optimization steps of the protocol were needed to achieve active RO-derived serotonergic neurons. Surprisingly, 2D serotonergic neurons (data not shown) or RO-dissociated cultures did not need extra maturation steps. Hence, the maturation of serotonergic neurons in 3D organoids emerged to be more complex and needed additional clues. In this context, two recent publications of the Studer group shedding light on the role of the epigenome in the context of neuronal maturation could be helpful. They identified genes, which transiently inhibited, facilitate a rapid maturation (Ciceri *et al.*, 2022). A defined mix of four factors was presented which fosters neuronal maturation more efficiently than other common approaches (Hergenreder *et al.*, 2022). Moreover, they proof the universal validity of their agents by successfully applying them to motor neurons and even melanocytes (Hergenreder *et al.*, 2022). Thus, it is likely that the application of their compounds to RO would enhance the maturation significantly.

Although others tried to achieve functional serotonergic neurons in the organoid system before, they lacked appropriate characterization (Eura *et al.*, 2020; Valiulahi *et al.*, 2021). Valiuhali *et al.* published a report on 2D serotonergic neurons as well as hindbrain organoids derived from iPSCs (Valiulahi et al., 2021). While achieving a remarkable efficiency in their 2D-protocol and notable hindbrain marker expression, they lack a proper characterization of the mature organoid. Notably, in contrast to the 2D neurons, their immunofluorescence staining for serotonin and TPH2 in the organoid showed a purely nuclear signal. Surprisingly, they described serotonergic neurons in ventricular areas which normally solely consist of progenitors (Eura *et al.*, 2020; Valiulahi *et al.*, 2021). A second report publication developed organoids representing the brainstem which includes the raphe nuclei (Hornung, 2003; Eura *et al.*, 2020). However, the authors do not further describe serotonergic neurons in their organoid cultures (Eura *et al.*, 2020).

The presented RO-CO assembloid were made possible by several optimization steps, including functionality boost media, slicing and ALI culturing. Previous experiments did not show sufficient neuronal outgrowth and interconnection between RO and CO, although published approaches were applied (Bagley *et al.*, 2017; Xiang *et al.*, 2017, 2019).

The distinguishment between ventricular structures in the final proliferation quantification was based on the presence of serotonergic projections identified by a positive serotonin labeling. This assay did not allow to confirm for actual innervation for all samples. Thus, timepoint of analysis of the

assembloids was extrapolated from previous experiments to ensure proper interconnection. The analysis of RO-CO assembloid focused on the role and effect of RO-derived serotonergic neurons. Possible other ingrowing or active neuronal subtypes, which may have also an effect on progenitor proliferation, were neglected (Crandall *et al.*, 2007; Andäng *et al.*, 2008a, 2008b). Likewise, identified proliferation differences were not further assessed as all mitotic progenitors were included. It is to assume that results obtained using exogenous serotonin can be transferred here. Thus, the disparity in proliferation behavior was likely caused by serotonin induced mitosis in apical and basal progenitors.

Assembloids could be further improved, for instance by utilizing a serotonergic reporter cell line. Expressing a fluorescence protein under a serotonergic transcription factor would label precisely serotonergic neurons. This would enable tracing the development of serotonergic neurons as well as their projections in the assembloid. However, establishing a vector expressing mCherry under a FEV promotor, remained fruitless during this thesis. A recent report by Xu and colleagues demonstrated a successful approach using a TPH2-EGFP construct, which could have been applied here as well (Xu *et al.*, 2022).

7.5 Detecting serotonin using sDarken

The validation of sDarken in the human system was achieved using hiPSC-derived cortical neurons. The differentiation protocol was based on work from Kemp *et al*. and Telezhkin *et al.* and was further advanced in the group of Philipp Koch (Telezhkin *et al.*, 2015; Kemp *et al.*, 2016). The developed Koch-protocol achieves ultimately a functional active interconnected network of pure cortical neurons (Wilkens *et al.*, 2022). This high level of maturation was not needed for the validation purpose in this study; therefore, a shortened protocol version was applied. Nevertheless, this approach still yielded in pure cortical neuron cultures and thus, relevant for test purposes. The experiments demonstrated that sDarken can detect serotonin in human cultures (Kubitschke *et al.*, 2022). It proved being reliable even in low concentrations and can respond repeatedly upon stimulation. The sensor was also capable to detect endogenous serotonin as the dissociation experiments have shown.

Fluorescence intensity changes of sDarken observed in RO slice cultures experiments clearly demonstrated binding of serotonin. As there was no exogenous serotonin in the culture, the detected serotonin was released by RO-derived serotonergic neurons. The short recovery time of the signal implies that serotonin is removed from the sensor rapidly. Thus, efficient measurements must be in place to clear serotonin, for instance SERT (Zhou *et al.*, 1998; Lau and Schloss, 2012). This indicates the presence of synaptic structures rather than volume transmission (Zoli *et al.*, 1999; Courtney and Ford, 2016; Kubitschke *et al.*, 2022). Volume transmission refers to an often-tonic release of

neuromodulators in the extra-synaptic space with long lasting effects of several seconds to minutes (Agnati *et al.*, 1995; Quentin, Belmer and Maroteaux, 2018).

Unfortunately, the efficiency of pLVX-EF1α-sDarken transfection was not limited and just a small subset of cells showed an expression of the sensor. Adjusting the virus exposure time and the addition of polybrene improved the transfection (Denning *et al.*, 2013; Sloan *et al.*, 2018). Nevertheless, generating a cell line with a stable expression of sDarken should be considered for future experiments. This could be achieved by inserting the construct in a safe-harbor location in combination with a selection possibility (Bagley *et al.*, 2017; Pellenz *et al.*, 2019).

However, the sDarken results do not allow to draw conclusions about the number of active neurons. In contrast to other activity markers, for instance calcium imaging calcium imaging, sDarken does not mark the active cell, but instead the innervated counterpart. Surprisingly, the intensity changes across ROIs showed high synchronicity. It is well established that serotonergic neurons display a rhythmic activity (Trulson and Jacobs, 1979). A recent study identified correlated activity patterns in clusters of neurons within the raphe nuclei, so called ensembles (Paquelet et al., 2022). Neurons within one ensemble show high levels of synchronicity and similar response to emotional behavior (Paquelet *et al.*, 2022). Whether or not serotonergic neurons in RO display comparable ensemble-like behavior, remains to be examined. Serotonergic neurons have shown to connect a large number of cells, hence it would be possible that just one neuron provided all innervation found in RO (Jacobs and Azmitia, 1992).

The fact that sDarken detects the cell which is being innervated instead of the active cell, helped validating the RO-CO assembloid. SDarken was introduced to CO, to ensure analyzing serotonergic innervations in cortical cells. As there was no exogenous serotonin present, all serotonin was provided by RO-derived serotonergic neurons. This allowed the conclusion, that indeed RO-derived serotonergic neurons were innervating cells of assembled COs.

7.6 The significance of the endogenous serotonergic system in humans

Human and rodent cortices differ in composition, features and complexity (Geschwind and Rakic, 2013). Recent studies have also shown important differences between the human and the rodent serotonergic system. Serotonergic receptors were shown to be differently and more abundantly expressed in the human (Xing and Huttner, 2020). Moreover, Hodge and colleagues compared human and mouse gene expression data and identified most serotonin receptors differ between homologous cell types (Hodge *et al.*, 2019). Serotonergic receptors were determined as the second most divergent gene class between mouse and human, indicating different roles and significance (Hodge et al., 2019; Mayer et al., 2019; Xing and Huttner, 2020).

Few developmental processes are similarly well understood between human and rodent corticogenesis; however, some show remarkable differences. For instance, the proportion of areas within the ganglionic eminences where migrating interneurons differ (Hansen *et al.*, 2013a; Laclef and Métin, 2018). Moreover, the effect of serotonin on migrating interneurons seems to be more ample, as serotonin also effects of human MGE-derived interneurons which was excluded in rodents (Frazer, Otomo and Dayer, 2015; Bajaj et al., 2021).

Taking all evidence into account, one might come to the conclusion that endogenous serotonin might play a more important role in the human corticogenesis compared to the rodent situation. Rodent and human differ in the importance of the different progenitor types (Betizeau et al., 2013; Lewitus, Kelava and Huttner, 2013b; Florio and Huttner, 2014). While bRGs are fundamental for humans, IPs are the most abundant progenitors in rodents. and show oppositional results regarding serotonin (Wang *et al.*, 2011). The results of this thesis and of others showed, that bPCs including bRGs do express serotonergic receptors and cause an increase of proliferation upon activation (Figure 18) (Xing *et al.*, 2020). On the contrary, proliferation-inducing serotonergic receptors were not found in human nor in mouse IPs (Dakic et al., 2016, 2017; Xing and Huttner, 2020). Interestingly, was an excess of serotonin associated with a decrease of IP abundance (Cheng *et al.*, 2010).

The developing murine brain is supplied by maternal serotonin between E10.5 and E16.5, while first projecting serotonergic neurons arrive the cortex at E14 (Côté *et al.*, 2007; Bonnin *et al.*, 2011b). Thus, endogenous serotonin is just present after many developmental stages have passed, including the first neurogenic phase of aPCs, the division of the pre-plate or the migration of MGE-derived interneurons. Thus, endogenous serotonin may just play a role for a very limited number of developmental processes like the second neurogenic phase of IPs and the migration of CGE-derived interneurons. In contrast, the first human serotonergic neurons reach the cortical structures at GW8 and the SVZ/IZ by GW10, relatively seen earlier than in rodents (Sundström et al., 1993; Workman et al., 2013). The occurrence coincides with the PP division (GW 8-10) and the migration of interneurons of LME and GME (GW10). Thus, endogenous serotonin will be present when aRGs divide and subsequently generate bRGs (GW11-13), the expansion of the bRG pool and finally, the generation of the majority of neurons (<GW20). Hence, the here observed stimulated proliferation by serotonin in apical and basal radial progenitor cells would likely be caused by endogenous serotonin provided by raphe nuclei-derived serotonergic neurons. Given the presence of serotonergic neurons and a different expression profile of serotonergic receptors, the possibility emerges of a more diverse and significant function of serotonin during human corticogenesis.

Important roles during the brain development always harbors the risks of severe consequences in case of deviations of the system due to external effects or genetic predispositions. This makes serotonin

once more an interesting player in the context of the emergence of psychiatric diseases, particularly ASD (Schain and Freedman, 1961; Yang *et al.*, 2015; Muller, Anacker and Veenstra-VanderWeele, 2016) Many studies highlighted the relation between disturbances in the serotonergic, developmental abnormalities, behavioral changes and even ASD (Sodhi and Sanders-Bush, 2004; Booij *et al.*, 2015; Carvajal-Oliveros and Campusano, 2021). However, modeling the biological onset has proven to be difficult. Recent advances in the brain organoid field led to the development of brain assembloids have made this topic accessible. Specifically, the assembloid technology revealed how abnormal interneuronal migration may lead to Timothy syndrome and thus ASD (Birey *et al.*, 2017, 2022).

The here developed RO-CO assembloid might provide a suitable model to clarify the effect of certain genetic variants affecting the serotonergic signaling and developmental aberrations in the human context (Dixon and Muotri, 2022; Kelley and Pașca, 2022). Using patient derived iPSCs carrying genetic variants to generate the organoids, would allow to investigate in detail aspects of serotonergic innervation and associated developmental alterations and how this might lead to the disease's onset. This will improve our understanding on the causes of the disease and might open the possibility to find therapeutical targets and agents.

8 References

Aasen, T. and Belmonte, J.C.I. (2010) 'Isolation and cultivation of human keratinocytes from skin or plucked hair for the generation of induced pluripotent stem cells', *Nature Protocols*, 5(2), pp. 371–382. Available at: https://doi.org/10.1038/nprot.2009.241.

Abdolmaleky, H.M. *et al.* (2011) 'Epigenetic dysregulation of HTR2A in the brain of patients with schizophrenia and bipolar disorder', *Schizophrenia Research*, 129(2), pp. 183–190. Available at: https://doi.org/https://doi.org/10.1016/j.schres.2011.04.007.

Agnati, L.F. *et al.* (1995) 'Intercellular communication in the brain: Wiring versus volume transmission', *Neuroscience*, 69(3), pp. 711–726. Available at: https://doi.org/https://doi.org/10.1016/0306-4522(95)00308-6.

Alenina, N. *et al.* (2009) 'Growth retardation and altered autonomic control in mice lacking brain serotonin', *Proceedings of the National Academy of Sciences of the United States of America*. 2009/06/11, 106(25), pp. 10332–10337. Available at: https://doi.org/10.1073/pnas.0810793106.

Alonso, A. *et al.* (2013) 'Development of the serotonergic cells in murine raphe nuclei and their relations with rhombomeric domains', *Brain structure & function*. 2012/09/30, 218(5), pp. 1229–1277. Available at: https://doi.org/10.1007/s00429-012-0456-8.

Andäng, M. *et al.* (2008a) 'Histone H2AX-dependent GABAA receptor regulation of stem cell proliferation', *Nature*, 451(7177), pp. 460–464. Available at: https://doi.org/10.1038/nature06488.

Andäng, M. *et al.* (2008b) 'Histone H2AX-dependent GABAA receptor regulation of stem cell proliferation', *Nature*, 451(7177), pp. 460–464. Available at: https://doi.org/10.1038/nature06488.

Andersen, J. *et al.* (2020) 'Generation of Functional Human 3D Cortico-Motor Assembloids', *Cell*, 183(7), pp. 1913-1929.e26. Available at: https://doi.org/https://doi.org/10.1016/j.cell.2020.11.017.

Andrews, S. (2010) 'FastQC: a quality control tool for high throughput sequence data. Available online at: http://www.bioinformatics.babraham.ac.uk/projects/fastqc'.

Avery, M.C. and Krichmar, J.L. (2017) 'Neuromodulatory Systems and Their Interactions: A Review of Models, Theories, and Experiments', *Frontiers in Neural Circuits*, 11. Available at: https://www.frontiersin.org/articles/10.3389/fncir.2017.00108.

Azmitia, E.C. (2001) 'Modern views on an ancient chemical: serotonin effects on cell proliferation, maturation, and apoptosis', *Brain Research Bulletin*, 56(5), pp. 413–424. Available at: https://doi.org/https://doi.org/10.1016/S0361-9230(01)00614-1.

Bagley, J.A. *et al.* (2017) 'Fused cerebral organoids model interactions between brain regions', *Nature methods*. 2017/05/10, 14(7), pp. 743–751. Available at: https://doi.org/10.1038/nmeth.4304.

Bajaj, S. *et al.* (2021) 'Neurotransmitter signaling regulates distinct phases of multimodal human interneuron migration', *The EMBO journal*. 2021/10/18, 40(23), pp. e108714–e108714. Available at: https://doi.org/10.15252/embj.2021108714.

Baker, K.G. *et al.* (1991) 'Cytoarchitecture of serotonin-synthesizing neurons in the pontine tegmentum of the human brain', *Synapse*, 7(4), pp. 301–320. Available at: https://doi.org/https://doi.org/10.1002/syn.890070407.

Baković, P. *et al.* (2021) 'Differential Serotonin Uptake Mechanisms at the Human Maternal-Fetal Interface', *International journal of molecular sciences*, 22(15), p. 7807. Available at: https://doi.org/10.3390/ijms22157807.

Banasr, M. *et al.* (2004) 'Serotonin-Induced Increases in Adult Cell Proliferation and Neurogenesis are Mediated Through Different and Common 5-HT Receptor Subtypes in the Dentate Gyrus and the Subventricular Zone', *Neuropsychopharmacology*, 29(3), pp. 450–460. Available at: https://doi.org/10.1038/sj.npp.1300320.

Bang, S.J. *et al.* (2012) 'Projections and interconnections of genetically defined serotonin neurons in mice', *The European journal of neuroscience*. 2011/12/13, 35(1), pp. 85–96. Available at: https://doi.org/10.1111/j.1460-9568.2011.07936.x.

Benito-Kwiecinski, S. *et al.* (2021) 'An early cell shape transition drives evolutionary expansion of the human forebrain', *Cell*. 2021/03/24, 184(8), pp. 2084-2102.e19. Available at: https://doi.org/10.1016/j.cell.2021.02.050.

Berger, M., Gray, J.A. and Roth, B.L. (2009) 'The Expanded Biology of Serotonin', *Annual Review of Medicine*, 60(1), pp. 355–366. Available at: https://doi.org/10.1146/annurev.med.60.042307.110802.

Bershteyn, M. *et al.* (2017) 'Human iPSC-Derived Cerebral Organoids Model Cellular Features of Lissencephaly and Reveal Prolonged Mitosis of Outer Radial Glia', *Cell Stem Cell*, 20(4), pp. 435-449.e4. Available at: https://doi.org/10.1016/j.stem.2016.12.007.

Betizeau, M. *et al.* (2013) 'Precursor Diversity and Complexity of Lineage Relationships in the Outer Subventricular Zone of the Primate', *Neuron*, 80(2), pp. 442–457. Available at: https://doi.org/10.1016/j.neuron.2013.09.032.

Birey, F. *et al.* (2017) 'Assembly of functionally integrated human forebrain spheroids', *Nature*, 545(7652), pp. 54–59. Available at: https://doi.org/10.1038/nature22330.

Birey, F. *et al.* (2022) 'Dissecting the molecular basis of human interneuron migration in forebrain assembloids from Timothy syndrome', *Cell Stem Cell*, 29(2), pp. 248-264.e7. Available at: https://doi.org/10.1016/j.stem.2021.11.011.

Bithell, A. *et al.* (2008) 'Fibroblast Growth Factor 2 Maintains the Neurogenic Capacity of Embryonic Neural Progenitor Cells In Vitro but Changes Their Neuronal Subtype Specification', *STEM CELLS*, 26(6), pp. 1565–1574. Available at: https://doi.org/https://doi.org/10.1634/stemcells.2007-0832.

Bjork, J.M. *et al.* (1999) 'The effects of tryptophan depletion and loading on laboratory aggression in men: time course and a food-restricted control', *Psychopharmacology*, 142(1), pp. 24–30. Available at: https://doi.org/10.1007/s002130050858.

Bockaert, J., Sebben, M. and Dumuis, A. (1990) 'Pharmacological characterization of 5-hydroxytryptamine4(5-HT4) receptors positively coupled to adenylate cyclase in adult guinea pig hippocampal membranes: effect of substituted benzamide derivatives.', *Molecular Pharmacology*, 37(3), p. 408. Available at: http://molpharm.aspetjournals.org/content/37/3/408.abstract.

Bonnin, A. *et al.* (2006) 'Expression mapping of 5-HT1 serotonin receptor subtypes during fetal and early postnatal mouse forebrain development', *Neuroscience*, 141(2), pp. 781–794. Available at: https://doi.org/https://doi.org/10.1016/j.neuroscience.2006.04.036.

Bonnin, A. *et al.* (2011a) 'A transient placental source of serotonin for the fetal forebrain', *Nature*, 472(7343), pp. 347–350. Available at: https://doi.org/10.1038/nature09972.

Bonnin, A. *et al.* (2011b) 'A transient placental source of serotonin for the fetal forebrain', *Nature*, 472(7343), pp. 347–350. Available at: https://doi.org/10.1038/nature09972.

Bonnin, A. and Levitt, P. (2011) 'Fetal, maternal, and placental sources of serotonin and new implications for developmental programming of the brain', *Neuroscience*. 2011/10/08, 197, pp. 1–7. Available at: https://doi.org/10.1016/j.neuroscience.2011.10.005.

Booij, L. *et al.* (2015) 'Genetic and early environmental influences on the serotonin system: consequences for brain development and risk for psychopathology', *Journal of psychiatry & neuroscience : JPN*, 40(1), pp. 5–18. Available at: https://doi.org/10.1503/jpn.140099.

Bowker, R.M. and Abbott, L.C. (1990) 'Quantitative re-evaluation of descending serotonergic and non-serotonergic projections from the medulla of the rodent: evidence for extensive co-existence of serotonin and peptides in the same spinally projecting neurons, but not from the nucleus raphe magnus', *Brain Research*, 512(1), pp. 15–25. Available at: https://doi.org/https://doi.org/10.1016/0006-8993(90)91164-C.

Boylan, C.B., Blue, M.E. and Hohmann, C.F. (2007) 'Modeling early cortical serotonergic deficits in autism', *Behavioural brain research*. 2006/10/10, 176(1), pp. 94–108. Available at: https://doi.org/10.1016/j.bbr.2006.08.026.

Brennan, J. *et al.* (2001) 'Nodal signalling in the epiblast patterns the early mouse embryo', *Nature*, 411(6840), pp. 965–969. Available at: https://doi.org/10.1038/35082103.

Brennand, K.J. *et al.* (2011) 'Modelling schizophrenia using human induced pluripotent stem cells', *Nature*. 2011/04/13, 473(7346), pp. 221–225. Available at: https://doi.org/10.1038/nature09915.

Brewer, G.J. *et al.* (1993) 'Optimized survival of hippocampal neurons in B27-supplemented neurobasal™, a new serum-free medium combination', *Journal of Neuroscience Research*, 35(5), pp. 567–576. Available at: https://doi.org/https://doi.org/10.1002/jnr.490350513.

Briscoe, J. *et al.* (2000) 'A Homeodomain Protein Code Specifies Progenitor Cell Identity and Neuronal Fate in the Ventral Neural Tube', *Cell*, 101(4), pp. 435–445. Available at: https://doi.org/https://doi.org/10.1016/S0092-8674(00)80853-3.

Briscoe, J. and Ericson, J. (1999) 'The specification of neuronal identity by graded sonic hedgehog signalling', *Seminars in Cell & Developmental Biology*, 10(3), pp. 353–362. Available at: https://doi.org/https://doi.org/10.1006/scdb.1999.0295.

Britanova, O. *et al.* (2008) 'Satb2 Is a Postmitotic Determinant for Upper-Layer Neuron Specification in the Neocortex', *Neuron*, 57(3), pp. 378–392. Available at: https://doi.org/10.1016/j.neuron.2007.12.028.

Brodski, C. *et al.* (2003) 'Location and size of dopaminergic and serotonergic cell populations are controlled by the position of the midbrain-hindbrain organizer', *The Journal of neuroscience : the official journal of the Society for Neuroscience*, 23(10), pp. 4199–4207. Available at: https://doi.org/10.1523/JNEUROSCI.23-10-04199.2003.

Budday, S., Steinmann, P. and Kuhl, E. (2015) 'Physical biology of human brain development', *Frontiers in Cellular Neuroscience*, 9. Available at: https://www.frontiersin.org/article/10.3389/fncel.2015.00257.

Buznikov, G.A., Lambert, W.H. and Lauder, J.M. (2001) 'Serotonin and serotonin-like substances as regulators of early embryogenesis and morphogenesis', *Cell and Tissue Research*, 305(2), pp. 177–186. Available at: https://doi.org/10.1007/s004410100408.

Camp, J.G. *et al.* (2015) 'Human cerebral organoids recapitulate gene expression programs of fetal neocortex development', *Proceedings of the National Academy of Sciences of the United States of America*. 2015/12/07, 112(51), pp. 15672–15677. Available at: https://doi.org/10.1073/pnas.1520760112.

Cappello, S. *et al.* (2006) 'The Rho-GTPase cdc42 regulates neural progenitor fate at the apical surface', *Nature Neuroscience*, 9(9), pp. 1099–1107. Available at: https://doi.org/10.1038/nn1744.

Carvajal-Oliveros, A. and Campusano, J.M. (2021) 'Studying the Contribution of Serotonin to Neurodevelopmental Disorders. Can This Fly?', *Frontiers in Behavioral Neuroscience*, 14. Available at: https://www.frontiersin.org/articles/10.3389/fnbeh.2020.601449.

Chamberlain, S.R. *et al.* (2006) 'Neurochemical modulation of response inhibition and probabilistic learning in humans', *Science (New York, N.Y.)*, 311(5762), pp. 861–863. Available at: https://doi.org/10.1126/science.1121218.

Chambers, S.M. *et al.* (2009) 'Highly efficient neural conversion of human ES and iPS cells by dual inhibition of SMAD signaling', *Nature biotechnology*. 2009/03/01, 27(3), pp. 275–280. Available at: https://doi.org/10.1038/nbt.1529.

Chameau, P. *et al.* (2009) 'The N-terminal region of reelin regulates postnatal dendritic maturation of cortical pyramidal neurons', *Proceedings of the National Academy of Sciences of the United States of America*. 2009/04/06, 106(17), pp. 7227–7232. Available at: https://doi.org/10.1073/pnas.0810764106.

Chen, J.K. *et al.* (2002) 'Small molecule modulation of Smoothened activity', *Proceedings of the National Academy of Sciences of the United States of America*. 2002/10/21, 99(22), pp. 14071–14076. Available at: https://doi.org/10.1073/pnas.182542899.

Cheng, A. *et al.* (2010) 'Monoamine oxidases regulate telencephalic neural progenitors in late embryonic and early postnatal development', *The Journal of neuroscience : the official journal of the Society for Neuroscience*, 30(32), pp. 10752–10762. Available at: https://doi.org/10.1523/JNEUROSCI.2037-10.2010.

Cheng, L. *et al.* (2003) 'Lmx1b, Pet-1, and Nkx2.2 coordinately specify serotonergic neurotransmitter phenotype', *The Journal of neuroscience : the official journal of the Society for Neuroscience*, 23(31), pp. 9961–9967. Available at: https://doi.org/10.1523/JNEUROSCI.23-31-09961.2003.

Chugani, D.C. *et al.* (1999) 'Developmental changes in brain serotonin synthesis capacity in autistic and nonautistic children', *Annals of Neurology*, 45(3), pp. 287–295. Available at: https://doi.org/https://doi.org/10.1002/1531-8249(199903)45:3<287::AID-ANA3>3.0.CO;2-9.

Ciceri, G. *et al.* (2022) 'An epigenetic barrier sets the timing of human neuronal maturation', *bioRxiv*, p. 2022.06.02.490114. Available at: https://doi.org/10.1101/2022.06.02.490114.

Clevers, H. (2016) 'Modeling Development and Disease with Organoids', *Cell*, 165(7), pp. 1586–1597. Available at: https://doi.org/10.1016/j.cell.2016.05.082.

Côté, F. *et al.* (2007) 'Maternal serotonin is crucial for murine embryonic development', *Proceedings of the National Academy of Sciences*, 104(1), pp. 329–334. Available at: https://doi.org/10.1073/pnas.0606722104.

Courtney, N.A. and Ford, C.P. (2016) 'Mechanisms of 5-HT1A receptor-mediated transmission in dorsal raphe serotonin neurons', *The Journal of physiology*. 2015/12/30, 594(4), pp. 953–965. Available at: https://doi.org/10.1113/JP271716.

Coutinho, A.M. *et al.* (2004) 'Variants of the serotonin transporter gene (SLC6A4) significantly contribute to hyperserotonemia in autism', *Molecular Psychiatry*, 9(3), pp. 264–271. Available at: https://doi.org/10.1038/sj.mp.4001409.

Cox, W.G. and Hemmati-Brivanlou, A. (1995) 'Caudalization of neural fate by tissue recombination and bFGF', *Development*, 121(12), pp. 4349–4358. Available at: https://doi.org/10.1242/dev.121.12.4349.

Crandall, J.E. *et al.* (2004) 'Cocaine exposure decreases GABA neuron migration from the ganglionic eminence to the cerebral cortex in embryonic mice', *Cerebral cortex (New York, N.Y. : 1991)*. 2004/03/28, 14(6), pp. 665–675. Available at: https://doi.org/10.1093/cercor/bhh027.

Crandall, J.E. *et al.* (2007) 'Dopamine receptor activation modulates GABA neuron migration from the basal forebrain to the cerebral cortex', *The Journal of neuroscience : the official journal of the Society for Neuroscience*, 27(14), pp. 3813–3822. Available at: https://doi.org/10.1523/JNEUROSCI.5124-06.2007.

Craven, S.E. *et al.* (2004) 'Gata2 specifies serotonergic neurons downstream of sonic hedgehog', *Development*, 131(5), pp. 1165–1173. Available at: https://doi.org/10.1242/dev.01024.

Crawford, T.Q. and Roelink, H. (2007) 'The Notch response inhibitor DAPT enhances neuronal differentiation in embryonic stem cell-derived embryoid bodies independently of sonic hedgehog signaling', *Developmental Dynamics*, 236(3), pp. 886–892. Available at: https://doi.org/https://doi.org/10.1002/dvdy.21083.

Crossley, P.H., Martinez, S. and Martin, G.R. (1996) 'Midbrain development induced by FGF8 in the chick embryo', *Nature*, 380(6569), pp. 66–68. Available at: https://doi.org/10.1038/380066a0.

Csaba, G. (1993) 'Presence in and effects of pineal indoleamines at very low level of phylogeny', *Experientia*, 49(8), pp. 627–634. Available at: https://doi.org/10.1007/BF01923943.

Dakic, V. *et al.* (2016) 'Harmine stimulates proliferation of human neural progenitors', *PeerJ*, 4, pp. e2727–e2727. Available at: https://doi.org/10.7717/peerj.2727.

Dakic, V. *et al.* (2017) 'Short term changes in the proteome of human cerebral organoids induced by 5-MeO-DMT', *Scientific reports*, 7(1), p. 12863. Available at: https://doi.org/10.1038/s41598-017-12779-5.

Dean, I., Robertson, S.J. and Edwards, F.A. (2003) 'Serotonin drives a novel GABAergic synaptic current recorded in rat cerebellar purkinje cells: a Lugaro cell to Purkinje cell synapse', *The Journal of neuroscience : the official journal of the Society for Neuroscience*, 23(11), pp. 4457–4469. Available at: https://doi.org/10.1523/JNEUROSCI.23-11-04457.2003.

Deneris, E. and Gaspar, P. (2018a) 'Serotonin neuron development: shaping molecular and structural identities', *Wiley interdisciplinary reviews. Developmental biology*. 2017/10/26, 7(1), p. 10.1002/wdev.301. Available at: https://doi.org/10.1002/wdev.301.

Deneris, E. and Gaspar, P. (2018b) 'Serotonin neuron development: shaping molecular and structural identities', *Wiley interdisciplinary reviews. Developmental biology*. 2017/10/26, 7(1), pp. 10.1002 & #x2F;wdev.301-10.1002 & #x2F;wdev.301. Available at: https://doi.org/10.1002/wdev.301.

Deneris, E.S. and Wyler, S.C. (2012) 'Serotonergic transcriptional networks and potential importance to mental health', *Nature neuroscience*, 15(4), pp. 519–527. Available at: https://doi.org/10.1038/nn.3039.

Denning, W. *et al.* (2013) 'Optimization of the transductional efficiency of lentiviral vectors: effect of sera and polycations', *Molecular biotechnology*, 53(3), pp. 308–314. Available at: https://doi.org/10.1007/s12033-012-9528-5.

Descarries, L. *et al.* (1982) 'The serotonin neurons in nucleus raphe dorsalis of adult rat: A light and electron microscope radioautographic study', *Journal of Comparative Neurology*, 207(3), pp. 239–254. Available at: https://doi.org/https://doi.org/10.1002/cne.902070305.

Dias, J.M. *et al.* (2014) 'Tgfβ Signaling Regulates Temporal Neurogenesis and Potency of Neural Stem Cells in the CNS', *Neuron*, 84(5), pp. 927–939. Available at: https://doi.org/10.1016/j.neuron.2014.10.033.

Dieudonné, S. and Dumoulin, A. (2000) 'Serotonin-driven long-range inhibitory connections in the cerebellar cortex', *The Journal of neuroscience : the official journal of the Society for Neuroscience*, 20(5), pp. 1837–1848. Available at: https://doi.org/10.1523/JNEUROSCI.20-05-01837.2000.

Dimos, J.T. *et al.* (2008) 'Induced Pluripotent Stem Cells Generated from Patients with ALS Can Be Differentiated into Motor Neurons', *Science*, 321(5893), pp. 1218–1221. Available at: https://doi.org/10.1126/science.1158799.

Ding, Y.-Q. *et al.* (2003) 'Lmx1b is essential for the development of serotonergic neurons', *Nature Neuroscience*, 6(9), pp. 933–938. Available at: https://doi.org/10.1038/nn1104.

Dixon, T.A. and Muotri, A.R. (2022) 'Advancing preclinical models of psychiatric disorders with human brain organoid cultures', *Molecular Psychiatry* [Preprint]. Available at: https://doi.org/10.1038/s41380-022-01708-2.

Ducray, A. *et al.* (2006) 'GDNF family ligands display distinct action profiles on cultured GABAergic and serotonergic neurons of rat ventral mesencephalon', *Brain Research*, 1069(1), pp. 104–112. Available at: https://doi.org/https://doi.org/10.1016/j.brainres.2005.11.056.

Echelard, Y. *et al.* (1993) 'Sonic hedgehog, a member of a family of putative signaling molecules, is implicated in the regulation of CNS polarity', *Cell*, 75(7), pp. 1417–1430. Available at: https://doi.org/10.1016/0092-8674(93)90627-3.

Eiraku, M. *et al.* (2008) 'Self-Organized Formation of Polarized Cortical Tissues from ESCs and Its Active Manipulation by Extrinsic Signals', *Cell Stem Cell*, 3(5), pp. 519–532. Available at: https://doi.org/10.1016/j.stem.2008.09.002.

Eldar, E. *et al.* (2016) 'Mood as Representation of Momentum', *Trends in Cognitive Sciences*, 20(1), pp. 15–24. Available at: https://doi.org/10.1016/j.tics.2015.07.010.

Elhusseiny, A. and Hamel, E. (2001) 'Sumatriptan elicits both constriction and dilation in human and bovine brain intracortical arterioles', *British journal of pharmacology*, 132(1), pp. 55–62. Available at: https://doi.org/10.1038/sj.bjp.0703763.

El-Merahbi, R. *et al.* (2015) 'The roles of peripheral serotonin in metabolic homeostasis', *FEBS Letters*, 589(15), pp. 1728–1734. Available at: https://doi.org/https://doi.org/10.1016/j.febslet.2015.05.054.

Eshleman, A.J. *et al.* (2013) 'Substituted methcathinones differ in transporter and receptor interactions', *Biochemical pharmacology*. 2013/04/10, 85(12), pp. 1803–1815. Available at: https://doi.org/10.1016/j.bcp.2013.04.004.

Eura, N. *et al.* (2020) 'Brainstem Organoids From Human Pluripotent Stem Cells', *Frontiers in neuroscience*, 14, p. 538. Available at: https://doi.org/10.3389/fnins.2020.00538.

Evans, M.J. and Kaufman, M.H. (1981) 'Establishment in culture of pluripotential cells from mouse embryos', *Nature*, 292(5819), pp. 154–156. Available at: https://doi.org/10.1038/292154a0.

Fietz, S.A. *et al.* (2010) 'OSVZ progenitors of human and ferret neocortex are epithelial-like and expand by integrin signaling', *Nature Neuroscience*, 13(6), pp. 690–699. Available at: https://doi.org/10.1038/nn.2553.

Fischer, J. *et al.* (2022) 'Human-specific ARHGAP11B ensures human-like basal progenitor levels in hominid cerebral organoids', *EMBO reports*, 23(11), p. e54728. Available at: https://doi.org/https://doi.org/10.15252/embr.202254728.

Florio, M. *et al.* (2015) 'Human-specific gene ARHGAP11B promotes basal progenitor amplification and neocortex expansion', *Science*, 347(6229), pp. 1465–1470. Available at: https://doi.org/10.1126/science.aaa1975.

Florio, M. and Huttner, W.B. (2014) 'Neural progenitors, neurogenesis and the evolution of the neocortex', *Development*, 141(11), pp. 2182–2194. Available at: https://doi.org/10.1242/dev.090571.

Fontanilla, D. *et al.* (2009) 'The hallucinogen N,N-dimethyltryptamine (DMT) is an endogenous sigma-1 receptor regulator', *Science (New York, N.Y.)*, 323(5916), pp. 934–937. Available at: https://doi.org/10.1126/science.1166127.

Frazer, S., Otomo, K. and Dayer, A. (2015) 'Early-life serotonin dysregulation affects the migration and positioning of cortical interneuron subtypes', *Translational Psychiatry*, 5(9), pp. e644–e644. Available at: https://doi.org/10.1038/tp.2015.147.

Gabriele, S., Sacco, R. and Persico, A.M. (2014) 'Blood serotonin levels in autism spectrum disorder: A systematic review and meta-analysis', *European Neuropsychopharmacology*, 24(6), pp. 919–929. Available at: https://doi.org/https://doi.org/10.1016/j.euroneuro.2014.02.004.

Garbarino, V.R. *et al.* (2019) 'Extreme enhancement or depletion of serotonin transporter function and serotonin availability in autism spectrum disorder', *Pharmacological research*. 2018/07/24, 140, pp. 85–99. Available at: https://doi.org/10.1016/j.phrs.2018.07.010.

Garcia, R.A.P. *et al.* (2008) 'Insulin modulates norepinephrine-mediated melatonin synthesis in cultured rat pineal gland', *Life Sciences*, 82(1), pp. 108–114. Available at: https://doi.org/https://doi.org/10.1016/j.lfs.2007.10.016.

Gaspar, P. and Nedelec, S. (2016) 'Serotonin neurons in a dish', *Nature Biotechnology*, 34(1), pp. 41–42. Available at: https://doi.org/10.1038/nbt.3455.

Gershon, M.D. (2013) '5-Hydroxytryptamine (serotonin) in the gastrointestinal tract', *Current Opinion in Endocrinology, Diabetes and Obesity*, 20(1). Available at: https://journals.lww.com/co-endocrinology/Fulltext/2013/02000/5_Hydroxytryptamine__serotonin__in_the.4.aspx.

Gervasoni, D. *et al.* (2000) 'Role and origin of the GABAergic innervation of dorsal raphe serotonergic neurons', *The Journal of neuroscience : the official journal of the Society for Neuroscience*, 20(11), pp. 4217–4225. Available at: https://doi.org/10.1523/JNEUROSCI.20-11-04217.2000.

Geschwind, D.H. and Rakic, P. (2013) 'Cortical Evolution: Judge the Brain by Its Cover', *Neuron*, 80(3), pp. 633–647. Available at: https://doi.org/10.1016/j.neuron.2013.10.045.

Giandomenico, S.L. *et al.* (2019) 'Cerebral organoids at the air-liquid interface generate diverse nerve tracts with functional output', *Nature neuroscience*. 2019/03/18, 22(4), pp. 669–679. Available at: https://doi.org/10.1038/s41593-019-0350-2.

Götz, M. and Huttner, W.B. (2005) 'The cell biology of neurogenesis', *Nature Reviews Molecular Cell Biology*, 6(10), pp. 777–788. Available at: https://doi.org/10.1038/nrm1739.

Hansen, D. v *et al.* (2010) 'Neurogenic radial glia in the outer subventricular zone of human neocortex', *Nature*, 464(7288), pp. 554–561. Available at: https://doi.org/10.1038/nature08845.

Hansen, D. v *et al.* (2013a) 'Non-epithelial stem cells and cortical interneuron production in the human ganglionic eminences', *Nature neuroscience*. 2013/10/06, 16(11), pp. 1576–1587. Available at: https://doi.org/10.1038/nn.3541.

Hansen, D. v *et al.* (2013b) 'Non-epithelial stem cells and cortical interneuron production in the human ganglionic eminences', *Nature neuroscience*. 2013/10/06, 16(11), pp. 1576–1587. Available at: https://doi.org/10.1038/nn.3541.

Hao, Y. *et al.* (2021) 'Integrated analysis of multimodal single-cell data', *Cell*, 184(13), pp. 3573-3587.e29. Available at: https://doi.org/https://doi.org/10.1016/j.cell.2021.04.048.

Haubensak, W. *et al.* (2004) 'Neurons arise in the basal neuroepithelium of the early mammalian telencephalon: a major site of neurogenesis', *Proceedings of the National Academy of Sciences of the United States of America*. 2004/02/12, 101(9), pp. 3196–3201. Available at: https://doi.org/10.1073/pnas.0308600100.

Hawthorne, A.L. *et al.* (2010) 'Serotonergic neurons migrate radially through the neuroepithelium by dynamin-mediated somal translocation', *The Journal of neuroscience : the official journal of the Society for Neuroscience*, 30(2), pp. 420–430. Available at: https://doi.org/10.1523/JNEUROSCI.2333-09.2010.

Heck, N. *et al.* (2007) 'GABA-A Receptors Regulate Neocortical Neuronal Migration In Vitro and In Vivo', *Cerebral Cortex*, 17(1), pp. 138–148. Available at: https://doi.org/10.1093/cercor/bhj135.

Hendrickx, M., Van, X.H. and Leyns, L. (2009) 'Anterior–posterior patterning of neural differentiated embryonic stem cells by canonical Wnts, Fgfs, Bmp4 and their respective antagonists', *Development, Growth & Differentiation*, 51(8), pp. 687–698. Available at: https://doi.org/https://doi.org/10.1111/j.1440-169X.2009.01128.x.

Hergenreder, E. *et al.* (2022) 'Combined small molecule treatment accelerates timing of maturation in human pluripotent stem cell-derived neurons', *bioRxiv*, p. 2022.06.02.494616. Available at: https://doi.org/10.1101/2022.06.02.494616.

Hevner, R.F. *et al.* (2001) 'Tbr1 Regulates Differentiation of the Preplate and Layer 6', *Neuron*, 29(2), pp. 353–366. Available at: https://doi.org/10.1016/S0896-6273(01)00211-2.

Hillion, J. *et al.* (1993) 'Prenatal Developmental Expression of Rat Brain 5-HT1A Receptor Gene Followed by PCR', *Biochemical and Biophysical Research Communications*, 191(3), pp. 991–997. Available at: https://doi.org/https://doi.org/10.1006/bbrc.1993.1315.

Hitoshi, S. *et al.* (2002) 'Neural stem cell lineages are regionally specified, but not committed, within distinct compartments of the developing brain', *Development*, 129(1), pp. 233–244. Available at: https://doi.org/10.1242/dev.129.1.233.

Hodge, R.D. *et al.* (2019) 'Conserved cell types with divergent features in human versus mouse cortex', *Nature*, 573(7772), pp. 61–68. Available at: https://doi.org/10.1038/s41586-019-1506-7.

Höglund, E., Øverli, Ø. and Winberg, S. (2019) 'Tryptophan Metabolic Pathways and Brain Serotonergic Activity: A Comparative Review', *Frontiers in Endocrinology*, 10. Available at: https://www.frontiersin.org/articles/10.3389/fendo.2019.00158.

Hornung, J.-P. (2003) 'The human raphe nuclei and the serotonergic system', *Journal of Chemical Neuroanatomy*, 26(4), pp. 331–343. Available at: https://doi.org/https://doi.org/10.1016/j.jchemneu.2003.10.002.

Huang, S.-M.A. *et al.* (2009) 'Tankyrase inhibition stabilizes axin and antagonizes Wnt signalling', *Nature*, 461(7264), pp. 614–620. Available at: https://doi.org/10.1038/nature08356.

Ideno, H. *et al.* (2022) 'Human PSCs determine the competency of cerebral organoid differentiation via FGF signaling and epigenetic mechanisms', *iScience*, 25(10), p. 105140. Available at: https://doi.org/https://doi.org/10.1016/j.isci.2022.105140.

Iefremova, V. *et al.* (2017) 'An Organoid-Based Model of Cortical Development Identifies Non-Cell-Autonomous Defects in Wnt Signaling Contributing to Miller-Dieker Syndrome', *Cell Reports*, 19(1), pp. 50–59. Available at: https://doi.org/10.1016/j.celrep.2017.03.047.

Imai, H., Steindler, D.A. and Kitai, S.T. (1986) 'The organization of divergent axonal projections from the midbrain raphe nuclei in the rat', *Journal of Comparative Neurology*, 243(3), pp. 363–380. Available at: https://doi.org/https://doi.org/10.1002/cne.902430307.

Invernizzi, R. *et al.* (1997) 'Effect of 5-HT1A Receptor Antagonists on Citalopram-induced Increase in Extracellular Serotonin in the Frontal Cortex, Striatum and Dorsal Hippocampus', *Neuropharmacology*, 36(4), pp. 467–473. Available at: https://doi.org/https://doi.org/10.1016/S0028-3908(97)00060-9.

Jabali, A. *et al.* (2022) 'Human cerebral organoids reveal progenitor pathology in EML1-linked cortical malformation', *EMBO reports*. 2022/03/15, 23(5), pp. e54027–e54027. Available at: https://doi.org/10.15252/embr.202154027.

Jacob, J. *et al.* (2007a) 'Transcriptional repression coordinates the temporal switch from motor to serotonergic neurogenesis', *Nature Neuroscience*, 10(11), pp. 1433–1439. Available at: https://doi.org/10.1038/nn1985.

Jacob, J. *et al.* (2007b) 'Transcriptional repression coordinates the temporal switch from motor to serotonergic neurogenesis', *Nature Neuroscience*, 10(11), pp. 1433–1439. Available at: https://doi.org/10.1038/nn1985.

Jacobs, B.L. and Azmitia, E.C. (1992) 'Structure and function of the brain serotonin system', *Physiological Reviews*, 72(1), pp. 165–229. Available at: https://doi.org/10.1152/physrev.1992.72.1.165.

Jähnichen, S., Glusa, E. and Pertz, H.H. (2005) 'Evidence for 5-HT2B and 5-HT7 receptor-mediated relaxation in pulmonary arteries of weaned pigs', *Naunyn-Schmiedeberg's Archives of Pharmacology*, 371(1), pp. 89–98. Available at: https://doi.org/10.1007/s00210-004-1006-6.

Janusonis, S., Gluncic, V. and Rakic, P. (2004) 'Early serotonergic projections to Cajal-Retzius cells: relevance for cortical development', *The Journal of neuroscience : the official journal of the Society for Neuroscience*, 24(7), pp. 1652–1659. Available at: https://doi.org/10.1523/JNEUROSCI.4651-03.2004.

Jin, L., Hu, X. and Feng, L. (2005) 'NT3 inhibits FGF2-induced neural progenitor cell proliferation via the PI3K/GSK3 pathway', *Journal of Neurochemistry*, 93(5), pp. 1251–1261. Available at: https://doi.org/https://doi.org/10.1111/j.1471-4159.2005.03118.x.

Jo, J. *et al.* (2016) 'Midbrain-like Organoids from Human Pluripotent Stem Cells Contain Functional Dopaminergic and Neuromelanin-Producing Neurons', *Cell stem cell*. 2016/07/28, 19(2), pp. 248–257. Available at: https://doi.org/10.1016/j.stem.2016.07.005.

Kadowaki, M. *et al.* (2007) 'N-cadherin mediates cortical organization in the mouse brain', *Developmental Biology*, 304(1), pp. 22–33. Available at: https://doi.org/https://doi.org/10.1016/j.ydbio.2006.12.014.

Kalebic, N. *et al.* (2019) 'Neocortical Expansion Due to Increased Proliferation of Basal Progenitors Is Linked to Changes in Their Morphology', *Cell Stem Cell*, 24(4), pp. 535-550.e9. Available at: https://doi.org/https://doi.org/10.1016/j.stem.2019.02.017.

Kaluthantrige Don, F. and Kalebic, N. (2022) 'Forebrain Organoids to Model the Cell Biology of Basal Radial Glia in Neurodevelopmental Disorders and Brain Evolution', *Frontiers in Cell and Developmental Biology*, 10. Available at: https://www.frontiersin.org/article/10.3389/fcell.2022.917166.

Karzbrun, E. *et al.* (2018) 'Human brain organoids on a chip reveal the physics of folding', *Nature Physics*, 14(5), pp. 515–522. Available at: https://doi.org/10.1038/s41567-018-0046-7.

Kaumann, A.J. and Levy, F.O. (2006) '5-Hydroxytryptamine receptors in the human cardiovascular system', *Pharmacology & Therapeutics*, 111(3), pp. 674–706. Available at: https://doi.org/https://doi.org/10.1016/j.pharmthera.2005.12.004.

Kawashima, T. (2018) 'The role of the serotonergic system in motor control', *Neuroscience Research*, 129, pp. 32–39. Available at: https://doi.org/https://doi.org/10.1016/j.neures.2017.07.005.

Kelava, I. *et al.* (2022) 'Androgens increase excitatory neurogenic potential in human brain organoids', *Nature*. 2022/01/19, 602(7895), pp. 112–116. Available at: https://doi.org/10.1038/s41586-021-04330-4.

Kelava, I. and Lancaster, M.A. (2016) 'Stem Cell Models of Human Brain Development', *Cell Stem Cell*, 18(6), pp. 736–748. Available at: https://doi.org/10.1016/j.stem.2016.05.022.

Kelley, K.W. and Pașca, S.P. (2022) 'Human brain organogenesis: Toward a cellular understanding of development and disease', *Cell*, 185(1), pp. 42–61. Available at: https://doi.org/10.1016/j.cell.2021.10.003.

Kelly, C.R. and Sharif, N.A. (2006) 'Pharmacological Evidence for a Functional Serotonin-2B Receptor in a Human Uterine Smooth Muscle Cell Line', *Journal of Pharmacology and Experimental Therapeutics*, 317(3), p. 1254. Available at: https://doi.org/10.1124/jpet.105.100172.

Kemp, P.J. *et al.* (2016) 'Improving and accelerating the differentiation and functional maturation of human stem cell-derived neurons: role of extracellular calcium and GABA', *The Journal of physiology*, 594(22), pp. 6583–6594. Available at: https://doi.org/10.1113/JP270655.

Kiecker, C. and Niehrs, C. (2001) 'A morphogen gradient of Wnt/β-catenin signalling regulates anteroposterior neural patterning in Xenopus', *Development*, 128(21), pp. 4189–4201. Available at: https://doi.org/10.1242/dev.128.21.4189.

Kim, H. *et al.* (2010) 'Serotonin regulates pancreatic beta cell mass during pregnancy', *Nature Medicine*, 16(7), pp. 804–808. Available at: https://doi.org/10.1038/nm.2173.

Kim, J.-H. *et al.* (2002) 'Dopamine neurons derived from embryonic stem cells function in an animal model of Parkinson's disease', *Nature*, 418(6893), pp. 50–56. Available at: https://doi.org/10.1038/nature00900.

Kimelman, D. and Kirschner, M. (1987) 'Synergistic induction of mesoderm by FGF and TGF-β and the identification of an mRNA coding for FGF in the early xenopus embryo', *Cell*, 51(5), pp. 869–877. Available at: https://doi.org/https://doi.org/10.1016/0092-8674(87)90110-3.

Kinney, H.C. *et al.* (2007) 'The development of the medullary serotonergic system in early human life', *Autonomic Neuroscience*, 132(1), pp. 81–102. Available at: https://doi.org/https://doi.org/10.1016/j.autneu.2006.11.001.

Kittappa, R., Kehler, J. and Barr, C.S. (2017) 'Regulation of the serotonin neuron fate in stem cells by foxa2 and shh', *Journal of Stem Cell Research & Therapeutics*, 3.

Kiyasova, V. and Gaspar, P. (2011) 'Development of raphe serotonin neurons from specification to guidance', *European Journal of Neuroscience*, 34(10), pp. 1553–1562. Available at: https://doi.org/https://doi.org/10.1111/j.1460-9568.2011.07910.x.

Klempin, F. *et al.* (2010) 'Oppositional Effects of Serotonin Receptors 5-HT1a, 2, and 2c in the Regulation of Adult Hippocampal Neurogenesis', *Frontiers in Molecular Neuroscience*, 3. Available at: https://www.frontiersin.org/articles/10.3389/fnmol.2010.00014.

Kliman, H.J. *et al.* (2018) 'Pathway of Maternal Serotonin to the Human Embryo and Fetus', *Endocrinology*, 159(4), pp. 1609–1629. Available at: https://doi.org/10.1210/en.2017-03025.

Kolk, S.M. and Rakic, P. (2022) 'Development of prefrontal cortex', *Neuropsychopharmacology : official publication of the American College of Neuropsychopharmacology*. 2021/10/13, 47(1), pp. 41–57. Available at: https://doi.org/10.1038/s41386-021-01137-9.

Krefft, O. *et al.* (2018) 'Generation of Standardized and Reproducible Forebrain-type Cerebral Organoids from Human Induced Pluripotent Stem Cells', *Journal of visualized experiments : JoVE*, (131), p. 56768. Available at: https://doi.org/10.3791/56768.

Kubitschke, M. *et al.* (2022) 'sDarken: Next generation genetically encoded fluorescent sensors for serotonin', *bioRxiv*, p. 2022.03.10.483799. Available at: https://doi.org/10.1101/2022.03.10.483799.

Laclef, C. and Métin, C. (2018) 'Conserved rules in embryonic development of cortical interneurons', *Seminars in Cell & Developmental Biology*, 76, pp. 86–100. Available at: https://doi.org/https://doi.org/10.1016/j.semcdb.2017.09.017.

Lancaster, M.A. *et al.* (2013) 'Cerebral organoids model human brain development and microcephaly', *Nature*. 2013/08/28, 501(7467), pp. 373–379. Available at: https://doi.org/10.1038/nature12517.

Lancaster, M.A. *et al.* (2017) 'Guided self-organization and cortical plate formation in human brain organoids', *Nature Biotechnology*, 35(7), pp. 659–666. Available at: https://doi.org/10.1038/nbt.3906.

Lau, T. and Schloss, P. (2012) 'Differential regulation of serotonin transporter cell surface expression', *Wiley Interdisciplinary Reviews: Membrane Transport and Signaling*, 1(3), pp. 259–268. Available at: https://doi.org/https://doi.org/10.1002/wmts.10.

Lee, J. *et al.* (2020) 'In vitro generation of functional murine heart organoids via FGF4 and extracellular matrix', *Nature Communications*, 11(1), p. 4283. Available at: https://doi.org/10.1038/s41467-020-18031-5.

Lesurtel, M. *et al.* (2006) 'Platelet-Derived Serotonin Mediates Liver Regeneration', *Science*, 312(5770), pp. 104–107. Available at: https://doi.org/10.1126/science.1123842.

Letinic, K., Zoncu, R. and Rakic, P. (2002) 'Origin of GABAergic neurons in the human neocortex', *Nature*, 417(6889), pp. 645–649. Available at: https://doi.org/10.1038/nature00779.

Lewitus, E., Kelava, I. and Huttner, W.B. (2013a) 'Conical expansion of the outer subventricular zone and the role of neocortical folding in evolution and development', *Frontiers in Human Neuroscience*, 7. Available at: https://www.frontiersin.org/articles/10.3389/fnhum.2013.00424.

Lewitus, E., Kelava, I. and Huttner, W.B. (2013b) 'Conical expansion of the outer subventricular zone and the role of neocortical folding in evolution and development', *Frontiers in Human Neuroscience*, 7. Available at: https://www.frontiersin.org/articles/10.3389/fnhum.2013.00424.

Li, Y. *et al.* (2017) 'Induction of Expansion and Folding in Human Cerebral Organoids', *Cell stem cell*. 2016/12/29, 20(3), pp. 385-396.e3. Available at: https://doi.org/10.1016/j.stem.2016.11.017.

Liem, K.F., Jessell, T.M. and Briscoe, J. (2000) 'Regulation of the neural patterning activity of sonic hedgehog by secreted BMP inhibitors expressed by notochord and somites', *Development*, 127(22), pp. 4855–4866. Available at: https://doi.org/10.1242/dev.127.22.4855.

Lin, M., Lachman, H.M. and Zheng, D. (2016) 'Transcriptomics analysis of iPSC-derived neurons and modeling of neuropsychiatric disorders', *Molecular and cellular neurosciences*. 2015/11/26, 73, pp. 32–42. Available at: https://doi.org/10.1016/j.mcn.2015.11.009.

Lin, S.L. *et al.* (2002) 'Differential coupling of 5-HT(1) receptors to G proteins of the G(i) family', *British journal of pharmacology*, 136(7), pp. 1072–1078. Available at: https://doi.org/10.1038/sj.bjp.0704809.

Liu, N. *et al.* (2021) 'The Mechanism of Secretion and Metabolism of Gut-Derived 5-Hydroxytryptamine', *International Journal of Molecular Sciences*, 22(15). Available at: https://doi.org/10.3390/ijms22157931.

Longmire, T.A. *et al.* (2012) 'Efficient derivation of purified lung and thyroid progenitors from embryonic stem cells', *Cell stem cell*, 10(4), pp. 398–411. Available at: https://doi.org/10.1016/j.stem.2012.01.019.

LoTurco, J.J. *et al.* (1995) 'GABA and glutamate depolarize cortical progenitor cells and inhibit DNA synthesis', *Neuron*, 15(6), pp. 1287–1298. Available at: https://doi.org/10.1016/0896-6273(95)90008-X.

Lu, J. *et al.* (2016) 'Generation of serotonin neurons from human pluripotent stem cells', *Nature biotechnology*. 2015/12/14, 34(1), pp. 89–94. Available at: https://doi.org/10.1038/nbt.3435.

Luppi, P.-H. and Fort, P. (2019) ‘Chapter 23 - Sleep–wake physiology’, in K.H. Levin and P. Chauvel (eds) *Handbook of Clinical Neurology*. Elsevier, pp. 359–370. Available at: https://doi.org/https://doi.org/10.1016/B978-0-444-64032-1.00023-0.

Malek, Z.S. *et al.* (2007) ‘Daily Rhythm of Tryptophan Hydroxylase-2 Messenger Ribonucleic Acid within Raphe Neurons Is Induced by Corticoid Daily Surge and Modulated by Enhanced Locomotor Activity’, *Endocrinology*, 148(11), pp. 5165–5172. Available at: https://doi.org/10.1210/en.2007-0526.

Marklund, U. *et al.* (2014) ‘Detailed expression analysis of regulatory genes in the early developing human neural tube’, *Stem cells and development*. 2013/10/08, 23(1), pp. 5–15. Available at: https://doi.org/10.1089/scd.2013.0309.

Martínez-Cerdeño, V. *et al.* (2012) ‘Comparative Analysis of the Subventricular Zone in Rat, Ferret and Macaque: Evidence for an Outer Subventricular Zone in Rodents’, *PLOS ONE*, 7(1), pp. e30178-. Available at: https://doi.org/10.1371/journal.pone.0030178.

de Masi, C. *et al.* (2020) ‘Application of CRISPR/Cas9 to human-induced pluripotent stem cells: from gene editing to drug discovery’, *Human Genomics*, 14(1), p. 25. Available at: https://doi.org/10.1186/s40246-020-00276-2.

Massa, S.M. *et al.* (2010) ‘Small molecule BDNF mimetics activate TrkB signaling and prevent neuronal degeneration in rodents’, *The Journal of Clinical Investigation*, 120(5), pp. 1774–1785. Available at: https://doi.org/10.1172/JCI41356.

Matsuda, M. *et al.* (2004) ‘Serotonin Regulates Mammary Gland Development via an Autocrine-Paracrine Loop’, *Developmental Cell*, 6(2), pp. 193–203. Available at: https://doi.org/10.1016/S1534-5807(04)00022-X.

Mayer, S. *et al.* (2019) ‘Multimodal Single-Cell Analysis Reveals Physiological Maturation in the Developing Human Neocortex’, *Neuron*. 2019/02/12, 102(1), pp. 143-158.e7. Available at: https://doi.org/10.1016/j.neuron.2019.01.027.

McComish, S.F. and Caldwell, M.A. (2018) ‘Generation of defined neural populations from pluripotent stem cells’, *Philosophical transactions of the Royal Society of London. Series B, Biological sciences*, 373(1750), p. 20170214. Available at: https://doi.org/10.1098/rstb.2017.0214.

McDougle, C. *et al.* (1996) ‘Effects of Tryptophan Depletion in Drug-Free Adults With Autistic Disorder’, *Archives of General Psychiatry*, 53(11), pp. 993–1000. Available at: https://doi.org/10.1001/archpsyc.1996.01830110029004.

McGrew, L.L., Hoppler, S. and Moon, R.T. (1997) ‘Wnt and FGF pathways cooperatively pattern anteroposterior neural ectoderm in Xenopus’, *Mechanisms of Development*, 69(1), pp. 105–114. Available at: https://doi.org/https://doi.org/10.1016/S0925-4773(97)00160-3.

Melander, H. *et al.* (2008) ‘A regulatory Apologia — A review of placebo-controlled studies in regulatory submissions of new-generation antidepressants’, *European Neuropsychopharmacology*, 18(9), pp. 623–627. Available at: https://doi.org/https://doi.org/10.1016/j.euroneuro.2008.06.003.

Meltzer, H.Y. and Roth, B.L. (2013) ‘Lorcaserin and pimavanserin: emerging selectivity of serotonin receptor subtype-targeted drugs’, *The Journal of clinical investigation*. 2013/12/02, 123(12), pp. 4986–4991. Available at: https://doi.org/10.1172/JCI70678.

Mendlin, A. *et al.* (1996) 'Neuronal Release of Serotonin in the Cerebellum of Behaving Rats: An In Vivo Microdialysis Study', *Journal of Neurochemistry*, 67(2), pp. 617–622. Available at: https://doi.org/https://doi.org/10.1046/j.1471-4159.1996.67020617.x.

Michely, J. *et al.* (2020) 'A mechanistic account of serotonin's impact on mood', *Nature communications*, 11(1), p. 2335. Available at: https://doi.org/10.1038/s41467-020-16090-2.

Migliarini, S. *et al.* (2013) 'Lack of brain serotonin affects postnatal development and serotonergic neuronal circuitry formation', *Molecular Psychiatry*, 18(10), pp. 1106–1118. Available at: https://doi.org/10.1038/mp.2012.128.

Millan, M.J. *et al.* (2005) 'Anxiolytic properties of agomelatine, an antidepressant with melatoninergic and serotonergic properties: role of 5-HT2C receptor blockade', *Psychopharmacology*, 177(4), pp. 448–458. Available at: https://doi.org/10.1007/s00213-004-1962-z.

Mistlberger, R.E. *et al.* (2000) 'Behavioral and Serotonergic Regulation of Circadian Rhythms', *Biological Rhythm Research*, 31(3), pp. 240–283. Available at: https://doi.org/10.1076/0929-1016(200007)31:3;1-K;FT240.

Miura, Y. *et al.* (2020) 'Generation of human striatal organoids and cortico-striatal assembloids from human pluripotent stem cells', *Nature biotechnology*. 2020/12/03, 38(12), pp. 1421–1430. Available at: https://doi.org/10.1038/s41587-020-00763-w.

Molnár, Z. *et al.* (2019) 'New insights into the development of the human cerebral cortex', *Journal of anatomy*. 2019/08/02, 235(3), pp. 432–451. Available at: https://doi.org/10.1111/joa.13055.

Moore, R.Y., Halaris, A.E. and Jones, B.E. (1978) 'Serotonin neurons of the midbrain raphe: Ascending projections', *Journal of Comparative Neurology*, 180(3), pp. 417–438. Available at: https://doi.org/https://doi.org/10.1002/cne.901800302.

Muguruma, K. *et al.* (2010) 'Ontogeny-recapitulating generation and tissue integration of ES cell–derived Purkinje cells', *Nature Neuroscience*, 13(10), pp. 1171–1180. Available at: https://doi.org/10.1038/nn.2638.

Muguruma, K. *et al.* (2015) 'Self-Organization of Polarized Cerebellar Tissue in 3D Culture of Human Pluripotent Stem Cells', *Cell Reports*, 10(4), pp. 537–550. Available at: https://doi.org/10.1016/j.celrep.2014.12.051.

Muller, C.L., Anacker, A.M.J. and Veenstra-VanderWeele, J. (2016) 'The serotonin system in autism spectrum disorder: From biomarker to animal models', *Neuroscience*. 2015/11/11, 321, pp. 24–41. Available at: https://doi.org/10.1016/j.neuroscience.2015.11.010.

Müller, F. and O'Rahilly, R. (2006) 'The amygdaloid complex and the medial and lateral ventricular eminences in staged human embryos', *Journal of anatomy*, 208(5), pp. 547–564. Available at: https://doi.org/10.1111/j.1469-7580.2006.00553.x.

Murphy, F. *et al.* (2002) 'The effects of tryptophan depletion on cognitive and affective processing in healthy volunteers', *Psychopharmacology*, 163(1), pp. 42–53. Available at: https://doi.org/10.1007/s00213-002-1128-9.

Murphy, F.C. *et al.* (1999) 'Emotional bias and inhibitory control processes in mania and depression', *Psychological Medicine*. 1999/11/01, 29(6), pp. 1307–1321. Available at: https://doi.org/DOI: 10.1017/S0033291799001233.

Murphy, S.E. *et al.* (2006) 'Tryptophan supplementation induces a positive bias in the processing of emotional material in healthy female volunteers', *Psychopharmacology*, 187(1), pp. 121–130. Available at: https://doi.org/10.1007/s00213-006-0401-8.

Murthy, S. *et al.* (2014) 'Serotonin receptor 3A controls interneuron migration into the neocortex', *Nature Communications*, 5(1), p. 5524. Available at: https://doi.org/10.1038/ncomms6524.

Nebigil, C.G. *et al.* (2000) 'Serotonin 2B receptor is required for heart development', *Proceedings of the National Academy of Sciences of the United States of America*, 97(17), pp. 9508–9513. Available at: https://doi.org/10.1073/pnas.97.17.9508.

Nichols, A.J. and Olson, E.C. (2010) 'Reelin Promotes Neuronal Orientation and Dendritogenesis during Preplate Splitting', *Cerebral Cortex*, 20(9), pp. 2213–2223. Available at: https://doi.org/10.1093/cercor/bhp303.

Nichols, D.E. and Nichols, C.D. (2008) 'Serotonin Receptors', *Chemical Reviews*, 108(5), pp. 1614–1641. Available at: https://doi.org/10.1021/cr078224o.

Nolbrant, S. *et al.* (2017) 'Generation of high-purity human ventral midbrain dopaminergic progenitors for in vitro maturation and intracerebral transplantation', *Nature Protocols*, 12(9), pp. 1962–1979. Available at: https://doi.org/10.1038/nprot.2017.078.

Nowakowski, T.J. *et al.* (2016) 'Transformation of the Radial Glia Scaffold Demarcates Two Stages of Human Cerebral Cortex Development', *Neuron*, 91(6), pp. 1219–1227. Available at: https://doi.org/10.1016/j.neuron.2016.09.005.

Oikonomou, G. *et al.* (2019) 'The Serotonergic Raphe Promote Sleep in Zebrafish and Mice', *Neuron*. 2019/06/24, 103(4), pp. 686-701.e8. Available at: https://doi.org/10.1016/j.neuron.2019.05.038.

Okaty, B.W. *et al.* (2015) 'Multi-Scale Molecular Deconstruction of the Serotonin Neuron System', *Neuron*. 2015/11/05, 88(4), pp. 774–791. Available at: https://doi.org/10.1016/j.neuron.2015.10.007.

Ossewaarde, J.M. *et al.* (1996) 'Application of a Mycoplasma group-specific PCR for monitoring decontamination of Mycoplasma-infected Chlamydia sp. strains', *Applied and Environmental Microbiology*, 62(2), pp. 328–331. Available at: https://doi.org/10.1128/aem.62.2.328-331.1996.

Paquelet, G.E. *et al.* (2022) 'Single-cell activity and network properties of dorsal raphe nucleus serotonin neurons during emotionally salient behaviors', *Neuron*, 110(16), pp. 2664-2679.e8. Available at: https://doi.org/10.1016/j.neuron.2022.05.015.

Paredes, M.F. *et al.* (2016) 'Extensive migration of young neurons into the infant human frontal lobe', *Science (New York, N.Y.)*, 354(6308), p. aaf7073. Available at: https://doi.org/10.1126/science.aaf7073.

Parnavelas, J.G. and Blue, M.E. (1982) 'The role of the noradrenergic system on the formation of synapses in the visual cortex of the rat', *Developmental Brain Research*, 3(1), pp. 140–144. Available at: https://doi.org/https://doi.org/10.1016/0165-3806(82)90082-7.

Pașca, S.P. *et al.* (2022) 'A nomenclature consensus for nervous system organoids and assembloids', *Nature*, 609(7929), pp. 907–910. Available at: https://doi.org/10.1038/s41586-022-05219-6.

Pattyn, A. *et al.* (2000) 'Control of hindbrain motor neuron differentiation by the homeobox gene Phox2b', *Development*, 127(7), pp. 1349–1358. Available at: https://doi.org/10.1242/dev.127.7.1349.

Pattyn, A. *et al.* (2003) 'Coordinated temporal and spatial control of motor neuron and serotonergic neuron generation from a common pool of CNS progenitors', *Genes & development*, 17(6), pp. 729–737. Available at: https://doi.org/10.1101/gad.255803.

Paulmann, N. *et al.* (2009) 'Intracellular Serotonin Modulates Insulin Secretion from Pancreatic β-Cells by Protein Serotonylation', *PLOS Biology*, 7(10), pp. e1000229-. Available at: https://doi.org/10.1371/journal.pbio.1000229.

Paulsen, B. *et al.* (2022) 'Autism genes converge on asynchronous development of shared neuron classes', *Nature*. 2022/02/02, 602(7896), pp. 268–273. Available at: https://doi.org/10.1038/s41586-021-04358-6.

Pellegrini, L. *et al.* (2020) 'SARS-CoV-2 Infects the Brain Choroid Plexus and Disrupts the Blood-CSF Barrier in Human Brain Organoids', *Cell stem cell*. 2020/10/13, 27(6), pp. 951-961.e5. Available at: https://doi.org/10.1016/j.stem.2020.10.001.

Pellenz, S. *et al.* (2019) 'New Human Chromosomal Sites with "Safe Harbor" Potential for Targeted Transgene Insertion', *Human gene therapy*. 2019/03/28, 30(7), pp. 814–828. Available at: https://doi.org/10.1089/hum.2018.169.

Pelosi, B. *et al.* (2015) 'Generation of a Tph2 Conditional Knockout Mouse Line for Time- and Tissue-Specific Depletion of Brain Serotonin', *PLOS ONE*, 10(8), pp. e0136422-. Available at: https://doi.org/10.1371/journal.pone.0136422.

Penisson, M. *et al.* (2019) 'Genes and Mechanisms Involved in the Generation and Amplification of Basal Radial Glial Cells', *Frontiers in Cellular Neuroscience*, 13. Available at: https://www.frontiersin.org/articles/10.3389/fncel.2019.00381.

Peroutka, S.J. and Howell, T.A. (1994) 'The molecular evolution of G protein-coupled receptors: Focus on 5-hydroxytryptamine receptors', *Neuropharmacology*, 33(3), pp. 319–324. Available at: https://doi.org/https://doi.org/10.1016/0028-3908(94)90060-4.

Piccolo, S. *et al.* (1996) 'Dorsoventral patterning in Xenopus: inhibition of ventral signals by direct binding of chordin to BMP-4', *Cell*, 86(4), pp. 589–598. Available at: https://doi.org/10.1016/s0092-8674(00)80132-4.

Pickard, G.E. *et al.* (1999) '5-HT1B receptor-mediated presynaptic inhibition of retinal input to the suprachiasmatic nucleus', *The Journal of neuroscience : the official journal of the Society for Neuroscience*, 19(10), pp. 4034–4045. Available at: https://doi.org/10.1523/JNEUROSCI.19-10-04034.1999.

Pickard, G.E. and Rea, M.A. (1997) 'TFMPP, a 5HT1B receptor agonist, inhibits light-induced phase shifts of the circadian activity rhythm and c-Fos expression in the mouse suprachiasmatic nucleus', *Neuroscience Letters*, 231(2), pp. 95–98. Available at: https://doi.org/https://doi.org/10.1016/S0304-3940(97)00534-X.

Pilz, G.-A. *et al.* (2013) 'Amplification of progenitors in the mammalian telencephalon includes a new radial glial cell type', *Nature Communications*, 4(1), p. 2125. Available at: https://doi.org/10.1038/ncomms3125.

Pollen, A.A. *et al.* (2015) 'Molecular Identity of Human Outer Radial Glia during Cortical Development', *Cell*, 163(1), pp. 55–67. Available at: https://doi.org/10.1016/j.cell.2015.09.004.

Pollen, A.A. *et al.* (2019) 'Establishing Cerebral Organoids as Models of Human-Specific Brain Evolution', *Cell*, 176(4), pp. 743-756.e17. Available at: https://doi.org/10.1016/j.cell.2019.01.017.

Popolo, M., McCarthy, D.M. and Bhide, P.G. (2004) 'Influence of dopamine on precursor cell proliferation and differentiation in the embryonic mouse telencephalon', *Developmental neuroscience*, 26(2–4), pp. 229–244. Available at: https://doi.org/10.1159/000082140.

Portas, C.M. *et al.* (1996) 'Microdialysis perfusion of 8-hydroxy-2-(di-n-propylamino)tetralin (8-OH-DPAT) in the dorsal raphe nucleus decreases serotonin release and increases rapid eye movement sleep in the freely moving cat', *The Journal of Neuroscience*, 16(8), p. 2820. Available at: https://doi.org/10.1523/JNEUROSCI.16-08-02820.1996.

Portas, C.M. *et al.* (1998) 'On-line detection of extracellular levels of serotonin in dorsal raphe nucleus and frontal cortex over the sleep/wake cycle in the freely moving rat', *Neuroscience*, 83(3), pp. 807–814. Available at: https://doi.org/https://doi.org/10.1016/S0306-4522(97)00438-7.

Pourhamzeh, M. *et al.* (2022) 'The Roles of Serotonin in Neuropsychiatric Disorders', *Cellular and Molecular Neurobiology*, 42(6), pp. 1671–1692. Available at: https://doi.org/10.1007/s10571-021-01064-9.

Qi, Y.-X. *et al.* (2014) 'Larvae of the small white butterfly, Pieris rapae, express a novel serotonin receptor', *Journal of Neurochemistry*, 131(6), pp. 767–777. Available at: https://doi.org/https://doi.org/10.1111/jnc.12940.

Qian, X. *et al.* (2016) 'Brain-Region-Specific Organoids Using Mini-bioreactors for Modeling ZIKV Exposure', *Cell*. 2016/04/22, 165(5), pp. 1238–1254. Available at: https://doi.org/10.1016/j.cell.2016.04.032.

Qian, X. *et al.* (2017) 'Using brain organoids to understand Zika virus-induced microcephaly', *Development*, 144(6), pp. 952–957. Available at: https://doi.org/10.1242/dev.140707.

Qian, X. *et al.* (2020) 'Sliced Human Cortical Organoids for Modeling Distinct Cortical Layer Formation', *Cell stem cell*. 2020/03/05, 26(5), pp. 766-781.e9. Available at: https://doi.org/10.1016/j.stem.2020.02.002.

Qian, X., Song, H. and Ming, G. (2019) 'Brain organoids: advances, applications and challenges', *Development*, 146(8), p. dev166074. Available at: https://doi.org/10.1242/dev.166074.

Quadrato, G. *et al.* (2017) 'Cell diversity and network dynamics in photosensitive human brain organoids', *Nature*, 545(7652), pp. 48–53. Available at: https://doi.org/10.1038/nature22047.

Quadrato, G., Brown, J. and Arlotta, P. (2016) 'The promises and challenges of human brain organoids as models of neuropsychiatric disease', *Nature Medicine*, 22(11), pp. 1220–1228. Available at: https://doi.org/10.1038/nm.4214.

Quentin, E., Belmer, A. and Maroteaux, L. (2018) 'Somato-Dendritic Regulation of Raphe Serotonin Neurons; A Key to Antidepressant Action', *Frontiers in Neuroscience*, 12. Available at: https://www.frontiersin.org/articles/10.3389/fnins.2018.00982.

Quist, J.F. *et al.* (2003) 'The serotonin 5-HT1B receptor gene and attention deficit hyperactivity disorder', *Molecular Psychiatry*, 8(1), pp. 98–102. Available at: https://doi.org/10.1038/sj.mp.4001244.

Rapport, M.M., Green, Arda.Alden. and Page, I.H. (1948) 'SERUM VASOCONSTRICTOR (SEROTONIN): IV. ISOLATION AND CHARACTERIZATION', *Journal of Biological Chemistry*, 176(3), pp. 1243–1251. Available at: https://doi.org/https://doi.org/10.1016/S0021-9258(18)57137-4.

Rash, B.G. *et al.* (2019) 'Gliogenesis in the outer subventricular zone promotes enlargement and gyrification of the primate cerebrum', *Proceedings of the National Academy of Sciences*, 116(14), pp. 7089–7094. Available at: https://doi.org/10.1073/pnas.1822169116.

Riccio, O. *et al.* (2009) 'Excess of serotonin affects embryonic interneuron migration through activation of the serotonin receptor 6', *Molecular Psychiatry*, 14(3), pp. 280–290. Available at: https://doi.org/10.1038/mp.2008.89.

Riccio, O. *et al.* (2011) 'Excess of serotonin affects neocortical pyramidal neuron migration', *Translational psychiatry*, 1(10), pp. e47–e47. Available at: https://doi.org/10.1038/tp.2011.49.

Rosebrock, D. *et al.* (2022) 'Enhanced cortical neural stem cell identity through short SMAD and WNT inhibition in human cerebral organoids facilitates emergence of outer radial glial cells', *Nature cell biology*. 2022/06/13, 24(6), pp. 981–995. Available at: https://doi.org/10.1038/s41556-022-00929-5.

Rose'meyer, R. (2013) 'A review of the serotonin transporter and prenatal cortisol in the development of autism spectrum disorders', *Molecular autism*, 4(1), p. 37. Available at: https://doi.org/10.1186/2040-2392-4-37.

Rossetti, A. *et al.* (2022) 'Capturing the pathomechanisms of different disease severities in a human cerebral organoid model of LIS1-lissencephaly', *submitted* [Preprint].

Roth, B.L. *et al.* (1984) 'Aortic recognition sites for serotonin (5HT) are coupled to phospholipase C and modulate phosphatidylinositol turnover', *Neuropharmacology*, 23(10), pp. 1223–1225. Available at: https://doi.org/https://doi.org/10.1016/0028-3908(84)90244-2.

Rumajogee, P. *et al.* (2005) 'Rapid up-regulation of the neuronal serotoninergic phenotype by brain-derived neurotrophic factor and cyclic adenosine monophosphate: Relations with raphe astrocytes', *Journal of Neuroscience Research*, 81(4), pp. 481–487. Available at: https://doi.org/https://doi.org/10.1002/jnr.20572.

Saitow, F., Murano, M. and Suzuki, H. (2009) 'Modulatory Effects of Serotonin on GABAergic Synaptic Transmission and Membrane Properties in the Deep Cerebellar Nuclei', *Journal of Neurophysiology*, 101(3), pp. 1361–1374. Available at: https://doi.org/10.1152/jn.90750.2008.

Samuelsen, G.B. *et al.* (2003) 'The Changing Number of Cells in the Human Fetal Forebrain and its Subdivisions: A Stereological Analysis', *Cerebral Cortex*, 13(2), pp. 115–122. Available at: https://doi.org/10.1093/cercor/13.2.115.

Sato, K. (2013) 'Placenta-derived hypo-serotonin situations in the developing forebrain cause autism', *Medical Hypotheses*, 80(4), pp. 368–372. Available at: https://doi.org/https://doi.org/10.1016/j.mehy.2013.01.002.

Schain, R.J. and Freedman, D.X. (1961) 'Studies on 5-hydroxyindole metabolism in autistic and other mentally retarded children', *The Journal of Pediatrics*, 58(3), pp. 315–320. Available at: https://doi.org/https://doi.org/10.1016/S0022-3476(61)80261-8.

Schoeffter, P. and Hoyer, D. (1988) 'Centrally acting hypotensive agents with affinity for 5-HT1A binding sites inhibit forskolin-stimulated adenylate cyclase activity in calf hippocampus', *British*

Journal of Pharmacology, 95(3), pp. 975–985. Available at: https://doi.org/https://doi.org/10.1111/j.1476-5381.1988.tb11728.x.

Schweighofer, N., Doya, K. and Kuroda, S. (2004) 'Cerebellar aminergic neuromodulation: towards a functional understanding', *Brain Research Reviews*, 44(2), pp. 103–116. Available at: https://doi.org/https://doi.org/10.1016/j.brainresrev.2003.10.004.

Shang, Z. *et al.* (2018) 'Single-cell RNA-seq reveals dynamic transcriptome profiling in human early neural differentiation', *GigaScience*, 7(11), p. giy117. Available at: https://doi.org/10.1093/gigascience/giy117.

Shin, D.-M. *et al.* (2004) 'Ascorbic acid responsive genes during neuronal differentiation of embryonic stem cells', *NeuroReport*, 15(12). Available at: https://journals.lww.com/neuroreport/Fulltext/2004/08260/Ascorbic_acid_responsive_genes_during_neuronal.25.aspx.

Sinha, S. and Chen, J.K. (2006) 'Purmorphamine activates the Hedgehog pathway by targeting Smoothened', *Nature Chemical Biology*, 2(1), pp. 29–30. Available at: https://doi.org/10.1038/nchembio753.

Sloan, S.A. *et al.* (2018) 'Generation and assembly of human brain region-specific three-dimensional cultures', *Nature protocols*, 13(9), pp. 2062–2085. Available at: https://doi.org/10.1038/s41596-018-0032-7.

Smidt, M.P. and van Hooft, J.A. (2013) 'Subset specification of central serotonergic neurons', *Frontiers in cellular neuroscience*, 7, p. 200. Available at: https://doi.org/10.3389/fncel.2013.00200.

Smith, B.N. *et al.* (2001) 'Serotonergic Modulation of Retinal Input to the Mouse Suprachiasmatic Nucleus Mediated by 5-HT1B and 5-HT7 Receptors', *Journal of Biological Rhythms*, 16(1), pp. 25–38. Available at: https://doi.org/10.1177/074873040101600104.

Sodhi, M.S.K. and Sanders-Bush, E. (2004) 'Serotonin and brain development', in *International Review of Neurobiology*. Academic Press, pp. 111–174. Available at: https://doi.org/https://doi.org/10.1016/S0074-7742(04)59006-2.

Soiza-Reilly, M. and Gaspar, P. (2020) 'Chapter 2 - From B1 to B9: a guide through hindbrain serotonin neurons with additional views from multidimensional characterization', in C.P. Müller and K.A. Cunningham (eds) *Handbook of Behavioral Neuroscience*. Elsevier, pp. 23–40. Available at: https://doi.org/https://doi.org/10.1016/B978-0-444-64125-0.00002-5.

Sos, K.E. *et al.* (2017) 'Cellular architecture and transmitter phenotypes of neurons of the mouse median raphe region', *Brain structure & function*. 2016/04/04, 222(1), pp. 287–299. Available at: https://doi.org/10.1007/s00429-016-1217-x.

Spence, J.R. *et al.* (2011) 'Directed differentiation of human pluripotent stem cells into intestinal tissue in vitro', *Nature*. 2010/12/12, 470(7332), pp. 105–109. Available at: https://doi.org/10.1038/nature09691.

Spohn, S.N. *et al.* (2016) 'Protective Actions of Epithelial 5-Hydroxytryptamine 4 Receptors in Normal and Inflamed Colon', *Gastroenterology*, 151(5), pp. 933-944.e3. Available at: https://doi.org/https://doi.org/10.1053/j.gastro.2016.07.032.

Spohn, S.N. and Mawe, G.M. (2017) 'Non-conventional features of peripheral serotonin signalling - the gut and beyond', *Nature reviews. Gastroenterology & hepatology*. 2017/05/10, 14(7), pp. 412–420. Available at: https://doi.org/10.1038/nrgastro.2017.51.

Staerk, J. *et al.* (2010) 'Reprogramming of human peripheral blood cells to induced pluripotent stem cells', *Cell stem cell*, 7(1), pp. 20–24. Available at: https://doi.org/10.1016/j.stem.2010.06.002.

Stahl, R. *et al.* (2013) 'Trnp1 Regulates Expansion and Folding of the Mammalian Cerebral Cortex by Control of Radial Glial Fate', *Cell*, 153(3), pp. 535–549. Available at: https://doi.org/10.1016/j.cell.2013.03.027.

Steenbergen, L. *et al.* (2016) 'Tryptophan supplementation modulates social behavior: A review', *Neuroscience & Biobehavioral Reviews*, 64, pp. 346–358. Available at: https://doi.org/https://doi.org/10.1016/j.neubiorev.2016.02.022.

Stepien, B.K. *et al.* (2020) 'Lengthening Neurogenic Period during Neocortical Development Causes a Hallmark of Neocortex Expansion', *Current Biology*, 30(21), pp. 4227-4237.e5. Available at: https://doi.org/https://doi.org/10.1016/j.cub.2020.08.046.

Stirling, D.R. *et al.* (2021) 'CellProfiler 4: improvements in speed, utility and usability', *BMC Bioinformatics*, 22(1), p. 433. Available at: https://doi.org/10.1186/s12859-021-04344-9.

Stunes, A.K. *et al.* (2011) 'Adipocytes express a functional system for serotonin synthesis, reuptake and receptor activation', *Diabetes, Obesity and Metabolism*, 13(6), pp. 551–558. Available at: https://doi.org/https://doi.org/10.1111/j.1463-1326.2011.01378.x.

Subramanian, L. *et al.* (2017) 'Dynamic behaviour of human neuroepithelial cells in the developing forebrain', *Nature Communications*, 8(1), p. 14167. Available at: https://doi.org/10.1038/ncomms14167.

Sumara, G. *et al.* (2012) 'Gut-Derived Serotonin Is a Multifunctional Determinant to Fasting Adaptation', *Cell Metabolism*, 16(5), pp. 588–600. Available at: https://doi.org/https://doi.org/10.1016/j.cmet.2012.09.014.

Sundström, E. *et al.* (1993) 'Neurochemical differentiation of human bulbospinal monoaminergic neurons during the first trimester', *Developmental Brain Research*, 75(1), pp. 1–12. Available at: https://doi.org/https://doi.org/10.1016/0165-3806(93)90059-J.

Sutcliffe, J.S. *et al.* (2005) 'Allelic Heterogeneity at the Serotonin Transporter Locus (SLC6A4) Confers Susceptibility to Autism and Rigid-Compulsive Behaviors', *The American Journal of Human Genetics*, 77(2), pp. 265–279. Available at: https://doi.org/10.1086/432648.

Szabo, A. *et al.* (2016) 'The Endogenous Hallucinogen and Trace Amine N,N-Dimethyltryptamine (DMT) Displays Potent Protective Effects against Hypoxia via Sigma-1 Receptor Activation in Human Primary iPSC-Derived Cortical Neurons and Microglia-Like Immune Cells', *Frontiers in neuroscience*, 10, p. 423. Available at: https://doi.org/10.3389/fnins.2016.00423.

Szebényi, K. *et al.* (2021) 'Human ALS/FTD brain organoid slice cultures display distinct early astrocyte and targetable neuronal pathology', *Nature Neuroscience*, 24(11), pp. 1542–1554. Available at: https://doi.org/10.1038/s41593-021-00923-4.

Taipale, J. *et al.* (2002) 'Patched acts catalytically to suppress the activity of Smoothened', *Nature*, 418(6900), pp. 892–896. Available at: https://doi.org/10.1038/nature00989.

Takahashi, E. *et al.* (2012) 'Emerging cerebral connectivity in the human fetal brain: an MR tractography study', *Cerebral cortex (New York, N.Y. : 1991)*. 2011/06/13, 22(2), pp. 455–464. Available at: https://doi.org/10.1093/cercor/bhr126.

Takahashi, K. *et al.* (2007) 'Induction of Pluripotent Stem Cells from Adult Human Fibroblasts by Defined Factors', *Cell*, 131(5), pp. 861–872. Available at: https://doi.org/10.1016/j.cell.2007.11.019.

Takahashi, K. and Yamanaka, S. (2006) 'Induction of Pluripotent Stem Cells from Mouse Embryonic and Adult Fibroblast Cultures by Defined Factors', *Cell*, 126(4), pp. 663–676. Available at: https://doi.org/https://doi.org/10.1016/j.cell.2006.07.024.

Takahashi, T. *et al.* (1999) 'Sequence of neuron origin and neocortical laminar fate: relation to cell cycle of origin in the developing murine cerebral wall', *The Journal of neuroscience : the official journal of the Society for Neuroscience*, 19(23), pp. 10357–10371. Available at: https://doi.org/10.1523/JNEUROSCI.19-23-10357.1999.

Takebe, T. *et al.* (2013) 'Vascularized and functional human liver from an iPSC-derived organ bud transplant', *Nature*, 499(7459), pp. 481–484. Available at: https://doi.org/10.1038/nature12271.

Tamir, H. *et al.* (1985) 'Human serotonectin: a blood glycoprotein that binds serotonin and is associated with platelets and white blood cells', *Journal of Cell Science*, 73(1), pp. 187–206. Available at: https://doi.org/10.1242/jcs.73.1.187.

Tanaka, Y. and Park, I.-H. (2021) 'Regional specification and complementation with non-neuroectodermal cells in human brain organoids', *Journal of molecular medicine (Berlin, Germany)*. 2021/03/02, 99(4), pp. 489–500. Available at: https://doi.org/10.1007/s00109-021-02051-9.

Telezhkin, V. *et al.* (2015) 'Forced cell cycle exit and modulation of GABAA, CREB, and GSK3β signaling promote functional maturation of induced pluripotent stem cell-derived neurons', *American Journal of Physiology-Cell Physiology*, 310(7), pp. C520–C541. Available at: https://doi.org/10.1152/ajpcell.00166.2015.

Thomson, J.A. *et al.* (1998) 'Embryonic Stem Cell Lines Derived from Human Blastocysts', *Science*, 282(5391), pp. 1145–1147. Available at: https://doi.org/10.1126/science.282.5391.1145.

Tick, B. *et al.* (2016) 'Heritability of autism spectrum disorders: a meta-analysis of twin studies', *Journal of child psychology and psychiatry, and allied disciplines*. 2015/12/27, 57(5), pp. 585–595. Available at: https://doi.org/10.1111/jcpp.12499.

Tieng, V. *et al.* (2014) 'Engineering of Midbrain Organoids Containing Long-Lived Dopaminergic Neurons', *Stem Cells and Development*, 23(13), pp. 1535–1547. Available at: https://doi.org/10.1089/scd.2013.0442.

Trulson, M.E. and Jacobs, B.L. (1979) 'Raphe unit activity in freely moving cats: Correlation with level of behavioral arousal', *Brain Research*, 163(1), pp. 135–150. Available at: https://doi.org/https://doi.org/10.1016/0006-8993(79)90157-4.

Urresti, J. *et al.* (2021) 'Cortical organoids model early brain development disrupted by 16p11.2 copy number variants in autism', *Molecular psychiatry*. 2021/08/26, 26(12), pp. 7560–7580. Available at: https://doi.org/10.1038/s41380-021-01243-6.

Vadodaria, K.C. *et al.* (2016) 'Generating human serotonergic neurons in vitro: Methodological advances', *BioEssays*, 38(11), pp. 1123–1129. Available at: https://doi.org/https://doi.org/10.1002/bies.201600127.

Vadodaria, K.C. *et al.* (2019) 'Serotonin-induced hyperactivity in SSRI-resistant major depressive disorder patient-derived neurons', *Molecular Psychiatry*, 24(6), pp. 795–807. Available at: https://doi.org/10.1038/s41380-019-0363-y.

Valiulahi, P. *et al.* (2021) 'Generation of caudal-type serotonin neurons and hindbrain-fate organoids from hPSCs', *Stem cell reports*. 2021/07/08, 16(8), pp. 1938–1952. Available at: https://doi.org/10.1016/j.stemcr.2021.06.006.

van der Veen, F.M. *et al.* (2007) 'Effects of Acute Tryptophan Depletion on Mood and Facial Emotion Perception Related Brain Activation and Performance in Healthy Women with and without a Family History of Depression', *Neuropsychopharmacology*, 32(1), pp. 216–224. Available at: https://doi.org/10.1038/sj.npp.1301212.

Veenstra-VanderWeele, J. *et al.* (2012) 'Autism gene variant causes hyperserotonemia, serotonin receptor hypersensitivity, social impairment and repetitive behavior', *Proceedings of the National Academy of Sciences of the United States of America*. 2012/03/19, 109(14), pp. 5469–5474. Available at: https://doi.org/10.1073/pnas.1112345109.

Velasco, S. *et al.* (2019) 'Individual brain organoids reproducibly form cell diversity of the human cerebral cortex', *Nature*. 2019/06/05, 570(7762), pp. 523–527. Available at: https://doi.org/10.1038/s41586-019-1289-x.

Verney, C., Lebrand, C. and Gaspar, P. (2002) 'Changing distribution of monoaminergic markers in the developing human cerebral cortex with special emphasis on the serotonin transporter', *The Anatomical Record*, 267(2), pp. 87–93. Available at: https://doi.org/https://doi.org/10.1002/ar.10089.

Virgintino, D. *et al.* (2000) 'Immunogold cytochemistry of the blood–brain barrier glucose transporter GLUT1 and endogenous albumin in the developing human brain11Published on the World Wide Web on 24 August 2000.', *Developmental Brain Research*, 123(1), pp. 95–101. Available at: https://doi.org/https://doi.org/10.1016/S0165-3806(00)00086-9.

Vitalis, T. *et al.* (2007a) 'Embryonic depletion of serotonin affects cortical development', *European Journal of Neuroscience*, 26(2), pp. 331–344. Available at: https://doi.org/https://doi.org/10.1111/j.1460-9568.2007.05661.x.

Vitalis, T. *et al.* (2007b) 'Embryonic depletion of serotonin affects cortical development', *European Journal of Neuroscience*, 26(2), pp. 331–344. Available at: https://doi.org/https://doi.org/10.1111/j.1460-9568.2007.05661.x.

Wallace, J.A. and Lauder, J.M. (1983) 'Development of the serotonergic system in the rat embryo: An immunocytochemical study', *Brain Research Bulletin*, 10(4), pp. 459–479. Available at: https://doi.org/https://doi.org/10.1016/0361-9230(83)90144-2.

Walther, D.J. *et al.* (2003) 'Synthesis of Serotonin by a Second Tryptophan Hydroxylase Isoform', *Science*, 299(5603), p. 76. Available at: https://doi.org/10.1126/science.1078197.

Walther, D.J. and Bader, M. (2003) 'A unique central tryptophan hydroxylase isoform', *Biochemical Pharmacology*, 66(9), pp. 1673–1680. Available at: https://doi.org/https://doi.org/10.1016/S0006-2952(03)00556-2.

Wang, D.D. and Kriegstein, A.R. (2008) 'GABA regulates excitatory synapse formation in the neocortex via NMDA receptor activation', *The Journal of neuroscience : the official journal of the*

Society for Neuroscience, 28(21), pp. 5547–5558. Available at: https://doi.org/10.1523/JNEUROSCI.5599-07.2008.

Wang, Q. *et al.* (2021) 'Constitutive Activity of Serotonin Receptor 6 Regulates Human Cerebral Organoids Formation and Depression-like Behaviors', *Stem cell reports*. 2020/12/23, 16(1), pp. 75–88. Available at: https://doi.org/10.1016/j.stemcr.2020.11.015.

Wang, X. *et al.* (2011) 'A new subtype of progenitor cell in the mouse embryonic neocortex', *Nature neuroscience*. 2011/04/10, 14(5), pp. 555–561. Available at: https://doi.org/10.1038/nn.2807.

Watanabe, K. *et al.* (2005) 'Directed differentiation of telencephalic precursors from embryonic stem cells', *Nature Neuroscience*, 8(3), pp. 288–296. Available at: https://doi.org/10.1038/nn1402.

Watanabe, M. *et al.* (2017) 'Self-Organized Cerebral Organoids with Human-Specific Features Predict Effective Drugs to Combat Zika Virus Infection', *Cell reports*, 21(2), pp. 517–532. Available at: https://doi.org/10.1016/j.celrep.2017.09.047.

Watanabe, M. *et al.* (2022) 'TGFβ superfamily signaling regulates the state of human stem cell pluripotency and capacity to create well-structured telencephalic organoids', *Stem Cell Reports* [Preprint]. Available at: https://doi.org/10.1016/j.stemcr.2022.08.013.

Wataya, T. *et al.* (2008) 'Minimization of exogenous signals in ES cell culture induces rostral hypothalamic differentiation', *Proceedings of the National Academy of Sciences*, 105(33), pp. 11796–11801. Available at: https://doi.org/10.1073/pnas.0803078105.

Wen, Z. (2017) 'Modeling neurodevelopmental and psychiatric diseases with human iPSCs', *Journal of Neuroscience Research*, 95(5), pp. 1097–1109. Available at: https://doi.org/https://doi.org/10.1002/jnr.24031.

Wilkens, R. *et al.* (2022) 'Diverse maturity-dependent and complementary anti-apoptotic brakes safeguard human iPSC-derived neurons from cell death', *Cell Death & Disease*, 13(10), p. 887. Available at: https://doi.org/10.1038/s41419-022-05340-4.

Willins, D.L., Deutch, A.Y. and Roth, B.L. (1997) 'Serotonin 5-HT2A receptors are expressed on pyramidal cells and interneurons in the rat cortex', *Synapse*, 27(1), pp. 79–82. Available at: https://doi.org/https://doi.org/10.1002/(SICI)1098-2396(199709)27:1<79::AID-SYN8>3.0.CO;2-A.

Workman, A.D. *et al.* (2013) 'Modeling transformations of neurodevelopmental sequences across mammalian species', *The Journal of neuroscience : the official journal of the Society for Neuroscience*, 33(17), pp. 7368–7383. Available at: https://doi.org/10.1523/JNEUROSCI.5746-12.2013.

Wylie, C.J. *et al.* (2010) 'Distinct Transcriptomes Define Rostral and Caudal Serotonin Neurons', *The Journal of Neuroscience*, 30(2), p. 670. Available at: https://doi.org/10.1523/JNEUROSCI.4656-09.2010.

Xiang, Y. *et al.* (2017) 'Fusion of Regionally Specified hPSC-Derived Organoids Models Human Brain Development and Interneuron Migration', *Cell stem cell*. 2017/07/27, 21(3), pp. 383-398.e7. Available at: https://doi.org/10.1016/j.stem.2017.07.007.

Xiang, Y. *et al.* (2019) 'hESC-Derived Thalamic Organoids Form Reciprocal Projections When Fused with Cortical Organoids', *Cell stem cell*. 2019/02/21, 24(3), pp. 487-497.e7. Available at: https://doi.org/10.1016/j.stem.2018.12.015.

Xiang, Y., Cakir, B. and Park, I.-H. (2021) 'Deconstructing and reconstructing the human brain with regionally specified brain organoids', *Seminars in Cell & Developmental Biology*, 111, pp. 40–51. Available at: https://doi.org/https://doi.org/10.1016/j.semcdb.2020.05.023.

Xing, L. *et al.* (2020) 'Serotonin Receptor 2A Activation Promotes Evolutionarily Relevant Basal Progenitor Proliferation in the Developing Neocortex', *Neuron*, 108(6), pp. 1113-1129.e6. Available at: https://doi.org/10.1016/j.neuron.2020.09.034.

Xing, L. and Huttner, W.B. (2020) 'Neurotransmitters as Modulators of Neural Progenitor Cell Proliferation During Mammalian Neocortex Development', *Frontiers in Cell and Developmental Biology*, 8. Available at: https://www.frontiersin.org/articles/10.3389/fcell.2020.00391.

Xu, T. *et al.* (2022) 'Generation of a TPH2-EGFP reporter cell line for purification and monitoring of human serotonin neurons in vitro and in vivo', *Stem Cell Reports*, 17(10), pp. 2365–2379. Available at: https://doi.org/https://doi.org/10.1016/j.stemcr.2022.08.012.

Yadav, V.K. *et al.* (2008) 'Lrp5 Controls Bone Formation by Inhibiting Serotonin Synthesis in the Duodenum', *Cell*, 135(5), pp. 825–837. Available at: https://doi.org/https://doi.org/10.1016/j.cell.2008.09.059.

Yang, C.-J. *et al.* (2015) 'The combined role of serotonin and interleukin-6 as biomarker for autism', *Neuroscience*, 284, pp. 290–296. Available at: https://doi.org/https://doi.org/10.1016/j.neuroscience.2014.10.011.

Yang, T. *et al.* (2016) 'A small molecule TrkB/TrkC neurotrophin receptor co-activator with distinctive effects on neuronal survival and process outgrowth', *Neuropharmacology*, 110, pp. 343–361. Available at: https://doi.org/https://doi.org/10.1016/j.neuropharm.2016.06.015.

Yasmine, C.-A. *et al.* (2012) 'Decreased osteoclastogenesis in serotonin-deficient mice', *Proceedings of the National Academy of Sciences*, 109(7), pp. 2567–2572. Available at: https://doi.org/10.1073/pnas.1117792109.

Yavarone, M.S. *et al.* (1993) 'Serotonin and cardiac morphogenesis in the mouse embryo', *Teratology*, 47(6), pp. 573–584. Available at: https://doi.org/https://doi.org/10.1002/tera.1420470609.

Ye, W. *et al.* (1998) 'FGF and Shh Signals Control Dopaminergic and Serotonergic Cell Fate in the Anterior Neural Plate', *Cell*, 93(5), pp. 755–766. Available at: https://doi.org/https://doi.org/10.1016/S0092-8674(00)81437-3.

Yoon, S.-J. *et al.* (2019) 'Reliability of human cortical organoid generation', *Nature methods*. 2018/12/20, 16(1), pp. 75–78. Available at: https://doi.org/10.1038/s41592-018-0255-0.

Zafeiriou, D.I., Ververi, A. and Vargiami, E. (2009) 'The serotonergic system: its role in pathogenesis and early developmental treatment of autism', *Current neuropharmacology*, 7(2), pp. 150–157. Available at: https://doi.org/10.2174/157015909788848848.

Zhang, W. *et al.* (2019) 'Modeling microcephaly with cerebral organoids reveals a WDR62–CEP170–KIF2A pathway promoting cilium disassembly in neural progenitors', *Nature Communications*, 10(1), p. 2612. Available at: https://doi.org/10.1038/s41467-019-10497-2.

Zhou, F.C. *et al.* (1998) 'Serotonin transporters are located on the axons beyond the synaptic junctions: anatomical and functional evidence', *Brain Research*, 805(1), pp. 241–254. Available at: https://doi.org/https://doi.org/10.1016/S0006-8993(98)00691-X.

Zoli, M. *et al.* (1999) 'Volume transmission in the CNS and its relevance for neuropsychopharmacology', *Trends in Pharmacological Sciences*, 20(4), pp. 142–150. Available at: https://doi.org/https://doi.org/10.1016/S0165-6147(99)01343-7.

V. Danksagungen

Dr. Julia Ladewig möchte ich zunächst für die Themenstellung und die Möglichkeit in ihrer Arbeitsgruppe meine Promotion durchzuführen. Besonders möchte ich mich für die Freiheiten bedanken, die es mir erlaubt haben dieses Projekt mit meinen eigenen Ideen zu gestalten, sowie die fachliche Betreuung.

Prof. Dr. Philipp Koch gebührt der zweite Dank für die Möglichkeit Teil des Hector Institut für Translationale Hirnforschung zu sein sowie für die Betreuung meiner Arbeit als Gutachter.

Ebenso möchte ich mich bei Prof. Dr. Valery Grinevich als meinen Fakultätsgutachter bedanken und sc

Den Vorsitz meines Prüfungskomitee hat Prof. Dr. Schuster übernommen, wofür ich ihm sehr dankbar bin.

Zudem gilt mein Dank auch Dr. Julieta Alfonso für die Bereitschaft mein Prüfungskomitee zu vervollständigen.

Ohne die aktuellen und ehemaligen Mitglieder der Arbeitsgruppen von Julia Ladewig und Philipp Koch wäre diese Arbeit nie zustande gekommen. Viele hilfreiche Ratschläge und Diskussionen haben die Ideen entwickelt, um diese Arbeit voranzutreiben. Ganz ausschlaggebend war allerdings der moralische Support des Teams. Dabei möchte ich Speziellen Ammar, Bettina, Anne, Ruven, Isa, Andrea, Raquel und Annasara hervorheben.

Besonders möchte ich mich bei Isabel für Ihre Liebe, Unterstützung und die kleinen Ablenkungen im letzten Jahr bedanken. Zu guter Letzt möchte ich mich bei meinen langjährigen Freunden und meiner Familie für die langanhaltende und bedingungslose Unterstützung in verschiedensten Formen bedanken.